ROLE OF PROα2(I) COLLAGEN CHAINS AND COLLAGEN CROSSLINKING IN THORACIC AORTIC BIOMECHANICAL INTEGRITY DURING AGING USING THE *OIM* MOUSE MODEL

A Dissertation
presented to
the Faculty of the Graduate School
University of Missouri-Columbia

In Partial Fulfillment
of the Requirements for the Degree
Doctor of Philosophy

---

by

BRENT J. PFEIFFER

Dr. Charlotte L. Phillips, Dissertation Supervisor

May 2006

The undersigned, appointed by the Dean of the Graduate School, have examined the dissertation entitled

ROLE OF PROα2(I) COLLAGEN CHAINS AND COLLAGEN CROSSLINKING IN THORACIC AORTIC BIOMECHANICAL INTEGRITY DURING AGING USING THE *OIM* MOUSE MODEL

Presented by Brent J. Pfeiffer

A candidate for the degree of Doctor of Philosophy of Biochemistry

And hereby certify that in their opinion it is worthy of acceptance.
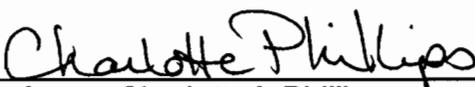

Professor Charlotte L Phillips
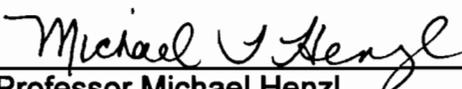
Professor Michael Henzl

Professor Dennis Lubahn

Professor Craig Franklin
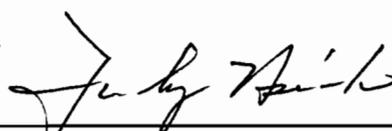
Professor Fu-hung Hsieh

DEDICATION

I dedicate this work to my parents (Stephen Pfeiffer and Phyllis O'Connor), my siblings (Ryan, Jeri, and Meghan Pfeiffer), and friends (Nathan Oehrle, Amanda Brodeur, Stephanie Carleton, and Matthew Schmitz). I am appreciative for the love and support they provided, which made it possible for me to attain this accomplishment. In addition, I want to thank my high school science teacher, Scott Dauve, for initiating my interest in the biological sciences.

ACKNOWLEDGEMENTS

TABLE OF CONTENTS

CHAPTERS

              The Collagen Family

              Type I Collagen

              Thoracic Aortic Integrity

              Mechanisms of Aging

              Inherited Connective Tissue Disorders

              The *Oim* (Osteogenesis Imperfecta Murine) Model

              Goals of the Study

              Introduction

              Material and Methods

              Results

              Discussion

              Introduction

              Material and Methods

Results

Discussion

Introduction

Materials and Methods

Results

Discussion

APPENDIX

LIST OF FIGURES

LIST OF TABLES

ROLE OF PROα2(I) COLLAGEN CHAINS AND COLLAGEN CROSSLINKING IN THORACIC AORTIC BIOMECHANICAL INTEGRITY DURING AGING USING THE *OIM* MOUSE MODEL

Brent J. Pfeiffer

Dr Charlotte L. Phillips, Dissertation Supervisor

ABSTRACT

Vascular tissue extracellular matrix (ECM) is crucial to maintaining aortic wall integrity in the presence of hemodynamic forces. The major vascular ECM components are elastin and collagens. The predominant collagen, type I, is normally a heterotrimeric molecule composed of two $\alpha 1$(I) collagen chains and one genetically distinct $\alpha 2$(I) collagen chain. The *oim* mouse produces only the homotrimeric type I collagen, composed of three $\alpha 1$(I) collagen chains, as a result of homozygosity for a functional null mutation in the COL1A2 gene. We have investigated the impact of homotrimeric type I collagen on arterial wall integrity, morphology, collagen expression, and collagen specific/non-specific crosslinking in relation to aging. The absence of $\alpha 2$(I) collagen chains and/or presence of homotrimeric type I collagen molecules in *oim* and heterozygote thoracic aortas is responsible for reduced aortic integrity, which cannot be attributed to reduced collagen content alone. *Oim* and heterozygote aortas demonstrated increased pyridinoline crosslinks/collagen molecule, a mechanism potentially compensating for their altered biomechanical parameters or possibly indicating abnormal fibril alignment. Despite increased pyridinoline crosslinking,

homotrimeric fibrils remained inherently weaker than heterotrimeric fibrils.

Morphometric analyses demonstrated significant age-associated increases of

lumen diameter and wall thickness, independent of genotype. However,

pyridinoline crosslinks/collagen molecule ratios were not significantly altered with

increasing age and do not account for the increased biomechanical integrity seen

with increasing age. Advanced glycation end-products (AGE) were found

localized to the aortic collagen and may account for the observed age-associated

increases of aortic strength and stiffness in heterozygote and *oim* aortas at 18

months of age.

CHAPTER I

INTRODUCTION

Connective tissue provides protection from external stress and the capacity to maintain a defined shape. The extracellular matrix (ECM) of connective tissue fulfills the qualities needed to form insoluble fibers that offer a scaffolding and/or anchors of high tensile strength and polymers that provide resistance to compressive forces. During the last 40 years, there have been significant advances in technologies that have allowed the elucidation of the various ECM components. However, the ECM interactions that define tissue characteristics have proven to be far more complex and diverse than previously believed. The basic building blocks of connective tissues-- collagens, proteoglycans, glycaminoglycans, and glycoproteins-- represent large families of matrix macromolecules. The composite nature of these ECM components is what defines a tissue's biomechanical structure and function.

An example of the ECMs increasing complexity is highlighted by vertebrates depending on the integrity of their vascular system for the delivery of nutrients and removal of waste. The thoracic aorta illustrates this concept, functioning as a circumferential spring storing energy when accommodating large volumes of blood ejected from the heart by increasing its diameter. After systole, it is the release of this stored energy via gradual elastic recoil, decreasing its diameter, which provides continuous blood flow to tissue arteries, arterioles, and capillaries between heart beats. Several ECM components must interact in order to accomplish this integral aortic function, such as elastin and collagens. Yet the ECM is not a static material, the ECM of vascular tissue undergoes physiological remodeling and age-associated changes. Collagen and elastin are the main

aortic ECM components, and these components undergo age-associated changes, which correlate with increased vascular stiffness. The true nature of the age-associated aortic collagen alterations remains unclear. The purpose of this dissertation is to examine the function of type I collagen in thoracic aortic integrity by comparing a type I collagen mutant mouse model with its wildtype control. In addition, we examined alterations of aortic integrity, collagen characteristics, and aortic ECM components associated with increasing age.

The Collagen Family

The definition of collagen was traditionally based on our knowledge of the major collagen types found in skin, bone, cartilage, and tendon. Collagens type I, II, and III are quantitatively the most important and abundant collagens, accounting for over 70% of the total collagen in the entire body (Kietly 1993; Byers 2001). Thus, the definition of collagen was based on histological properties, chemical composition, physical properties, and X-ray diffraction patterns of the fibrillar collagens, mainly of type I collagen; hence, the collagen numbering system (Roman numerals for each collagen type and Arabic numerals for individual α chains) (Kietly 1993). Currently, the generally accepted definition of 'collagen' is a molecule composed of three polypeptides that form triple-helical molecules, with characteristic triplets of (Gly-X-Y)$_n$ repeats where X and Y are often proline/hydroxyproline residues, of which molecular aggregates form via

3

self-assembly in the extracellular space (Kietly 1993; Byers 2001). Clues to the
evolution of the different collagen types are revealed in the detailed analyses of
collagen gene structure, which demonstrates divergence between fibrillar and
nonfibrillar collagen gene families, suggesting that specific collagens
accommodate the variety of structural, physiological, mechanical, and functional
needs of tissues (Bernard, Myers et al. 1983; Chu, de Wet et al. 1984; Exposito
and Garrone 1990; Exposito, D'Alessio et al. 1992; Exposito, Cluzel et al. 2000;
Exposito, Cluzel et al. 2002).

As the number of collagen types defined in the literature increases
(currently at 28 unique human collagen types comprised of 43 unique genes and
23 unique mouse collagen orthologs with 36 unique collagen genes), it is
appropriate to discuss the collagen family in terms of groups
(http://www.informatics.jax.org/mgihome/nomen/genefamilies/collagen.shtml
2006; http://www.ncbi.nlm.nih.gov/entrez/query 2006). The current classification
system (see Table 1) uses data derived from amino acid and cDNA sequencing
analyses, allowing the identification of collagens based on classes. Collagen
classes are as follows: fibrillar, basement membrane, anchoring fibrils, short
chain, fibrillar-associated collagens with interrupted triple helices (FACIT),
meshwork-forming collagen, anchoring-fibrils, transmembrane, FACIT-like, and
multiplexin. A discussion of the various collagen classes will not be presented
here. The interested reader should consult Byers 2001(Byers 2001).

Collagen biosynthesis is a multi-stage process, beginning with collagen
gene transcription and finishing with the maturation of the collagen molecule

Table 1.1 Classifications of Human and Mouse Collagens

Type	Class	Gene	Alpha chain	Mouse Ortholog	Collagen Domain Lengths (Amino Acid Content)
I	Fibrillar	COL1A1	$\alpha1(I)$	COL1A1	1014
		COL1A2	$\alpha2(I)$	COL1A2	1014
II	Fibrillar	COL2A1	$\alpha1(II)$	COL2A1	1017
III	Fibrillar	COL3A1	$\alpha1(III)$	COL3A1	1029
IV	Basement Membrane	COL4A1	$\alpha1(IV)$	COL4A1	1398
		COL4A2	$\alpha2(IV)$	COL4A2	1428
		COL4A3	$\alpha3(IV)$	COL4A3	1428
		COL4A4	$\alpha4(IV)$	COL4A4	1405
		COL4A5	$\alpha5(IV)$	COL4A5	1421
		COL4A6	$\alpha6(IV)$	COL4A6	1417
V	Fibrillar	COL5A1	$\alpha1(V)$	COL5A1	1014
		COL5A2	$\alpha2(V)$	COL5A2	1014
		COL5A3	$\alpha3(V)$	COL5A3	1011
VI		COL6A1	$\alpha1(VI)$	COL6A1	336
		COL6A2	$\alpha2(VI)$	COL6A2	335
		COL6A3	$\alpha3(VI)$	COL6A3	336
VII	Anchoring	COL7A1	$\alpha1(VII)$	COL7A1	1530
VIII	Short Chain	COL8A1	$\alpha1(VIII)$	COL8A1	454
		COL8A2	$\alpha2(VIII)$	COL8A2	457
IX	FACIT	COL9A1	$\alpha1(IX)$	COL9A1	115 / 339 / 137
		COL9A2	$\alpha2(IX)$	COL9A2	115 / 339 / 137
		COL9A3	$\alpha3(IX)$	COL9A3	112 / 339 / 137
X	Short Chain	COL10A1	$\alpha1(X)$	COL10A1	463
XI	Fibrillar	COL11A1	$\alpha1(XI)$	COL11A1	1014
		COL11A2	$\alpha2(XI)$	COL11A2	1014
		COL2A1	$\alpha1(II)$		1017
XII	FACIT	COL12A1	$\alpha1(XII)$	COL12A1	103 / 152
XIII	Transmembrane	COL13A1	$\alpha1(XIII)$	COL13A1	95 / 172 / 209
XIV	FACIT	COL14A1	$\alpha1(XIV)$	COL14A1	106 / 149
XV	Multiplexin	COL15A1	$\alpha1(XV)$	COL15A1	577 discontinuous
XVI	FACIT-like	COL16A1	$\alpha1(XVI)$	COL16A1	106 / 422 / 15 / 52 / 138 / 71
XVII	Transmembrane	COL17A1	$\alpha1(XVII)$	COL17A1	918 discontinuous
XVIII	Multiplexin	COL18A1	$\alpha1(XVIII)$	COL18A1	688 discontinuous
XIX	FACIT-like	COL19A1	$\alpha1(XIX)$	COL19A1	70 / 168 / 108 / 224 / 144
XX	FACIT	COL20A1	$\alpha1(XX)$		103 / 155
XXI	FACIT	COL21A1	$\alpha1(XXI)$		112 / 339
XXII	FACIT	COL22A1	$\alpha1(XXII)$		109 / 339 / 234 / 374
XXIII	Transmembrane	COL23A1	$\alpha1(XXIII)$	COL23A1	186 / 75 / 111
XXIV	Fibrillar	COL24A1	$\alpha1(XXIV)$	COL24A1	931
XXV	Transmembrane	COL25A1	$\alpha1(XXV)$	COL25A1	44 / 238 / 189
XXVI	Multiplexin	COL26A1	$\alpha1(XXVI)$		69 / 33
XXVII	Fibrillar	COL27A1	$\alpha1(XXVII)$	COL27A1	997
XXVIII	Multiplexin	COL28A1	$\alpha1(XXVIII)$		96

assembled into a superstructure and/or linked with other ECM components. The

biosynthesis of type I collagen illustrates many of the common features of

collagen biosynthesis. Translation of the mRNAs encoding the procollagen α

chains begins on free ribosomes with the synthesis of an N-terminal signal leader

sequence, which is essential for the efficient targeting of procollagen mRNA to

the ER (Yamada, Mudryj et al. 1983; Gura, Hu et al. 1996). Intracellular ER

processing of the signal sequence and co-translational modifications occur as the

newly synthesizing procollagen α chains elongate (Rojkind 1979; Phillips 1992;

Gura, Hu et al. 1996). Co-translational modifications continue until triple-helix

formation occurs (Phillips 1992). The end result is procollagen molecules

containing hydroxyproline and hydroxylysine residues, which are required for

proper fibril thermal stability and fibril maturation, respectively (Kadler, Hojima et

al. 1988; Brodsky and Ramshaw 1997; Zafarullah, Sieron et al. 1997). The

intracellular ER enzymes responsible for these co-translational modifications are

specific prolyl-hydroxylases and lysyl-hydroxylases. In addition,

glycosyltransferases modify hydroxylysyl residues with carbohydrate adducts

(Phillips 1992; Kietly 1993; Gura, Hu et al. 1996).

After translation has been completed, chain association occurs to form the

different collagen molecules. The assembly of the type I collagen molecule

serves as a model for the complex process of triple-helical folding. It has been

proposed that chain selection begins with the attachment of the cytosol-initiated

signal peptide sequences, such that appropriate nascent procollagen α chains

may be inserted into the ER at a common entry site increasing chain selectivity

efficiency (Kirk, Evans et al. 1987). Chain association and alignment takes place only after the chains are fully elongated, such that folding proceeds in the C- to N-terminal domain direction (Kietly 1993; Alvares, Siddiqui et al. 1999; Byers 2001). Procollagen α chain folding begins with the selective association of C-terminal propeptides for specific procollagen α chains (i.e.: proα1(I) and proα2(I) collagen chains) (Alvares, Siddiqui et al. 1999). The association of procollagen α chains is believed to be initiated by non-covalent interactions between the C-terminal domain propeptides (Kietly 1993). However, once chain selection and association has occurred, the C-termini are stabilized by disulfide bond formation catalyzed by the enzyme protein disulfide isomerase (PDI) (Byers, Click et al. 1975; Wilson, Lees et al. 1998; Hosokawa and Nagata 2000). Afterwards, collagen triple helical chain folding proceeds through a series of events involving nucleation and propagation (Byers 2001; Pace, Kuslich et al. 2001; Xu, Bhate et al. 2002). Once assembled into the triple helical procollagen molecule, all ER co-translational modifications cease and the procollagen molecule is trafficked through the golgi and secreted outside of the cell for extracellular processing and fibril formation.

The next step in collagen biosynthesis is extracellular processing, fibrillogenesis, and fibril maturation. Although the aggregation of collagen molecules into ordered structures is a self-assembly process, factors that control the placement and distributions of collagen fibers in vivo are not well understood

(Meadows, Holmes et al. 2000; Canty and Kadler 2005). Before initiating

fibrillogenesis, specific enzymatic cleavage must occur at the procollagen N- and

C-terminal globular domains, making the collagen molecules insoluble under

physiological conditions. Two specific metalloproteinases (procollagen N-

proteinase and C-proteinase) cleave at specific peptide recognition sites,

allowing the processed fibrils to form tissue specific superstructure aggregates

(Kadler 1995; Bornstein, Walsh et al. 2002; Cabral, Makareeva et al. 2005; Canty

and Kadler 2005).

Lysyl oxidase, an extracellular enzyme, attaches to the collagen fibrils

early during fibrillogenesis (Rucker, Kosonen et al. 1998; Hornstra, Birge et al.

2003). This is an important extracellular processing step in which covalent

crosslinks form via adjacent collagen molecules. These crosslinks form at

specific lysyl and hydroxylysyl residues and are essential in providing the tensile

strength and mechanical stability to collagen fibrils present in tissues ECM

(Bailey, Paul et al. 1998; Knott and Bailey 1998). The crosslinking process is

spontaneous except for the initial step in which lysyl oxidase deaminates

telopeptide lysine and hydroxylysine residues (Bailey, Paul et al. 1998; Rucker,

Kosonen et al. 1998; Hornstra, Birge et al. 2003). The two major mature

crosslinks formed from this process are lysyl-pyridinoline, primarily formed in

skin, cornea, and sclera; and hydroxylysl-pyridinoline, primarily found in bone,

cartilage, ligaments, tendons, embryonic skin, and internal tissues (Bailey, Paul

et al. 1998). Studies related to inherited connective tissue disease (i.e.: cutis

laxa), acquired copper nutritional deficiency, copper transport defect (i.e.:

menkes), and lathyrism (i.e.: β-aminopropionitrile (BAPN) ingestion) demonstrate the importance of collagen crosslinking in determining proper tissue function (Oxlund, Andreassen et al. 1984; Yeowell and Pinnell 1993; Murakami, Kodama et al. 2002).

Type I Collagen

Type I collagen is a fibrillar collagen and the most abundant ubiquitous collagen in the body.   The organization of fibrillar collagen genes is similar and have been shown to be evolutionarily conserved, made up of 52 exons of which 42 comprise the triple helical region (Phillips 1992). Exons 6 and 48 are transition exons containing both triple helical and non-triple helical coding sequences (Phillips 1992). Type I collagen is long (300nm) rod-like molecules that self-assemble in a parallel, quarter-staggered, end over-lap arrangement, exhibiting a characteristic banding pattern, readily visualized by electron microscopy (Figure 1.1) (Kietly 1993; Brodsky and Ramshaw 1997).

The regulation of type I collagen gene expression is critically important. COL1A1 and COL1A2 genes are located on separate chromosomes, 17 and 7, respectively, and proα1(I) to proα2(I) are coordinately regulated in a 2:1 ratio, respectively (Prockop, Kadler et al. 1988; Phillips 1992; Slack, Liska et al. 1993; Hata 1995). In addition to coordinated expression, there are several levels of collagen regulation such as transcriptional elements, pretranslational mRNA
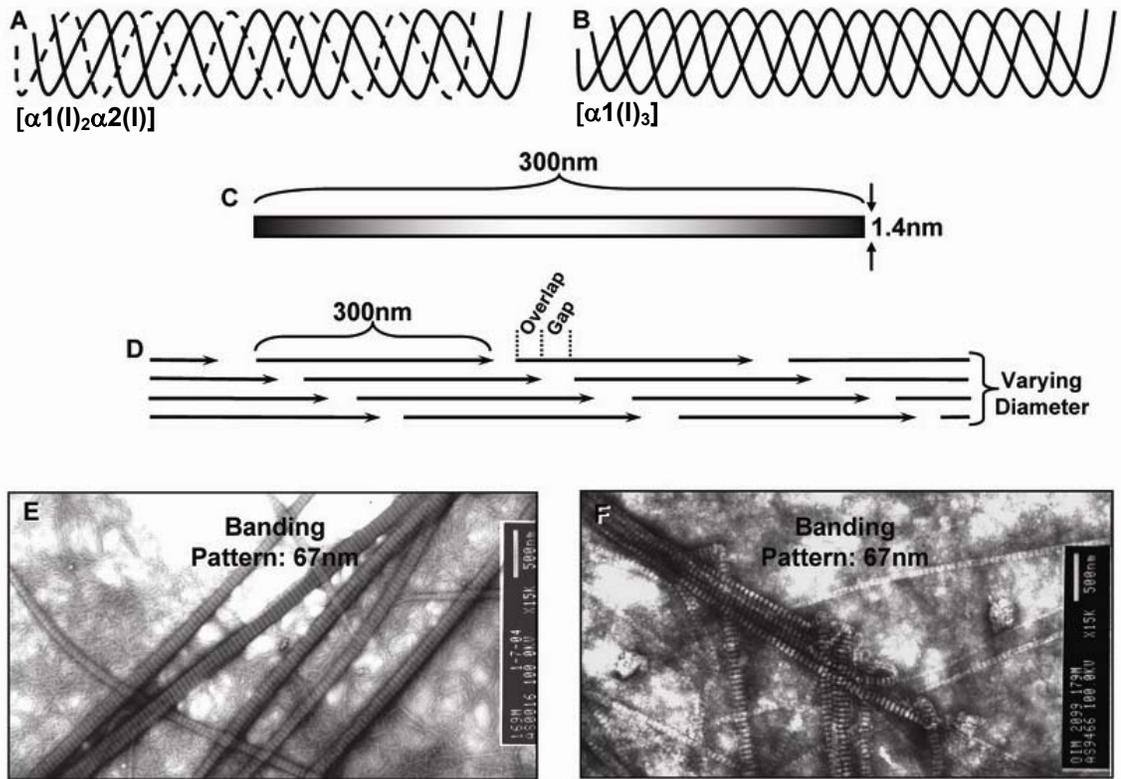
Figure 1.1 Collagen Fibril Schematic. Schematic of type I collagen illustrating the differences in heterotrimeric (A) and homotrimeric (B) collagen molecules. Three procollagen α chains assemble into a rod-like structure (C). The collagen fibrils self-assemble in the extracellular matrix in a staggered arrangement (D), giving rise the the characteristic collagen banding pattern by transmission electron microscopy (EM) (E & F). (E) is an EM of wildtype mouse type I collagen fibrils reconstituted from tail tendon collagen, and (F) is an of *oim* mouse type I collagen fibrils reconstituted from tail tendon collagen. Mangification is 1500X.

arrest, and posttranslational degradation (Byers 2001; Schwarze, Hata et al. 2004). Although type I collagen generally occurs as the heterotrimer $[\alpha1(I)_2,\alpha2(I)_1]$, low amounts of homotrimeric type I collagen are present in tissues; especially embryonically, in normal skin, at sites of wound healing, and during disease processes (Jimenez, Bashey et al. 1977; Uitto 1979; Rupard, Dimari et al. 1988; Kietly 1993). Homotrimeric type I collagen incorporates a third proα1(I) collagen chain instead of a proα2(I) collagen chain. Incorporating three proα1(I) chains to form the homotrimeric type I collagen isotype occurs at a much slower rate and requires a higher concentration of proα1(I) chains than that used in the formation of the heterotrimeric type I collagen isotype (Kadler, Hojima et al. 1987; McBride, Kadler et al. 1992). The difference between heterotrimeric and homotrimeric type I collagen are minor. Homotrimeric type I collagen molecules display an elevated 3-hydroxyproline content and additional lysyl/hydroxylysyl residues (McBride, Kadler et al. 1992). These modifications may confer greater fibril thermal stability and facilitate additional intermolecular collagen crosslinking, increasing the stability and tensile strength of various connective tissues (Hall and Reed 1957; Berg and Prockop 1973; Miles, Burjanadze et al. 1995; Bailey, Paul et al. 1998). Our interest in studying type I collagen focuses on the proα2 (I) collagen chain and its role in determining thoracic aorta integrity.

Thoracic Aortic Integrity

Multicellular organisms depend upon their circulatory system for survival; this requires proper vessel wall integrity throughout an organism's life span. The function of the thoracic aorta is to offer minimal resistance to blood flow by accommodating the ejected stroke volume from the heart and provide continuous blood flow to the body during diastole (Guyton and Hall 2000). The thoracic aorta has the ability to fulfill this function because of the aortic wall's composition (Fung 1993; Dobrin 1997). The thoracic aortic components that make distension possible are collagen, elastin, and smooth muscle cells (SMCs); these components work together to make the thoracic aortic wall strong, compliant, and reactive to continually oscillating blood pressures (Fung 1993; Dobrin 1997).

The basic architecture of blood vessels consists of three layers: the intima, media, and adventitia (Fung 1993; Dobrin 1997). The arteries, capillaries, and veins differ in the amounts of collagens, elastin, and SMCs present within each layer (Fung 1993). The intima is the innermost layer, composed of endothelial cells and basement membrane type IV collagen (Fung 1993; Dobrin 1997). The media is the middle layer and contains SMCs, elastin, and fibrillar collagens types I, III, V (Fung 1993; Dobrin 1997). SMCs exert active "force generated contractions" resulting in vasoconstriction via neural and humoral mechanisms (Dobrin 1997). Although SMCs constitute approximately 34% of the thoracic aorta, they are more abundant, nearly 61%, in medium-sized arteries and arterioles (Fung 1993; Dobrin 1997). However, the SMC component of the

thoracic aorta has a less significant influence over aortic wall strength and stiffness than that of collagen and elastin (Fung 1993).

Elastin and collagen are the passive components of the thoracic aorta, and each significantly influences aortic and large artery integrity (Fung 1993; Dobrin 1997). Elastin and collagen constitute 24% and 37% of the medial thoracic aortic layer, respectively (Fung 1993; Dobrin 1997). The adventitia layer, the outermost layer, is composed mainly of collagen and proteoglycans (Fung 1993; Dobrin 1997). Collagen fibers constitute 78% of the advential thoracic aorta layer, while elastin either has no or a minor presence in the adventitia (Fung 1993; Dobrin 1997). The ability of collagen to sustain an applied load depends on the orientation of its fibers. Collagen fibrils provide little strength in longitudinal extension or torsion of the vessel, but do exhibit high tensile strength in a vessel's diameter, termed circumferential extension. In addition to collagen fibril orientation, collagen fibril diameters also impact aortic wall integrity. As a general rule, increases in collagen fibril diameter increases tissue stiffness. Proteoglycan components are localized to the media and adventitia layers and have a role in viscoelastic properties correlating to tissue hydration; this does not significantly influence aortic strength and stiffness (Fung 1993; Dobrin 1997). In addition to differing aortic ECM components, the amount of ECM components significantly influences aortic wall integrity. The ratio of collagen to elastin increases as the aortic distance from the heart increases; thus, an increased collagen:elastin ratio in the descending thoracic aorta

correlates with a stiffer or less compliant aortic wall as compared to the ascending thoracic aorta (Fung 1993; Dobrin 1997).

To assess aortic wall integrity, we can examine stress/load-strain/extension curves. Vascular tissue does not obey Hooke's law—i.e., they do not show a linear stress/load-strain/extension relationship (Fung 1993; Fung 1993). Instead, vascular tissue demonstrates a nonlinear stress/load-strain/extension relationships, apparent by hysteresis loops and relaxation under constant strain studies (Figure 1.2) (Fung 1993; Fung 1993). This occurs because aortic integrity is determined by several components, i.e.: elastin and collagens (Fung 1993; Fung 1993). The primary collagens that determine aortic integrity are collagens type I, III, and V (Fung 1993).

It is critical to specify the directionality of the aortic wall extension because ECM components contribute to aortic integrity in different directions. Distention and deformation of blood vessel walls occurs in three orthogonal directions: circumferential, longitudinal, and radial (Fung 1993; Dobrin 1997). Enzyme degradation studies have previous demonstrated the contribution of collagen and elastin in each orthogonal direction (Dobrin, Baker et al. 1984; Dobrin and Canfield 1984; Fung 1993; Dobrin 1997). Elastin exerts a force in all three orthogonal directions and contributes to aortic wall compliance (extensibility), while collagen exerts a force mainly in the circumferential direction and contributes to aortic wall stiffness (Dobrin 1997). Collagen is inherently less compliant than elastin because of its rod-like molecular structure (Fung 1993; Dobrin 1997; Fratzl 1997). As physiological pressures and aortic diameter

14
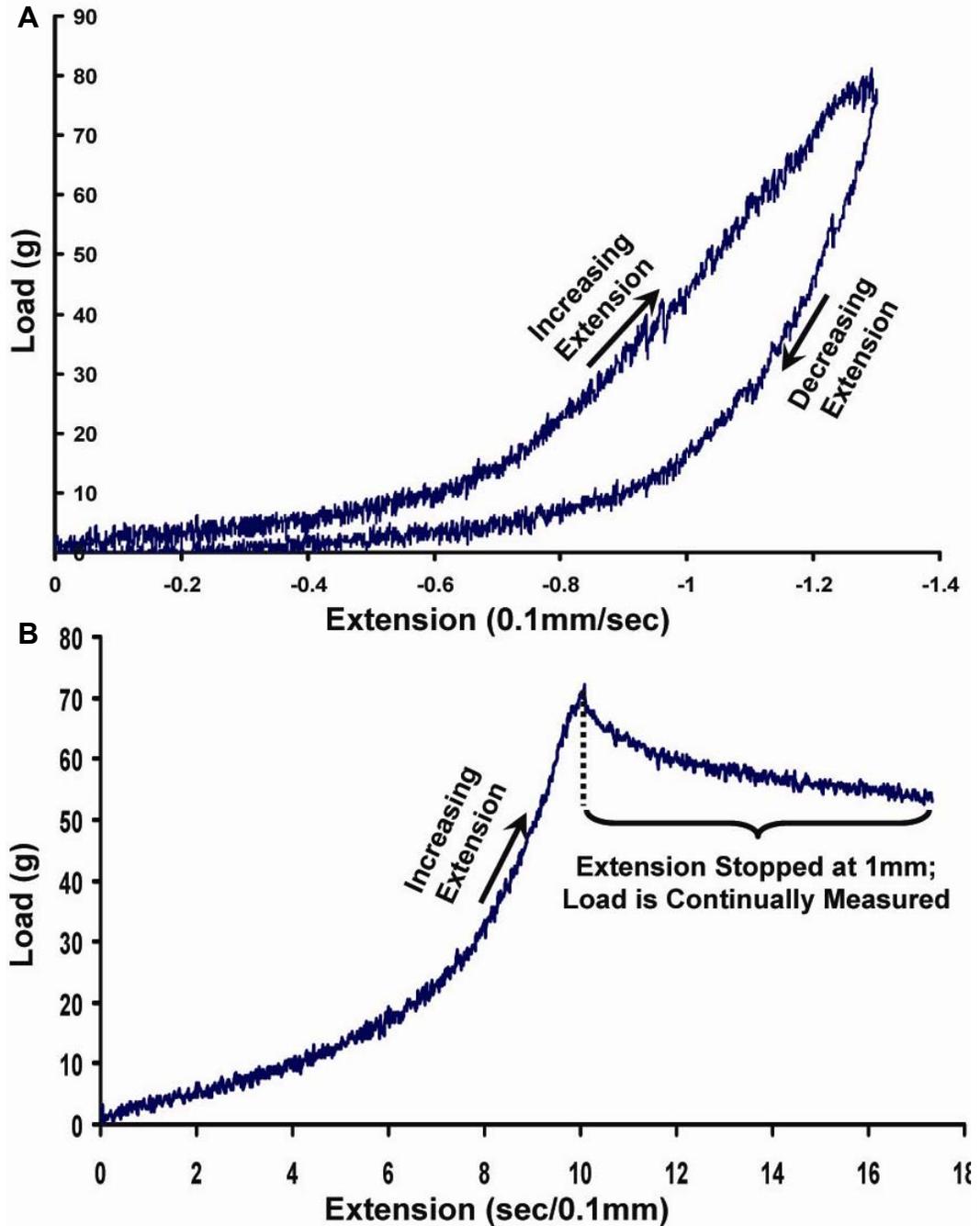
Figure 1.2 Load-Extension Curves. Load-extension curves of mouse thoracic aortas demonstrating extension at a constant speed recording load as either a function of distance (A) or time (B). (A) is an example of a hysteresis loop demonstrating difference in relaxation of the thoracic aorta post extension. (B) is an example of stress-relaxtion via a creep curve. Both curves allow for the calculation of viscoelastic properties of the thoracic aorta.

increase (> 100 mm Hg), elastin lamella are fully extended and collagen fibrils

must be recruited to manage the excess load of increasing pressure and aortic

diameter (Fung 1993; Dobrin 1997).

Quantitative aspects of describing thoracic aorta mechanical properties in

terms of the contribution from collagen will be limited to the circumferential and

longitudinal directions. An assumption must be made when mathematically

describing blood vessel mechanical properties. The assumption is that

equilibrium exists between the distending force and the reaction of the vessel

wall that opposes the distending force. This is known as Pascal's principle. At

equilibrium, the distending force is equivalent to the reactive force of the vessel

wall and thus resembles LaPlace's Law:

$$\sigma = P_T \times r/h$$

where σ is the stress on the vessel wall, P_T is the transmural pressure, r is the

radius of the vessel, and h is the wall thickness. For the purpose of

simplification, we may treat the blood vessel wall as an infinitely thin wall

distending axisymmetrically in the circumferential and longitudinal directions.

This simplifies the σ (stress) to Laplace's law:

$$T = P \times r$$

where T is wall tension, P is pressure, and r is radius. However, blood vessels

are subjected to changes in pressure and increases or decreases in diameter or

distension. This is denoted as deformation, and is quantitated either by strain or

extension ratio:

$$(strain)\ \varepsilon = (D-D_o)/\ D_o$$

$$\text{(extension ratio)} \ \lambda = D / D_o$$

where ε is the strain, λ is the extension ratio, D is the diameter after deformation, and D_o is the diameter before deformation. The relationship between strain and the extension ratio is:

$$\lambda = \varepsilon + 1$$

As the deformation of the blood vessel wall occurs via the distending force, the blood vessel wall exerts an increasing reactive force until equilibrium is achieved; therefore, the relationship between deformation and stress may be calculated:

$$E = \sigma/\varepsilon \ \text{ or } \ E = \sigma/\lambda$$

where E is the elastic modulus, a measure of stiffness. Because of the nonlinear stress-strain or stress-extension relationship of blood vessel walls, we are unable to calculate the overall elastic modulus of a blood vessel. However, the tangential elastic modulus or incremental elastic modulus more accurately depicts blood vessel stiffness at particular areas of the curve; this is shown in (Figures 1.2 and 1.3).

We assessed aortic integrity by load-extension curves comparing aortic breaking strength and high-degree extension stiffness. The purpose of this study is to addresses the role in which proα2(I) collagen chains and/or presence of homotrimeric type I collagen molecules influence thoracic aortic wall integrity and examine age-associated alterations in the presence and absence of heterotrimeric and homotrimeric the type I collagen molecules.
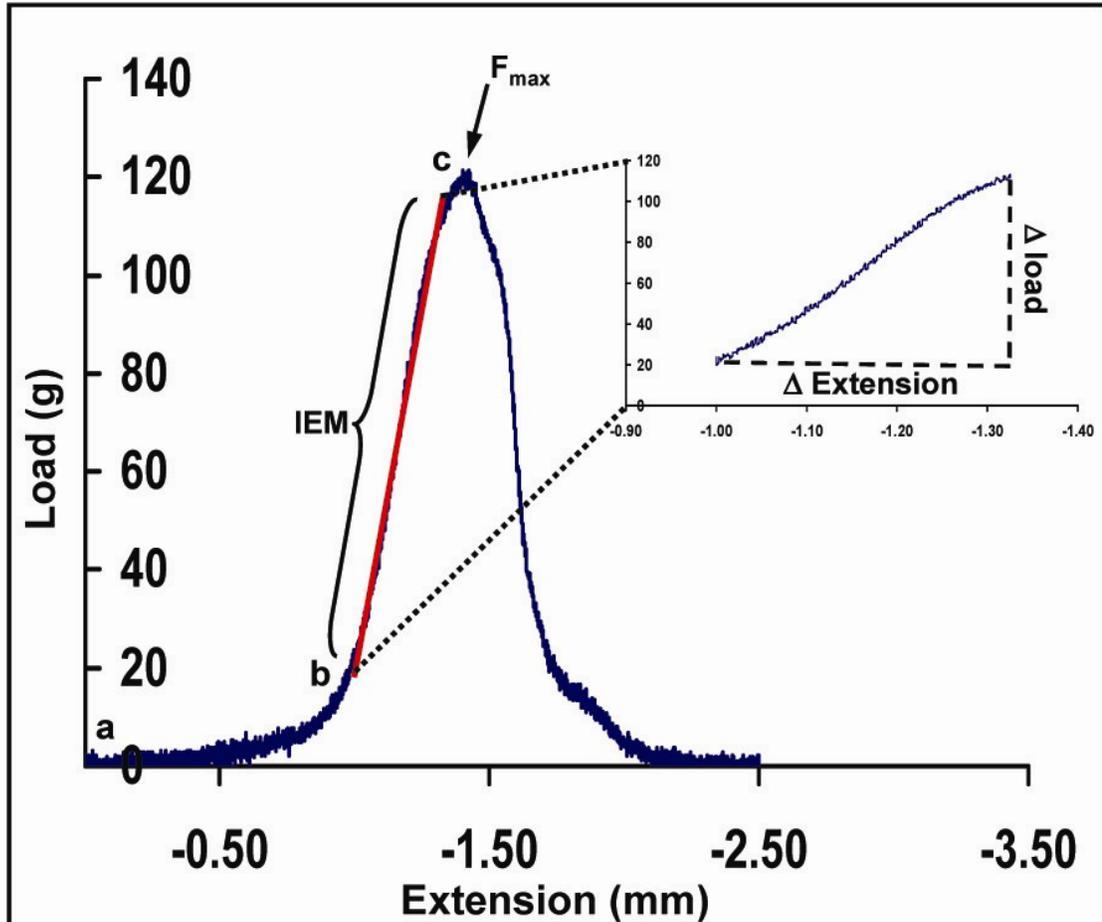
Figure 1.3 Strain-Stress Curve. A strain-stress curve demonstrating the non-linear relationship of blood vessels during load-extension studies. This graph is a circumferential load-extension curve obtained from a wildtype mouse descending thoracic aorta. The 'ab' segment represents low degree extension; elastin handles most of the load at this range of extension. The 'bc' segment represents high degree extension (1.5-2.0X the initial aortic diameter); collagen handles most of the load at this range of extension. The arrow indicating F_{max} represents the failure point of the aorta and is the vessels maximum strength. The inset is the linear analysis and best-fit line of segment 'bc'. This allows us to calculate the incremental elastic modulus (IEM = Δ load/ Δ extension) at high degree extension and compare the contribution of collagen molecules in determining aortic stiffness.

18

Mechanisms of Aging

Age-associated increases in aortic stiffness alter the hemodynamic parameter of blood pressure and function of the aorta, which is a risk factor for cardiovascular morbidity and mortality (Simon and Levenson 1991; Franklin 1999). Many factors influence aortic/arterial stiffness, such as physiology (age, gender, etc.), environment (nutrition, smoking, etc), and disease states (hypertension, atherosclerosis, diabetes, and inherited disorders) (Simon and Levenson 1991; Himmelmann, Hedner et al. 1998; Franklin 1999). However, in normal and disease populations, the primary predictors of aortic/arterial stiffness are age and blood pressure. Current epidemiological studies demonstrate that increased arterial stiffness, a reflection of elevated pulse pressure (increased systolic blood pressure without increased diastolic blood pressure), is a reliable predictor of cardiovascular disease (Glasser, Arnett et al. 1997; Franklin 1999). However, it is controversial whether the relationship between increased arterial stiffness associated with aging reflects a predisposition to the development of cardiovascular disease or a consequence of already established cardiovascular disease process. This ambiguity underscores the importance of understanding age-associated changes in vascular tissue.

Age-related changes in collagen reflect altered physical properties in many tissues, and these changes of collagen and elastin properties are potentially deleterious to vascular function (Figure 1.4). The formation of collagen crosslinks have been demonstrated to be important for proper tissue
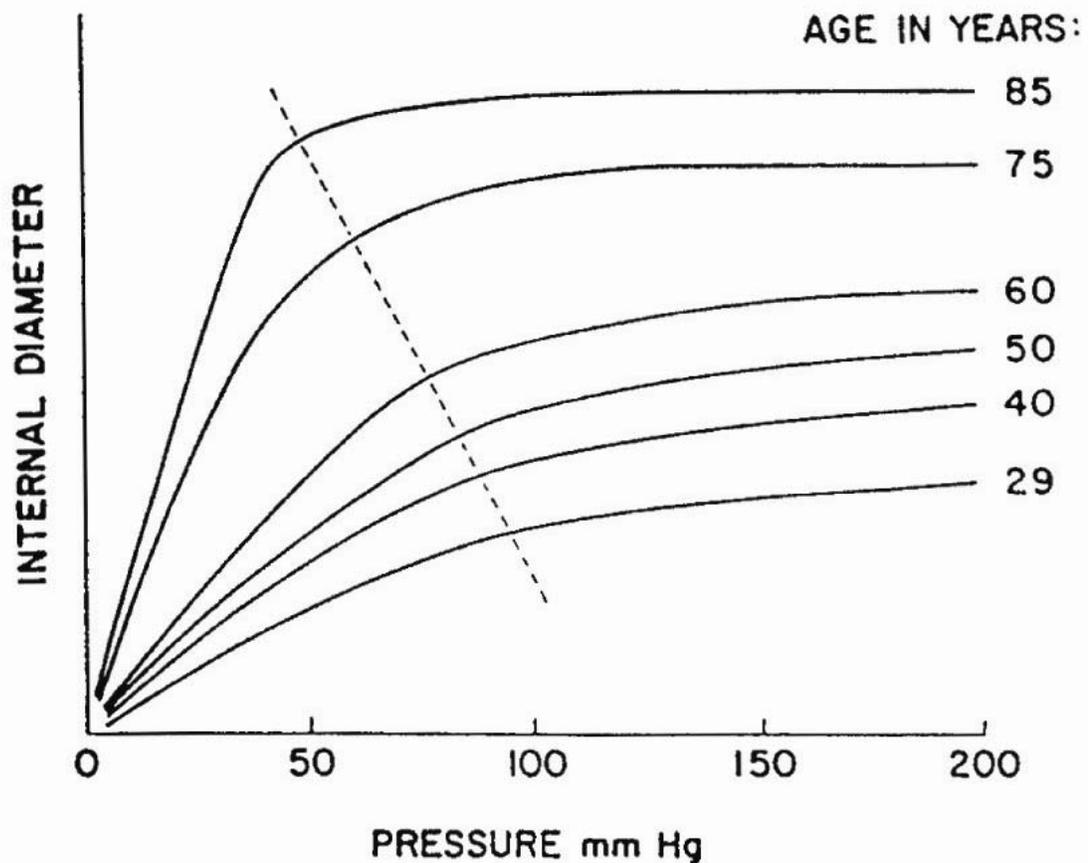
Figure 1.4 Pressure-Diameter Curves. Pressure-diameter curves of thoracic aortas of humans from ages 29 to 85 years of age, reconstructed data from Bader *et al* (Bader 1967). With age the aorta dilates, stiffening the elastin fibers causing collagen to handle more of the forces transmitted to the aortic wall. This results in increasing vessel stiffness at progressively lower blood pressures. The broken line demonstrates the transition from compliant to stiff vessels. There is a shift to lower blood pressures associated with aging. This figure is from Dobrin Physiology and Pathophysiology of Blood Vessels. In: The Basic Science of Vascular Disease (1997): pp 69 – 105.

structure/function and in aging (Vogel 1978; Spina, Garbisa et al. 1983; Bailey, Paul et al. 1998). Crosslinking involves two different mechanisms; one is a precise enzymatically initiated event during tissue maturation and the other is a non-enzymatic event known as glycation (Bailey, Paul et al. 1998).

In many tissues, the lysyl oxidase-initiated crosslinks form immature divalent crosslinks, which mature over time forming trivalent pyridinoline crosslinks demonstrated to be important for proper tissue function (Bailey, Paul et al. 1998). Bruel *et al.* demonstrated in rats that pyridinoline crosslinks contribute to aortic tissue tensile strength (Bruel and Oxlund 1996; Bruel, Ortoft et al. 1998). However, the number of mature lysyl oxidase-initiated crosslinks plateaus with age, rather than increasing in a linear manner, making pyridinoline crosslinks less likely to be responsible for age-associated increases in thoracic aortic stiffness. This has been observed in human and rat aging studies (Reiser 1994; Bruel, Ortoft et al. 1998).

Glycation-derived crosslinks, termed advanced glycation end-products (AGE), have been positively correlated in a linear manner with increasing amounts and age (Reiser 1991; Bailey, Paul et al. 1998). AGE are hypothesized to play a central role in the deleterious affects of joint and vascular tissue stiffness (Reiser 1991; Bailey, Paul et al. 1998). Nonenzymatic AGE crosslinks occur on ECM molecules and are derived from carbohydrate adducts. The nonenzymatic glycosylation of ECM proteins has been of interest since the association of poor diabetes mellitus outcomes correlating with increased amounts of glycosylated hemoglobin (Reiser 1991; Reiser 1998). All long-lived

ECM proteins are susceptible to carbohydrate groups reacting with the free amino group of lysine, hydroxylysine, or arginine residues. The addition of carbohydrate adducts involves a Maillard reaction-- the chemical reaction of a carbohydrate aldehyde or ketone with a free amino group of an amino acid-- to form a Schiff base (Reiser, McCormick et al. 1992; Bailey, Paul et al. 1998; Reiser 1998). The Schiff base then may undergo a rearrangement forming a stable ketoamine (an Amadori product), which may undergo condensation to form an AGE (Bailey, Paul et al. 1998). The occurrence and accumulation of these groups on stable low-turnover macromolecules has received considerable attention (Reiser, McCormick et al. 1992; Bailey, Paul et al. 1998).

A current hypothesis is that AGE modifications are responsible for the normal aging of tissues. During aging, changes occur in the collagenous framework. These changes alter the physical properties of collagen fibers and are reflected by the well-documented increases in stiffness found in skin, tendon, bone, joints, and vascular tissue (Reiser, McCormick et al. 1992; Reiser 1994; Bruel and Oxlund 1996; Bailey, Paul et al. 1998; Reiser 1998). Such changes are deleterious to the optimal functioning of an organ system. Changes in the tissue composition of collagen vary during development, disease processes, and often with increased age (Peleg, Greenfeld et al. 1993; Autio, Risteli et al. 1994; Dumas, Chaudagne et al. 1996; DeBacker, Putterman et al. 1998; de Souza 2002). Bruel *et al.* observed increased aortic stiffness in old rats, relative to young and adult rats, positively correlating increased AGE product formation with collagen molecules (Bruel and Oxlund 1996). Studies have yet to address or

identify whether a particular type I collagen domain is important for AGE modification or whether there is a predominant vascular AGE crosslink (Reiser, Amigable et al. 1992).

In addition to ECM crosslinking, changes in ECM composition also alter tissue properties. An example of this is the type III collagen content in embryonic dermis compared to post-natal dermis; postnatally, type III collagen is dramatically decreased correlating with an increase in skin stiffness (Bailey, Paul et al. 1998). This illustrates important temporal and spatial regulation of collagen genes and gene products and that tissue ECM components are constantly remodeled. The rate of collagen metabolism varies substantially with maturation and senescence, although the overall turnover rate is comparatively slow. Collagen synthesis decreases steadily with maturation and drops by approximately 10-fold in most tissues with aging (Bailey, Paul et al. 1998). In order to understand the mechanism of age-related changes, it is essential to 1) understand the role of collagen in determining the mechanical properties of tissues, 2) understand the changes in the crosslinking as it relates to mechanical properties, 3) understand the role of collagen types comprising the ECM connective tissue, and 4) understand changes in the activity or collagen type expression of cells during the aging process.

Inherited Connective Tissue Disorders

The primary components of the aortic wall, elastin and collagen, have been shown to be critical in disorders affecting vascular physiology (Ju and Dixon 1996; Dobrin 1997; Bailey, Paul et al. 1998; Arteaga-Solis, Gayraud et al. 2000). Abnormalities in the biosynthesis and structure of vascular components such as elastin, fibrillin, or collagen are known to cause cardiovascular pathologies, such as supravalvular aortic stenosis, Marfan syndrome, and various Ehlers-Danlos Syndrome (EDS) types (Yeowell and Pinnell 1993; Ju and Dixon 1996; Chowdhury and Reardon 1999; Arteaga-Solis, Gayraud et al. 2000). Much has been elucidated concerning the pathogenesis of elastin and fibrillin defects in cardiovascular function, whereas the impact by which collagen abnormalities influence mineralized and non-mineralized tissues, especially cardiovascular function, are largely undefined.

EDS represents a heterogeneous group of connective tissue disorders classified into types, such as hypermobility, classical, vascular, arthrochalasia, dermatosparaxis, and kyphoscoliosis (Yeowell and Pinnell 1993; Pope and Burrows 1997). Certain types of EDS demonstrate severe cardiovascular complications. These various EDS types are associated with defects in different collagen types or collagen co-translational enzymes. EDS type VI (Kyphoscoliosis Type) patients exhibit vascular fragility, resulting from deficiencies in lysyl hydroxylase, an enzyme which is crucial to collagen co-translational processing, causing a decrease in the amount of hydroxylysine

residues, which are essential for tissue specific intermolecular cross-linking (Yeowell and Pinnell 1993; Walker, Overstreet et al. 2004). Many EDS type VI patients have cardiovascular complications, including mitral valve prolapse, arterial aneurysms, and arterial dissections (Yeowell and Pinnell 1993; Walker, Overstreet et al. 2004). EDS type IV (Vascular Type) is caused by a molecular defect in type III collagen, which predisposes affected individuals to medium sized arterial rupture and provides clear evidence for the importance of type III collagen in determining arterial wall integrity (Yeowell and Pinnell 1993). Type III collagen is hypothesized to impart arterial wall compliance; however, studies have yet to confirm this hypothesis. Type V collagen, a minor constituent of vascular collagens, has been shown to impact fibrillogenesis and play a role in the regulation of type I collagen fibril diameter (Marchant, Hahn et al. 1996; Michalickova, Susic et al. 1998; Schwarze, Atkinson et al. 2000; Wenstrup, Florer et al. 2004; Wenstrup, Florer et al. 2004). Mutations in type V collagen have been shown to be responsible for EDS type I (Classical type) (Yeowell and Pinnell 1993; Wenstrup, Florer et al. 2000; Wenstrup, Florer et al. 2004; Wenstrup, Florer et al. 2004). EDS type I individuals often have valvular problems, specifically mitral valve prolapse (Yeowell and Pinnell 1993; Schwarze, Atkinson et al. 2000; Wenstrup, Florer et al. 2000; Wenstrup, Florer et al. 2004; Wenstrup, Florer et al. 2004). These and other studies emphasize the significant role of collagens in determining cardiovascular integrity via abnormalities in collagen biosynthesis, fibril assembly, and/or cross-linking.

Osteogenesis imperfecta (OI) is a heritable disorder of connective tissue characterized by type I collagen mutations primarily affecting mineralized tissue (i.e.: bone) and is classified into four types (I-V) based upon mode of inheritance and severity of skeletal, ocular, otologic, and dental abnormalities (Byers 2001; Byers 2001). The molecular defects responsible for causing OI are mutations in the proα1(I) or proα2(I) collagen chains (Byers 2001). Individuals with OI demonstrate varying degrees of bone involvement resulting in 'brittle bones' and an increased propensity for fractures. However, orthopedic problems associated with OI often overshadows possible extra-skeletal manifestations of type I collagen defects, since type I collagen is such a ubiquitous protein in the body (Byers 2001). Several case reports describing OI patients with cardiovascular dysfunction, as well as investigations into extra-skeletal complications associated with OI, have been reported since the 1980's (Hortop, Tsipouras et al. 1986; Kalath, Tsipouras et al. 1987; Sasaki, Arai et al. 1987; Wheeler, Cooley et al. 1988; Vetter, Maierhofer et al. 1989; Wong, Follis et al. 1995). Four studies examined OI populations to determine the prevalence of cardiovascular dysfunction (Hortop, Tsipouras et al. 1986; Kalath, Tsipouras et al. 1987; Wheeler, Cooley et al. 1988; Vetter, Maierhofer et al. 1989). In particular, Hortop *et al.* found aortic root dilatation in 12% in the OI population studied (Hortop, Tsipouras et al. 1986). Vetter *et al.* examined 58 children with OI types I, III, and IV finding that type III individuals exhibit aortic diameter enlargement (28%), septal thickening (40%) and left ventricular hypertrophy (68%) as compared to age-matched normal controls (Vetter, Maierhofer et al. 1989). However, these

studies examined heterogeneous OI populations, and because of the genetic and phenotypic heterogeneity of OI, it is unclear how and which type I collagen mutations may have affected cardiovascular integrity.

The purpose of this work is to determine the role of proα2(I) collagen chains in aortic integrity by studying a mouse model in which proα2(I) collagen chains are absent and only homotrimeric type I collagen molecules are present. Patients with the connective tissue disorders EDS and OI have been identified who exhibit proα2(I) collagen mutations and only form homotrimeric type I collagen molecules. In addition, this emphasizes important differences in clinical phenotypes EDS or OI based upon the cellular mechanism of proα2(I) collagen chain production. Two unrelated patients with EDS type I/II (Classical type) have been reported presenting with valvular dysfunction requiring surgical correction (Sasaki, Arai et al. 1987; Hata, Kurata et al. 1988) . Cultured skin fibroblast from these two patients demonstrated an absence of the proα2(I) collagen chain from type I collagen molecules. Recently, a series of EDS patients with cardiovascular valvular dysfunction were described by Schwarze *et al.* who had COL1A2 splicing mutations activating a nonsense-mediated RNA decay pathway resulting in the complete absence of proα2(I) collagen expression (Schwarze, Hata et al. 2004). A few reported cases of OI have demonstrated proα2(I) collagen chain absence (Pihlajaniemi, Dickson et al. 1984; Deak, van der Rest et al. 1985; Nicholls, Valler et al. 2001). In contrast to the nonsense-mediated RNA decay, these patients synthesize mutant proα2(I) collagen chains, but do not incorporate the mutant proα2(I) chains into the type I collagen molecule. This is

27

similar to the molecular defect in our mouse model, which is classified as a model for OI.

The *Oim* (Osteogenesis Imperfecta Murine) Model

The *oim* (osteogenesis imperfecta mouse) model was used in this study because of its naturally occurring spontaneous mutation in its COL1A2 collagen gene. A single nucleotide deletion in the COL1A2 gene results in a frameshift at the proα2(I) C-terminal domain, altering the last 48 amino acids, preventing the proα2(I) C-terminal domain association with the proα1(I) C-terminal domain (Chipman, Sweet et al. 1993; McBride and Shapiro 1994). Because of this defect, *oim* mice homozygous for the mutation do not synthesize functional proα2(I) collagen chains and are unable to form normal heterotrimeric type I collagen molecules. Instead they synthesize homotrimeric type I collagen molecules [α1(I)$_3$] (Chipman, Sweet et al. 1993). Homozygous *oim* mice have biochemical and phenotypic features similar to moderately severe nonlethal OI type III in humans, and heterozygous mice exhibit features similar to mild OI (Chipman, Sweet et al. 1993; Saban, Zussman et al. 1996). The structural/biomechanical properties of homotrimeric type I collagen molecules in *oim* mouse bone and tendon have been the focus of several laboratories. Their studies have demonstrated reduced biomechanical properties in these tissues, as well as altered mineral crystal size/content and reduced lateral packing of

fibrils (Camacho, Landis et al. 1996; McBride, Choe et al. 1997; Phillips, Bradley et al. 2000).

Goals of the Study

The *oim* mouse provides opportunities to investigate the role of proα2(I) collagen chains in mineralized and non-mineralized tissues and how this type I collagen chain influences structure/function. The objective of this study is to investigate the impact the absence of the α2(I) collagen chain from type I collagen molecules and/or presence of homotrimeric type I collagen molecules has on thoracic aortic integrity. In this study, we begin to elucidate the causative and/or contributory role of type I collagen defects in the development of vascular disease. In addition to understanding how the matrix architecture is impacted by the absence of the proα2(I) collagen chains from type I collagen molecules, the *oim* mouse promises to be a more generalized model for other proα2(I) collagen chain defects or polymorphisms, which may alter aortic integrity. We initially demonstrated that *oim* mice had significantly reduced thoracic aortic integrity without gross morphological alterations of other thoracic aortic components (Chapter II). Next we refined the biomechanical and biochemical assays by determining thoracic aortic integrity at a specified young age (3 months); in addition, we determined collagen characteristics such as collagen content and collagen crosslinking, which are known to contribute to aortic integrity (Chapter

III). Finally, we completed this study by examining *oim*, heterozygote, and wildtype mouse aortas at young, adult, and old age (3, 8 and 18 months, respectively). We assayed aortas for aortic integrity, collagen content, pretranslational ECM mRNA steady-state levels, and collagen specific and non-specific crosslinking (Chapter IV). In addition, we addressed the issue of age-associated alterations of aortic integrity, collagen content, collagen crosslinking, and ECM mRNA steady-state expression. This was done to determine important collagen characteristics that may affect aortic integrity.

The findings of this study demonstrate that the absence of $\alpha2(I)$ collagen chains from type I collagen and/or presence of homotrimeric type I collagen molecules in *oim* and heterozygote thoracic aortas is responsible for reduced aortic strength and stiffness, which cannot be attributed to reduced collagen content alone. We also demonstrated increased pyridinoline crosslinks/collagen molecule in oim thoracic aortas, a mechanism potentially compensating for altered biomechanical parameters. The increased pyridinoline may reflect altered fibril alignment and packing, which may influence fibril integrity and ultimately aortic strength and stiffness. In terms of age-associated changes, pyridinoline crosslinks/collagen molecule ratios did not significantly change with increasing age and do not account for the increased aortic integrity observed in 18 month old aortas. However, evidence of advanced glycation end-product crosslinking formation was demonstrated and may be the major contributor of increased aortic strength and stiffness in 18 month old aortas.

CHAPTER II

THE ROLE OF TYPE I COLLAGEN IN AORTIC WALL STRENGTH USING A HOMOTRIMERIC [α1(I)]$_3$ COLLAGEN MOUSE MODEL

Introduction

Elastin and collagen are the primary extracellular matrix components of

the aortic wall, providing the integrity to withstand the outward forces exerted by

arterial pressure (Nichols 1990; Dobrin 1997)(1,2). These elements make up

approximately 50% of the dry weight of normal arteries (Nichols 1990). The

dominant component in the thoracic aorta is elastin (approximately 60%),

whereas the composition is reversed in the abdominal aorta (70% collagen)

(Nichols 1990). Arterial collagen is comprised predominantly of type I and type III

(Morton and Barnes 1982).

The normal type I collagen isotype is a heterotrimeric molecule, composed

of two α1(I) chains and one similar, but genetically distinct α2(I) chain (Byers,

Marini et al. 1995; Phillips CL 1997). The homotrimeric type I collagen isotype,

composed of three α1(I) chains was originally discovered in certain tumors and

cultured cancer cell lines (Moro and Smith 1977; Rupard, Dimari et al. 1988;

Ghersi, La Fiura et al. 1989). Since then, homotrimeric type I collagen has been

shown to naturally occur at low levels in normal adult skin, during embryonic

development, and wound healing (Jimenez, Bashey et al. 1977; Uitto 1979; Kay

1986). Homotrimeric type I collagen has also been associated with certain forms

of Ehlers-Danlos syndrome (EDS) (Sasaki, Arai et al. 1987; Hata, Kurata et al.

1988; Kojima, Shinkai et al. 1988) and osteogenesis imperfecta (OI) (Nicholls,

Osse et al. 1984; Pihlajaniemi, Dickson et al. 1984).

Altered elastin content and structure have been implicated in the formation

of abdominal aortic aneurysms (Sumner, Hokanson et al. 1970; Dobrin 1997).

Since the tensile strength of collagen (1.0×10^9 N/m^2) is approximately 1000 times

greater than that of elastin (4.6×10^5 N/m^2), defects in collagen should alter

vascular integrity and contribute to aneurysmal development (Clark and Glagov

1985). Defects in type III collagen, responsible for EDS type IV, are strongly

associated with aortic aneurysmal degeneration (Byers 1996; Pope and Burrows

1997; Beighton, De Paepe et al. 1998). However, the role of type I collagen in

aortic wall integrity and aneurysmal development remains to be elucidated. The

objective of this study was to investigate the impact of the absence of the $\alpha 2$(I)

collagen chain and/or presence of homotrimeric type I collagen [$\alpha 1$(I)]$_3$ on the

biomechanical properties of the thoracic aorta and to begin to elucidate the

causative and/or contributory role of type I collagen defects and polymorphisms

in the development of vascular disease.

Material and Methods

Animals

Mice who were homozygous for the homotrimeric type I collagen

(*oim/oim*), heterozygous mice (*oim/+*), and wildtype mice (+/+) were purchased

from Jackson Laboratory (Bar Harbor, ME). Additional +/+ mice (B6C3Fe a/a)

were purchased to serve as additional control animals: the *oim* mutation is

maintained in the B6C3Fe a/a background (Chipman, Sweet et al. 1993). All
animals were housed in an AALAC approved facility, provided free access to
water and food (standard laboratory diet: autoclavable rodent laboratory chow,
5010, Purina Mills Inc., Richmond, Indiana), and handled according to an
approved protocol and the approved regulations of the facility. *Oim/oim, oim/+
and +/+* genotype was confirmed by polymerase chain reaction - restriction
fragment length polymorphism (PCR-RFLP) analysis (Phillips, Bradley et al.
2000). Mice (4-7 months old) were euthanized with CO_2 asphyxiation for
biomechanical and histological analyses.

Preparation of the aortic segments

Aortas were harvested using a Weck operating microscope with lens
magnification x 15. The chest of the animals was opened via median sternotomy
and the thoracic aorta was dissected from the surrounding adipose tissue, and
harvested from the aortic root to the diaphragmatic crurae. For circumferential
analyses, two 5mm long aortic rings were prepared: a proximal ring including
aortic root and aortic arch, and a distal aortic ring including the descending aorta
just below the take off of the left subclavian artery. A pair of 0.5-mm diameter
stainless steel hooks was inserted in each aortic ring. For longitudinal analyses,
the whole segment of the descending aorta from the left subclavian artery to the
diaphragm was excised for use in the longitudinal extension analyses. The

infrarenal aorta was not analyzed due to its decreased size (less than 5 mm in length and less than 1mm in diameter).

Biomechanical studies

To obtain circumferential load-extension curves, each aortic ring was attached to an TA-XT2 texture analyzer (tensile testing apparatus) (Texture Technologies, Corp., Scarsdale NY), placed in Krebs solution bath at room temperature (24 $\pm$1°C), and stretched at a constant tensile speed of 0.1 mm/s (Figure 2.1). During the aortic ring extension [length (l, mm)] the required tensile load [Force (F, g)] was recorded at 0.01 second intervals. The maximal tensile load (F_{max}) is the greatest load (force) prior to vessel breakage (Figure 2.1, value indicated by C). As the aortic segment is deformed by tensile load, the wall exerts an increasing reactive force aiming to a final equilibrium. Stiffness of the aortic ring results from the relationship between deformation (extension) and tensile load, and can be expressed as:

$$E=f/l$$

where E is the elastic modulus, f is the tensile load, and l is the extension. Due to the non-linear relationship, the incremental elastic modulus (IEM=$\Delta f/\Delta l$) was used to compare the stiffness of the aortic segments among the genotypes. The IEM was calculated as the ratio of the incremental load (g) to the incremental
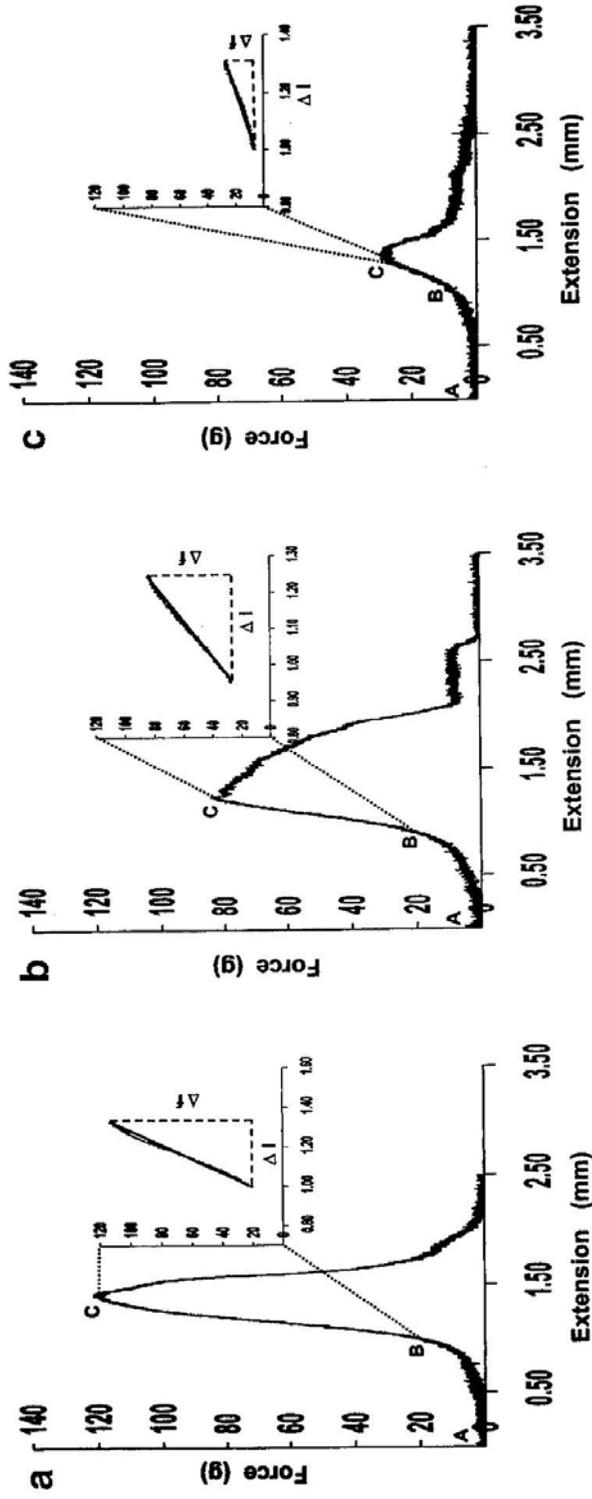
Figure 2.1 Circumferential Load-Extension Curves. Representative circumferential load-extension curves obtained from the descending aortic rings of wildtype (+/+; a), heterozygote (*oim*/+;b), and homozygous (*oim*/*oim*; c) mice. The AB segment represents low-degree extension, and the BC segment represents high-degree extension (1.5-2 x initial aortic diameter). Incremental elastic modulus was calculated from slope of BC segment, IEM = df/dl. Inset is linear analysis and best-fit line of segment BC. Figure is from Vouyouka, *et al*. J Vasc Surg 2001; 33, 6: 1263-70

36

extension (mm). The IEM was estimated by performing a linear regression analysis on each load-extension curve. Best-fit lines were obtained at low and high (1.5x to 2 x diameter) degrees of extension in the aortic rings. Elastin bears most of the load at low degrees of extension, whereas collagen bears most of the load at higher degrees. The slope of the regression line at high degrees of extension was used to estimate the IEM, since this is the region where differences in collagen structure are observed.   IEM and F_{max} values were standardized to dry mass weight of the respective aortic sample (mg). In the longitudinal direction, aortic segments of the whole descending aorta were extended at 0.1 mm/s along the longitudinal axis (axial stretching) and the F_{max} and the IEM determined. Figure 2.2 represents schematically the TA-XT2 texture analyzer used for the aortic tissue extension.

Hydroxyproline assay

The hydroxyproline content was used to determine the total amount of collagen in the aortic wall. Hydroxyproline represents 20-30% of the amino acids of mature collagen molecules (Kietly 1993). Following load-extension curve analyses, the aortic tissue was dried, weighed, and the total hydroxyproline content determined by a colorimetric assay (based on the oxidation of hydroxyproline to a compound which reacts with *p*-dimethylaminobenzaldehyde to form a chromophore) established by Stegemann and Stadler (Stegemann and Stalder 1967).
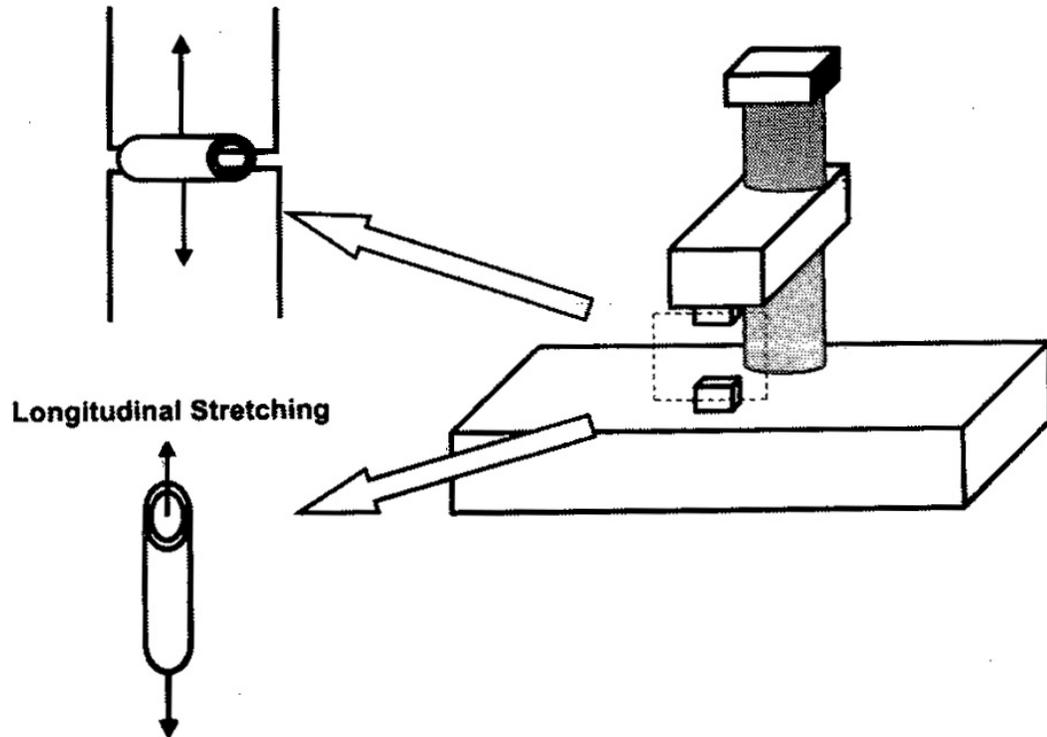
Figure 2.2 Schematic of TA-XT2 Texture Analyzer. Schematic representation of TA-XT2 texture analyzer system used for load-extension studies of the aortic samples. The TA-XT2 is a computer-controlled system that regulates the speed of extension (0.1mm/s) and measures the loading force (in grams) for each extension point (in millimeters). For circumferential extension analyses, a pair of stainless steel 0.5-mm hooks were threaded into aortic rings and secured to the TA96 system clamps. For longitudinal extension analyses, aortic segments were secured in the TA96 clamps directly. Figure is from Vouyouka, *et al*. J Vasc Surg 2001; 33, 6: 1263-70

Histological Analysis

Aortic sections were harvested for histological and morphological analyses from 2 *oim/oim* and 3 +/+ mice. Aortas were perfused at 112 mmHg, a pressure that mimics the normal *oim/oim* mouse systolic pressure as determined by tail cuff plethysmography. Perfusion was performed through the left ventricle with 0.9% NaCl (2 min) followed by neutral buffered 10% formalin fixation (3 min). Aortas were then harvested and processed for histological examination. Transverse sections were collected from the aortic arch, proximal descending thoracic aorta, and from the proximal abdominal aorta. Five micron sections of each aorta were stained with 1) hematoxylin and eosin to qualitatively assess cell number and morphology, 2) picrosirius red to assess collagen, and 3) Verhoff's-Van Gieson to assess elastin.

Statistical analysis

Differences in F_{max} and IEM between *oim/oim, oim/+* and +/+ were evaluated using analysis of variance, as well as by analysis of covariance with age as the covariant. Statistical significance was defined as $P < .05$.

Results

Six *oim/oim*, eight *oim/+*, and six *+/+* mice were sacrificed for the

circumferential analyses. The mean body weights of the *+/+*, *oim/+*, and *oim/oim*

mice were 25.0 ± 2.1 g, 26.3 ± 2.6 g, and 20.8 ± 2.1g, respectively. Though

oim/oim mice weighed 21% and 17% less than the *oim/+* (P=.001) and *+/+*

(P=.02) mice, there appeared to be no differences in aortic diameters or lengths.

Biomechanical studies

Representative circumferential load extension curves for the descending

aortic rings are depicted in Figure 2.1. Complete disruption of vessels was noted

at ring extensions that were 1.5 to 2 times the initial diameters for all genotypes

(indicated by the F_{max} value of C). As demonstrated by Figure 2.1, the curves

were nonlinear. At low degrees of stretch, small load increments resulted in

large size deformation (segment AB in the curve). At high degrees of ring

extension (1.3 to 2 times the diameter of the ring) where collagen bears most of

the load, the same load increments resulted in much smaller deformation

(segment BC). Linear regression analysis of the segment BC leads to the best fit

line (inset of Figure 2.1 a, b, and c), which was used to estimate the IEM.

Figure 2.3 summarizes the results from the load-extension curves

obtained from circumferential extension of the ascending aortas.

Circumferentially, the maximum tensile load (F_{max}) of the *oim/oim* ascending

aorta (132 ± 42 g/mg) was significantly reduced as compared to the F_{max} of the

Circumferential Extension of the Ascending Aorta
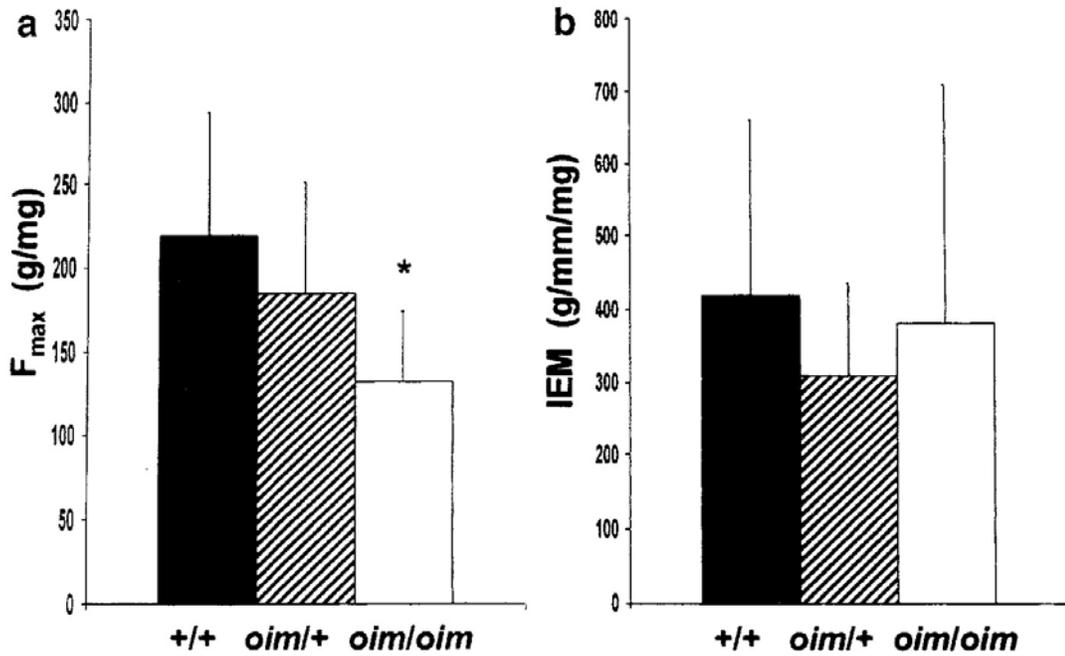
Figure 2.3 Circumferential F$_{max}$ and IEM of Ascending Aoratas. Circumferential maximum breaking strength (F$_{max}$; a) and incremental elastic modulus (IEM; b) of the ascending aorta of wildtype (+/+; n=6; black bar), heterozygote (*oim*/+;n=8; diagonal bar), and homozygous (*oim*/*oim*; n=6; open bar) mice. Values are expressed as the mean ± SD in grams (F$_{max}$) and grams per millimeter (IEM) per milligram of dried aortic tissue. * P ≤0.05. Figure is from Vouyouka, *et al*. J Vasc Surg 2001; 33, 6: 1263-70

+/+ ascending aorta (219 $\pm$ 75 g/mg, P=.04). The heterozygous mice

demonstrated intermediate values for F_{max} (185 $\pm$ 66 g/mg), although the results

were not significantly different from the *oim/oim* or +/+ groups (Figure 2.3 a).

When the stiffness of the ascending aorta was evaluated, the IEM of *oim/oim*

(IEM=379 $\pm$ 332 g/mg/mm), *oim/+* (IEM=309 $\pm$126 g/mg/mm), and +/+ (IEM= 417

$\pm$ 244 g/mg/mm) mice were not statistically different. However, there was a trend

for the *oim/oim* and *oim/+* aortas to be more extensible (lower IEM values) as

compared to +/+ ascending aortas (Figure 2.3 b).

In contrast, circumferential extension of the descending aortas

demonstrated significant differences in both the breaking strength and stiffness

between *oim/oim, oim/+*, and +/+ mice (Figure 2.4). The maximal load (F_{max})

required to circumferentially disrupt the distal aortic ring of +/+ mice was 447 $\pm$

124 g/mg, whereas the F_{max} of *oim/+* and *oim/oim* mice descending thoracic

aortas were 242 $\pm$ 112 g/mg (P= .002) and 103 $\pm$ 42 g/mg (P= .001), respectively

(Figure 2.4 a). Similarly, the +/+ mice had stiffer (less extensible) distal aortic

rings (IEM 788 $\pm$ 128 g/mg/mm) as compared to *oim/+* (486 $\pm$ 271 g/mg/mm, P=

.01) and *oim/oim* (188 $\pm$ 70 g/mg/mm, P= .0001) mice. (Figure 2.4 b)

Longitudinal extension studies of the descending thoracic aortas were

performed in five *oim/oim*, three *oim/+*, and seven +/+ mice. The F_{max} of the +/+

mice (41.7 $\pm$ 13.5 g/mm/mg) was significantly greater as compared to the

oim/oim (16.4 $\pm$ 8.5 g/mg, P=.003) and *oim/+* mice (13.11 $\pm$ 5.2 g/mg, P=.017)

(Figure 2.5 a). However, no significant difference was noted in the longitudinal

extensibility (IEM) of the +/+ descending aorta (10.7 $\pm$ 1.4 g/mm/mg) as

# Circumferential Extension of the Descending Aorta
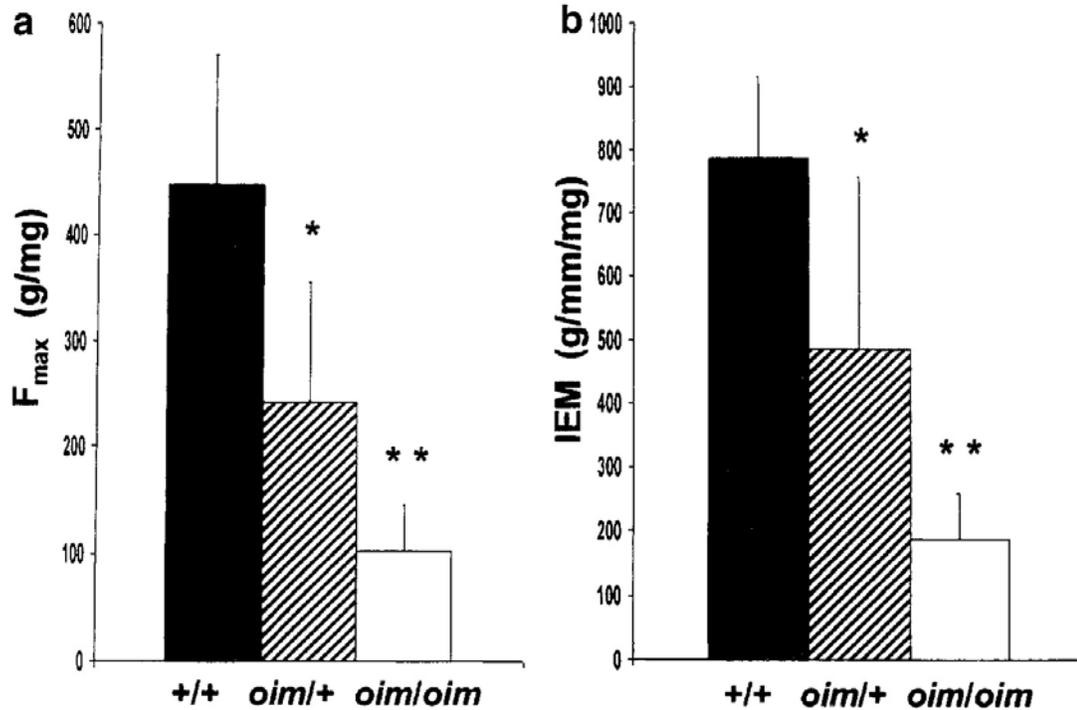
Figure 2.4 Circumferential F_{max} and IEM of Descending Aoratas. Circumferential maximum breaking strength (F_{max}; a) and incremental elastic modulus (IEM; b) of the descending aorta of wildtype (+/+; n=6; black bar), heterozygote (*oim*/+;n=8; diagonal bar), and homozygous (*oim*/*oim*; n=6; open bar) mice. Values are expressed as the mean ± SD in grams (F_{max}) and grams per millimeter (IEM) per milligram of dried aortic tissue. * P ≤0.01; ** P ≤0.001. Figure is from Vouyouka, *et al*. J Vasc Surg 2001; 33, 6: 1263-70

compared to the *oim/oim* descending aorta (9.8 ± 3.3 g/mm/mg, P= .512) (Figure

2.5 b). Interestingly, the IEM of the *oim/+* (5.9 ± 1.6 g/mm/mg) did appear

different from +/+ (P= .034), but the real significance of this is unclear and may

reflect in part the small sample number of *oim/+* (n=3).

Hydroxyproline assay

Hydroxyproline content (a measure of total collagen) was measured in six +/+,

three *oim/+*, and four *oim/oim* mice. There were no significant differences in the

amount of total collagen present in the descending thoracic aortas of the +/+

(13.5 ± 3.8 μg collagen/mg dry tissue), *oim/+* (12.0 ± 1.6 μg/mg), and *oim/oim*

(12.3 ± 3.0 μg/mg) mice. This suggests that the altered biomechanical properties

may not simply reflect quantitative differences in total collagen, but reflect more

qualitative alterations in the fibrillar organization and architecture.

Histological Analysis

Preliminary histological evaluation of the descending thoracic aorta was

performed in two *oim/oim* and three wild-type (+/+) mice (Figure 2.6). Though

only a limited number of animals were examined histologically, examination of

hematoxylin and eosin stained sections suggested there were no lesions or

major differences in cell numbers. Furthermore, there appeared to be no major

differences in aortic wall thickness or diameter between *oim/oim* and +/+ mouse

Longitudinal Extension of the Descending Aorta
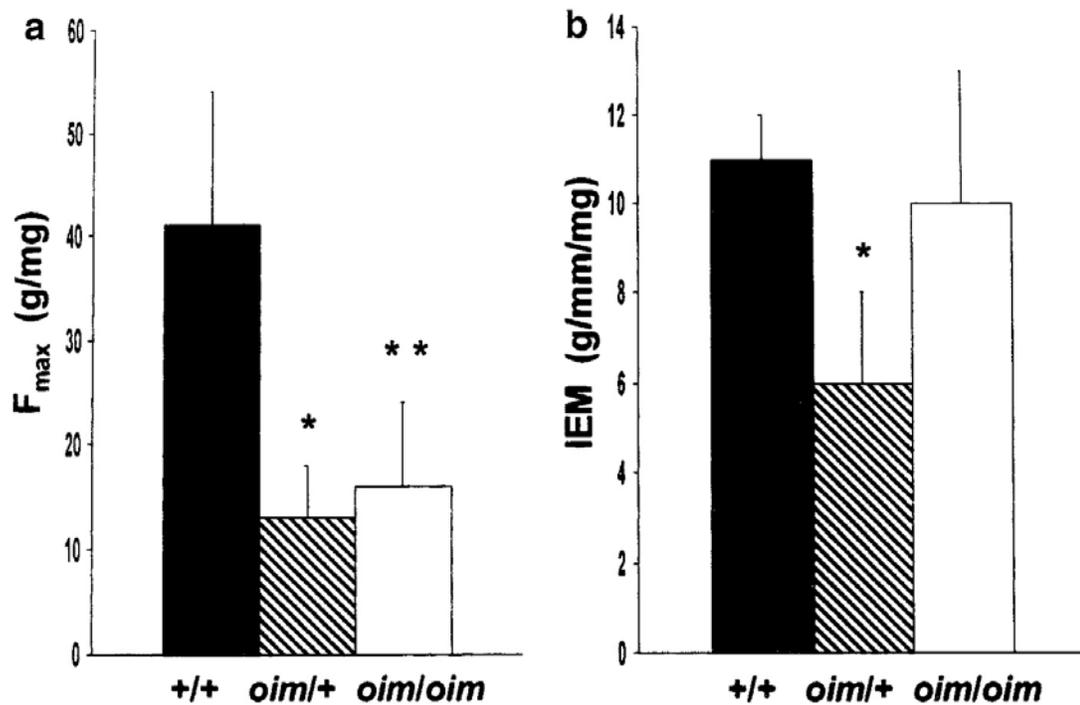
Figure 2.5 Longitudinal F_{max} and IEM of Descending Aoratas. Longitudinal maximum breaking strength (F_{max}; a) and incremental elastic modulus (IEM; b) of the descending aorta of wildtype (+/+; n=7; black bar), heterozygote (*oim*/+;n=3; diagonal bar), and homozygous (*oim*/*oim*; n=5; open bar) mice. Values are expressed as the mean ± SD in grams (F_{max}) and grams per millimeter (IEM) per milligram of dried aortic tissue. * P ≤0.05; ** P ≤0.003. Figure is from Vouyouka, *et al*. J Vasc Surg 2001; 33, 6: 1263-70
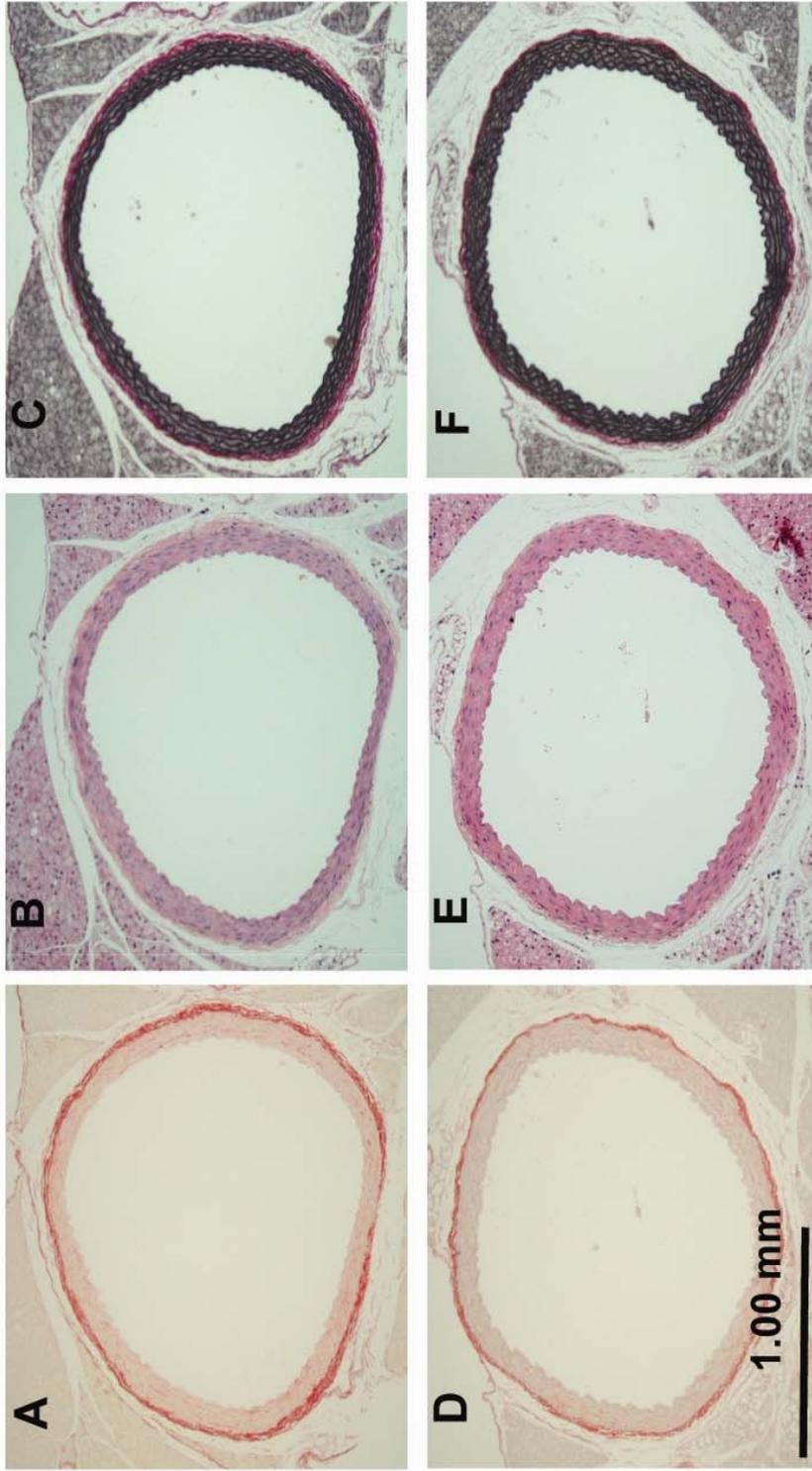
Figure 2.6 Histology of Thoracic Aortas. Histology of media thoracic aortic sections of 7-month-old wildtype (+/+; A,B,C) and homozygous (*oim/oim*; D,E,F) mice stained with picrosirius red (A,D), hematoxylin and eosin (B,E), and Verhoff-van Gieson (C,F); original magnification at 10X. Figure is from Vouyouka, *et al*. J Vasc Surg 2001; 33, 6: 1263-

aortas. In addition, there were no obvious histological abnormalities or differences in the lamellar or elastin organization between *oim/oim* and *+/+* mouse aortas.

Discussion

We present evidence that the thoracic aorta of the *oim/oim* mouse exhibits decreased breaking strength and greater extensibility in the absence of proα2(I) collagen chains and/or the presence of the homotrimeric type I collagen isotype. The most pronounced biomechanical differences were seen with circumferential extension of the descending aorta. The average breaking strength (F_{max}) circumferentially in the descending *oim/oim* mouse aorta was only 23% of the F_{max} in *+/+* (wildtype) mouse aorta. Similarly, the *oim/oim* mouse descending aorta had an IEM which was 24% of the value in *+/+* mouse aorta. Interestingly, the differences were not as dramatic during circumferential extension of the ascending aorta. Overall, the circumferential F_{max} of the ascending aorta (range 132 to 219 g/mg) was much lower than the F_{max} of the descending aorta (range 242 to 447 g/mg). The circumferential F_{max} of the ascending *oim/oim* aorta was approximately 60% of the value in the *+/+* aorta. These findings are consistent with our understanding that collagen and elastin bear the majority of the wall stress and determine the stiffness (compliance) of the aorta (2). With increasing distance of the vessel from the heart, the elastin content is known to decrease

and the collagen content to increase, with a net result of higher collagen to elastin ratios (Dobrin, Baker et al. 1984; Clark and Glagov 1985).

The aorta is an "elastic artery" and subsequently its media is composed of layers of smooth muscle cells interspersed with clearly defined lamellae of connective tissue. These lamellar units, composed predominantly of elastin and collagen lying in parallel, represent the functional and structural unit of the aortic wall that responds to pressure and tangential stress and are responsible for the passive mechanical properties of the vessel (Nichols 1990; Dobrin 1997). Several studies suggest that elastin determines the aortic compliance at low physiologic pressures, and that collagen progressively takes over load-bearing at higher pressures (Krafka 1940; Greene, Friedlander et al. 1966; Matsumura, Kawazoye et al. 1995; Dobrin 1997). Accordingly, aortic stiffness also progressively increases from the ascending and descending thoracic aorta to the abdominal aorta (Clark and Glagov 1985).

In addition, the aortic wall is anisotropic, having different mechanical properties in the three orthogonal directions: circumferential, longitudinal, and radial (Dobrin 1997). Enzymatic degradation studies demonstrated that elastin bears the load in all three directions, where as collagen bears the load almost exclusively in the circumferential direction, and smooth muscle cells do not significantly contribute directly to the passive "static" biomechanical properties of the aortic wall (Roach 1957; Dobrin, Baker et al. 1984; Dobrin and Canfield 1984; Bank, Wang et al. 1996; MacLean, Dudek et al. 1999). During the longitudinal stretching all the aortic samples, regardless of mouse genotype, demonstrated

much lower breaking strength (range 13 to 42 g/mg) and higher extensibility (range 6 to 11 g/mm/mg) than when they were stretched circumferentially. These findings are also consistent with the anisotropic nature of the aortic wall. Moreover, the longitudinal extension showed no differences in the stiffness of the aorta in *oim/oim* and *+/+* animals, which is also consistent with the decreased role of collagen along the longitudinal axis. However, to our surprise there was still a significant difference in F_{max} longitudinally between the genotypes, suggesting type I collagen does influence indirectly or directly the biomechanical properties along the longitudinal axis. One can easily postulate that deposits of the homotrimeric type I collagen isotype and/or the absence of the proα2(I) collagen chain may alter the fibrillar structure and architecture of the collagen fibrils as well as influence the structure and function of the other components of the lamellar units.

In addition, we found no significant differences in total collagen content or the morphological structure/organization of the aorta of *oim/oim* and *+/+* mice, suggesting that the absolute amount of collagen is not the only factor, which determines arterial wall strength. Further suggesting that the ultrastructural collagen composition and organization of the aortic wall must play a significant role.

It is quite likely that all three components, elastin and types I and III collagen, contribute to the ultimate structural integrity of the aorta. We postulate that a structural defect in any one or more of these components increases the load-bearing on the other components of the aortic wall, and thus, making the

49

vascular wall more susceptible to fatigue and failure. There is a great deal of

clinical evidence from the pathogenesis of certain connective tissue disorders,

which support this hypothesis. Ehlers Danlos Syndrome (EDS) types IV and VI

result from defects affecting type III and I collagens, respectively, and are

strongly associated with decreased arterial wall integrity and cardiovascular

deficits, including mitral valve prolapse, multiple arterial ruptures, and aortic

dissections (Wenstrup, Murad et al. 1989; Byers 1996; Pope and Burrows 1997;

Beighton, De Paepe et al. 1998). Two unrelated individuals with classical EDS

(EDS type I/II) have been previously described who synthesize only homotrimeric

type I collagen, and are biochemically similar to the *oim* mouse (Chipman, Sweet

et al. 1993) and certain recessive forms of human type III OI (Nicholls, Osse et

al. 1984; Pihlajaniemi, Dickson et al. 1984). Both individuals had cardiovascular

complications, a grade IV aortic regurgitation and severe mitral valve prolapse

(Sasaki, Arai et al. 1987; Hata, Kurata et al. 1988; Kojima, Shinkai et al. 1988).

However no data was presented regarding the integrity of their aortas. The

significance of our findings with the *oim* mouse aortas in the clinical course of

patients with aortic aneurysmal disease or with type I collagen deficiencies is yet

to be determined. The cardiovascular complications of OI, particularly in relation

to aortic diseases have not been well characterized. Only a handful of cases of

spontaneous aortic dissection directly related to osteogenesis imperfecta are

reported in literature (Ashraf, Shaukat et al. 1993; Moriyama, Nishida et al. 1995;

Cusimano 1996; Isotalo, Guindi et al. 1999). Vetter evaluated cardiovascular

function in 58 patients with types I, III and IV OI, and determined that patients

with OI type III were more likely to exhibit elastic aortas (Vetter, Maierhofer et al.

1989).   It is difficult to make any direct clinical correlation with the *oim/oim*

mouse, though it is clinically most similar to type III OI, since its molecular defect

is relatively rare (autosomal recessive inheritance of a functionally null COL1A2

gene), with only a few reported human cases (Nicholls, Osse et al. 1984;

Pihlajaniemi, Dickson et al. 1984).

Deficiencies in elastin and collagen have also been implicated in the

pathogenesis of aneurysmal degeneration in patients *without* Marfan Syndrome

or EDS (Sumner, Hokanson et al. 1970; Menashi, Campa et al. 1987; Powell and

Greenhalgh 1989; Baxter, McGee et al. 1992; Dobrin 1997). And although there

is well demonstrated correlation between elastin decrease and aneurysm

formation there still remains a lot of confusion in literature regarding the role of

collagen in aneurysmal aorta: collagen concentrations have been found to be

increased in some studies, decreased or unchanged in others (Sumner,

Hokanson et al. 1970; Thornell, Norrgard et al. 1986; Menashi, Campa et al.

1987; Powell and Greenhalgh 1989; Rizzo, McCarthy et al. 1989; Dobrin 1997).

This study demonstrates the biomechanical consequences of exclusive

expression of homotrimeric type I collagen on the thoracic aorta of the *oim/oim*

mouse and represents a unique model for investigating the role of the

proα2(I)collagen chain in the structure and function of the vasculature and for

defining the mechanisms and tissue specific adaptations to over expression of

the homotrimeric isotype of type I collagen. The *oim* mouse provides a potential

paradox for cardiovascular disease and aging. The increased extensibility of the

oim/oim aorta may protect the *oim/oim* mouse against the development of elevated arterial pressures, yet the *oim/oim* aorta with its significantly reduced breaking strength may also be significantly compromised when subjected to elevated arterial pressures or other vascular stressors. Long term follow up of these animals during aging as well as under cardiovascular stress, using serial ultrasonic imaging of their aortas, analysis of the aortic velocity profile under different conditions of systemic blood pressure, as well as analysis of the ultrastructure of the collagen should significantly contribute to our understanding of the role of the extracellular matrix architecture in vascular function and disease. Finally, the greatest significance of the *oim* mouse model is that it provides a foundation for future studies, in conjunction with other cardiovascular mouse models such as the elastin deficient mouse (Li, Brooke et al. 1998), it will allow for very defined breeding strategies, making it finally possible to systematically evaluate the role of multi-gene interactions in vascular and aneurysmal disease.

CHAPTER III

ALPHA 2(I) COLLAGEN DEFICIENT *OIM* MICE HAVE ALTERED BIOMECHANICAL INTEGRITY, COLLAGEN CONTENT, AND COLLAGEN CROSSLINKING OF THEIR THORACIC AORTA

Introduction

The extracellular matrix (ECM) performs a critical role in organ system development and biomechanical properties (Arteaga-Solis, Gayraud et al.). In this study we explore the vascular biomechanical properties imparted by the $\alpha2(I)$ collagen chain of type I collagen. The ECM is essential to maintain wall integrity while anisotropic forces are acting on it (Dobrin 1997). Vascular ECM components, elastin and collagen, are passive determinants of arterial wall integrity (Dobrin 1997). Elastin primarily contributes to arterial wall compliance (Dobrin 1997; Chowdhury and Reardon 1999; Arteaga-Solis, Gayraud et al. 2000), while collagen primarily contributes to arterial wall strength and stiffness, especially in the circumferential direction at high degrees of extension (Fung 1993; Dobrin 1997; Vouyouka, Pfeiffer et al. 2001). Abnormalities in elastin, fibrillin, or collagen biosynthesis are known to cause cardiovascular pathology including supravalvular aortic stenosis, Marfan syndrome, and Ehlers Danlos syndrome (Chowdhury and Reardon 1999; Arteaga-Solis, Gayraud et al. 2000; Schwarze, Hata et al. 2004). While much is known about the mechanisms and pathogenesis of elastin and fibrillin defects on cardiovascular function, the mechanisms in which collagen abnormalities influence non-mineralized tissues and cardiovascular function are not well understood (Hortop, Tsipouras et al. 1986; Wheeler, Cooley et al. 1988; Vetter, Maierhofer et al. 1989; Chowdhury and Reardon 1999; Arteaga-Solis, Gayraud et al. 2000; Schwarze, Hata et al. 2004). Collagens found in vascular tissues include types I, III, IV, and V, of which types I and III are the vast majority (Fung 1993; Kietly 1993). Types I, III

and V collagen are fibrillar collagens (Fung 1993; Kietly 1993), whereas type IV collagen is a nonfibrillar basement membrane collagen, and appears not to play a significant role in arterial integrity (Fung 1993; Kietly 1993). The primary contributor to aortic wall strength and stiffness is type I collagen (Fung 1993; Dobrin 1997), while type III collagen is believed to contribute to arterial wall compliance (Arteaga-Solis, Gayraud et al. 2000). Type V collagen, a minor constituent however, is hypothesized to have a role in fibrillogenesis and regulation of type I collagen fibril diameter (Marchant, Hahn et al. 1996; Wenstrup, Florer et al. 2004).

The predominant type I collagen isotype normally present in connective tissue is the heterotrimeric molecule composed of two $\alpha 1(I)$ collagen chains and one genetically distinct $\alpha 2(I)$ collagen chain, $[\alpha 1(I)_2 \alpha 2(I)]$ (Phillips 1992; Kietly 1993; Byers 2001). It is presumed that the maintenance of a heterotrimeric molecule has been evolutionarily conserved in higher vertebrates because of its greater stability, particularly to mechanical stress (Exposito, D'Alessio et al. 1992; Miles, Sims et al. 2002). A recent report by Schwartze *et al.* suggests that the $\alpha 2(I)$ collagen chain has a major role in cardiovascular disease (Schwarze, Hata et al. 2004). However, the precise role of the $\alpha 2(I)$ chain in the type I collagen molecule is unknown and remains the subject of great interest.

With the goal of understanding the role of the $\alpha 2(I)$ collagen chain in arterial wall integrity, we examined thoracic aortas from the osteogenesis imperfecta murine (*oim*) model. *Oim* mice produce only the homotrimeric type I collagen isotype composed of three $\alpha 1(I)$ collagen chains, $[\alpha 1(I)_3]$, as a result of

homozygosity for a functional null mutation in the COL1A2 gene (Chipman, Sweet et al. 1993). We previously demonstrated that 4-7 month old *oim* mice, relative to wildtype mice, had reduced thoracic aortic breaking strength and stiffness (Vouyouka, Pfeiffer et al. 2001). This in conjunction with the report by Weis *et al.* of the altered ventricular properties of the *oim* mouse spurred us to investigate whether the reduced vascular biomechanics of the thoracic aorta of *oim* mice are associated with alterations in collagen content and/ or crosslinking (Weis, Emery et al. 2000). Toward this end, we evaluated age-matched three-month-old *oim*, heterozygote, and wildtype mice ascending and descending thoracic aortas histologically, morphometrically, and biochemically to quantitate collagen and collagen crosslinks in relation to their biomechanical properties via circumferential load-extension analyses. The *oim* mouse is an ideal model to examine how homotrimeric type I collagen and/or the absence of the proα2(I) collagen chain impacts aortic integrity, aortic collagen content, and collagen crosslinks. The presence of the homotrimeric isotype of type I collagen during various developmental stages and pathological states suggests a potential physiologically relevant role for homotrimeric type I collagen and regulation of proα2(I) collagen expression to attain appropriate tissue maturation and mechanical integrity during development and/or disease processes (Jimenez, Bashey et al. 1977; Uitto 1979; Rupard, Dimari et al. 1988). We hypothesized that the biomechanical changes associated with the absence of α2(I) collagen chains and /or presence of homotrimeric type I collagen will correlate with altered collagen content and/or crosslinking content.

Materials and Methods

Mice

Heterozygous B6C3Fe-*a/a-Col1a2^{oim}/+* mice were purchased from Jackson Laboratory (Bar Harbor, ME) and bred to produce homozygous *oim* (*oim/oim*), heterozygous (*oim/+*), and wildtype (+/+) mice. All animals were housed in an American Association for Accreditation of Laboratory Animal Care (AAALAC) approved facility, provided free access to water and food (Rodent Laboratory Chow, 5100, Purina Mills, Richmond, IN), and handled according to an approved protocol and regulations for the facility. *Oim*, heterozygous, and wildtype genotypes were confirmed by means of PCR restriction fragment length polymorphism analysis (Phillips, Bradley et al. 2000). Three-month-old mice were euthanized with CO_2 asphyxiation for biomechanical, histological/morphological, and biochemical analyses.

Biomechanical Analysis

Thoracic aortas were dissected, separated into ascending and descending portions, threaded with stainless steel hooks and circumferential load-extension curves were obtained using on a TA-XT2 texture analyzer (Stable MicroSystems, NY), as described previously (Vouyouka, Pfeiffer et al. 2001). Load-extension curves were analyzed for thoracic aortic maximal breaking strength (F_{max}) and

incremental elastic modulus (IEM), as described previously (Vouyouka, Pfeiffer et al. 2001). Following mechanical testing, aortas were delipified and weighed prior to biochemical analyses.

Histological/Morphological Analysis

Aortas from each genotype were perfusion fixed and harvested for histological and morphological studies. Briefly, the right renal vein was cut to prevent fluid overload and the vasculature was perfused via the left ventricle at mouse systolic blood pressure (112 mmHg) with neutral buffered 10% formalin for 3 minutes. Aortas were embedded in paraffin and transverse sections at the ascending, medial descending, and distal descending thoracic portions were prepared. Five-micron sections of each aorta were stained with hematoxylin & eosin for cell numbers, picrosirius red for fibrillar collagens, Verhoff's-van Gieson for elastin, and Alcian Blue pH 1.0 for proteoglycans. Digital images were captured using an Olympus D11 digital camera (Olympus America Inc., NY) attached to a Ziess (Carl Ziess Inc., NY) microscope. Hematoxylin & eosin and picrosirius red images were converted to black and white tiff files in Adobe Photoshop 6.0 (Adobe Systems Incorporated, CA) and these tiff files were used for morphological studies of cell numbers, aortic wall diameter, aortic wall thickness and total fibrillar collagen content using Scion Image (Scion, MD). Fibrillar collagen content was determined using the density slice tool with the threshold set for white values 0-100 measuring the area (mm^2) corresponding to the picrosirius red staining.

Biochemical Analysis

Following biomechanical testing, dried delipified aortic tissue was
evaluated for total collagen content, hydroxylysine/lysine content,
hydroxyproline/proline content, and enzyme initiated collagen crosslink content
(hydroxylysyl-pyridinoline/lysyl-pyridinoline) using reverse phase high
performance liquid chromatography (HPLC), as previously described (Bank,
Beekman et al. 1997; Bank, Bayliss et al. 1998).

Amino Acid analysis of purified α1(I) collagen chains was evaluated using
isolated tail tendon collagen from wildtype, heterozygote, and *oim* mice. Ten
micrograms of collagen from each genotype were loaded onto 5% (2M Urea)
SDS-PAGE gels for alpha chain separation and ran at 40mA in Running Buffer
(192mM Glycine, 25mM Tris, 0.1% SDS, and 2M Urea). Following
electrophoresis the SDS-PAGE gel was equilibrated in Transfer Buffer (20mM
Bicine, 34.6mM Tris, 0.64mM EDTA, and 0.05% SDS) for 5 minutes (repeated 5
times). Collagen alpha chains were transferred by blotting to a BioRad Sequi-
Blot PVDF Membrane (7x8.4 cm) at 200mA for 3 hours at 4°C. The PVDF
membrane was stained with coomassie blue to visualize the collagen alpha
chains, and the α1(I) and α2(I) collagen chains were excised from the membrane
and prepared for amino acid derivitization and analysis, as previously described
(Woodson, Fujita et al. 1991).

Statistical Analysis

Data from each genotype and study were expressed as means $\pm$ standard deviation. Differences between the genotypes were detected by analysis of variance using SAS (SAS Institute Inc., NC) and expressed as p-values.

Results

Histology/Morphometry

Three-month-old *oim*, heterozygote and wildtype thoracic aortas were analyzed for histological and morphometric differences. *Oim* aortas demonstrated a reduction in picrosirius red fibrillar collagen staining relative to wildtype (Figure 3.1 A, C, & E). Though no gross histological differences were found in cell numbers, elastin, or proteoglycan staining between wildtype, heterozygote, and *oim* aortas (data not shown), *oim* and heterozygote descending aortas did exhibit significant reductions in outer diameter (700 $\pm$ 33 and 698 $\pm$ 36 μm, respectively) as compared to wildtype descending aortas (796 $\pm$ 76 μm); a 12% reduction in diameter for both genotypes (Figure 3.2 A).
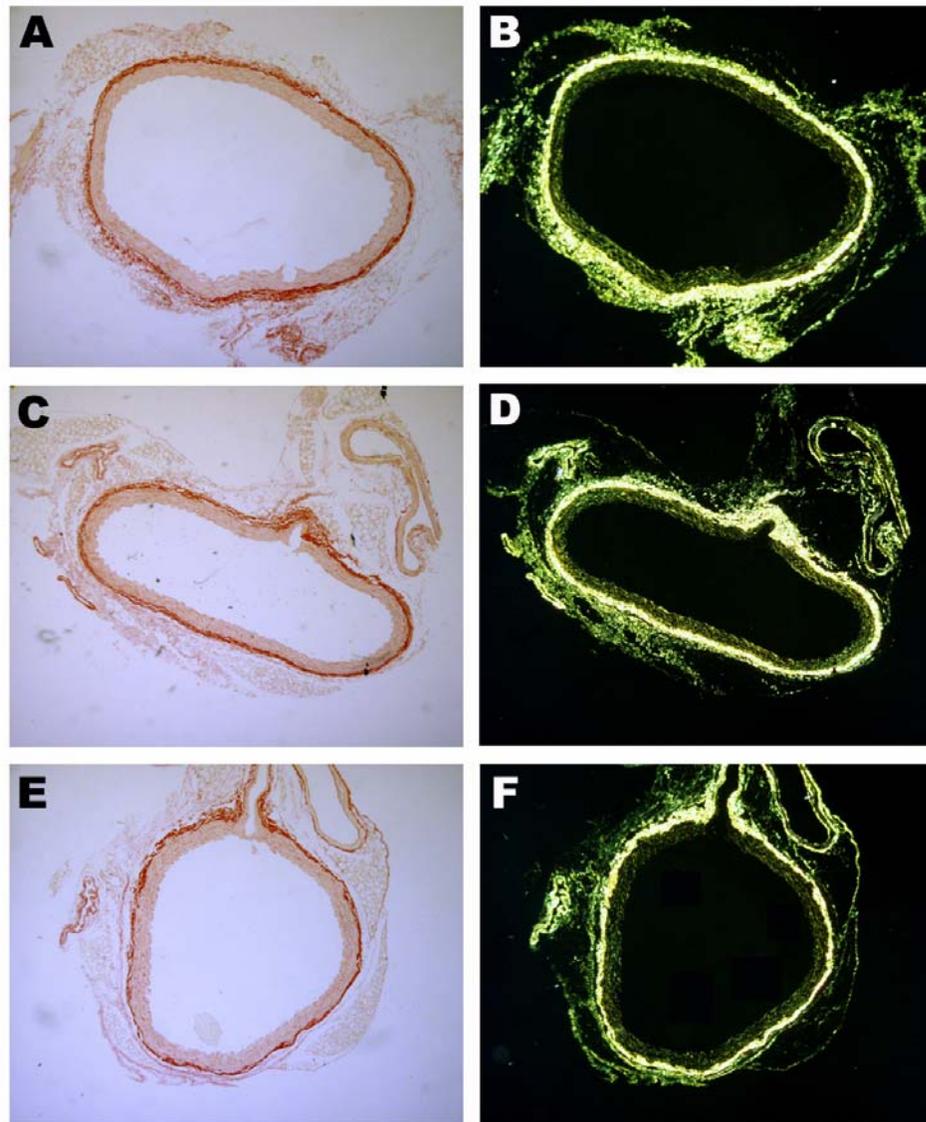
Figure 3.1 Histology of Wildtype and *Oim* Thoracic Aortas. Histological comparison of wildtype (A&B), heterozygote (C&D), and *oim* (E&F) descending aortas stained for collagen content via picrosirius red (A,C&E), collagen content via picrosirius red under polarized light (B,D&F). Figure is from Pfeiffer, *et al*. Matrix Biol 2005; 24, 7: 451-8

However, the same aortas did not demonstrate any difference in wall thickness as compared to wildtype (data not shown). An assessment of collagen content via picrosirius red staining indicated that the descending portion of *oim* and heterozygote aortas had 41% and 33% reductions in fibrillar collagen staining (987 $\pm$ 163 and 1114 $\pm$ 118 mm^2, respectively, as compared to wildtype (1668 $\pm$ 311 mm^2) (Figure 3.2 B).

Biomechanics

To more systematically quantitate and compare the biomechanical properties to biochemical parameters in the ascending and descending thoracic aortas we examined 3 month old *oim*, heterozygote, and wildtype mouse thoracic aortas by load extension curve analyses followed subsequently by biochemical evaluation of collagen content and enzyme initiated crosslinking in the same tissues. Load extension curve analyses demonstrated the expected significant decrease in breaking strength (maximum circumferential breaking strength; F_{max}) and stiffness (incremental elastic modulus; IEM), (Table 3.1) (Dobrin 1997; Fratzl 1997; Vouyouka, Pfeiffer et al. 2001). No significant differences of aortic mass demonstrated between *oim*, heterozygote, and wildtype mice.

Collagen Crosslinks and Collagen Content

The three-month-old *oim*, heterozygote, and wildtype ascending and descending thoracic aortas previously evaluated for biomechanical
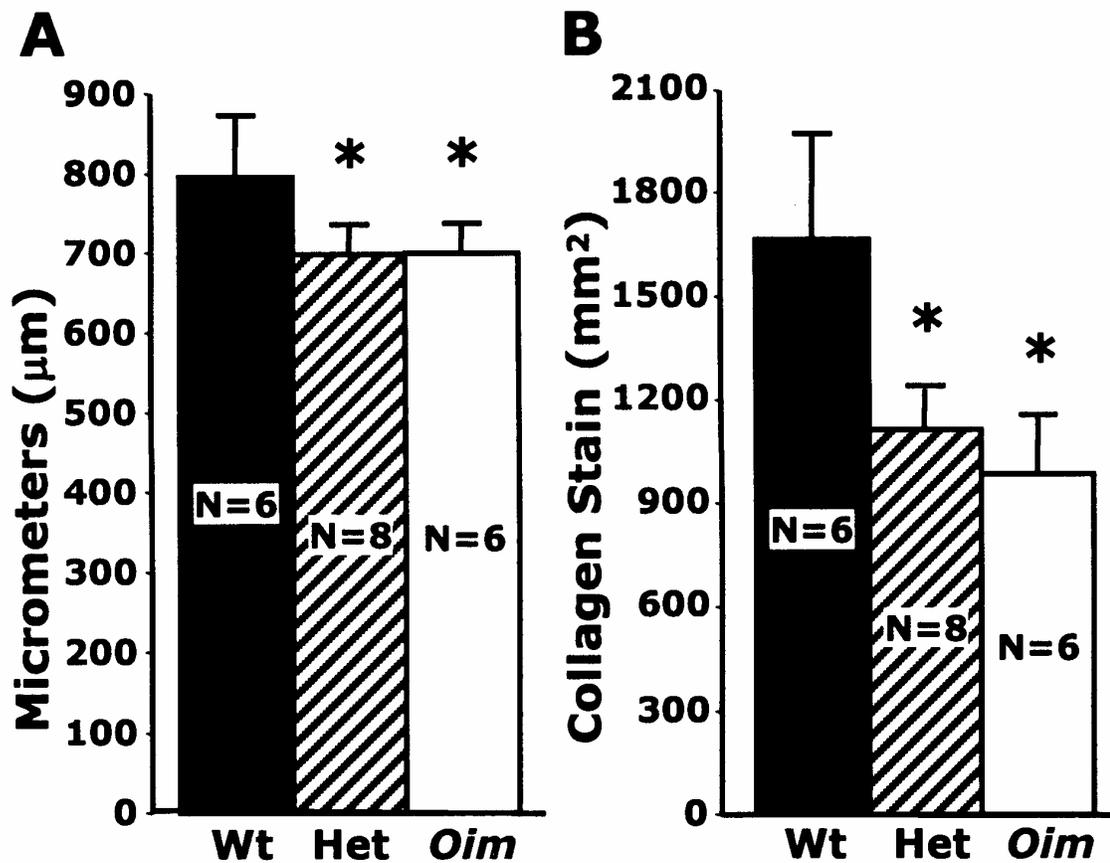
Figure 3.2. Thoracic Aortic Morphometry Measurements. Descending thoracic aortic

morphometry measurements of outside aortic diameter and fibrillar collagen histological

picrosirius red staining from *oim,* heterozygote and wildtype mice.   A, mean outside

aortic diameter for wildtype (Wt – *solid bars*), heterozygote (Het – *striped bars*), and *oim*

(*Oim – open bars*). B, mean area of fibrillar collagen staining (picrosirius red positive).

Data are expressed as mean ± S.D. of μm and area of collagen stain (mm^2). (*) indicates a

p < 0.05 relative to wildtype. Figure is from Pfeiffer, *et al*. Matrix Biol 2005; 24, 7: 451-8

Table 3.1 Circumferential Biomechanical Analysis of 3 Month Old Wildtype, Heterozygote and O*im* Ascending and Descending Thoracic Aortas

Genotype (N=Number)	F_{max} Force (g)/Aortic Weight (mg)		EIM Force (g)/Extension (mm)/ Aortic Weight (mg)	
	Ascending	Descending	Ascending	Descending
Wildtype (N=7)	254 ± 59	480 ± 120	374 ± 97	1171 ± 274
Heterozygote (N=8)	249 ± 69	314 ± 113*	457 ± 152	681 ± 276*
Oim (N=7)	135 ± 32*	165 ± 70*	256 ± 88	333 ± 98*

* p value < 0.05   Table is from Pfeiffer, *et al.* Matrix Biol 2005; 24, 7: 451-8

properties were subsequently analyzed for total collagen content (calculated from hydroxyproline content), hydroxyproline/proline, hydroxylysine/lysine, and non-reducible enzyme (lysyl oxidase) initiated collagen crosslinks (hydroxylysyl-pyridinoline/lysyl-pyridinoline). To ensure that hydroxyproline content was a valid measure of collagen content between wildtype, heterozygote, and *oim* mice, we isolated the α1(I) and α2(I) collagen chains from *oim* and wildtype mouse tail tendons and compared the individual alpha chains for amino acid composition and found no differences in hydroxyproline content between genotypes (data not shown).

Our results demonstrate that *oim* thoracic aortas have decreased collagen content per tissue weight with increased mature lysyl-oxidase initiated collagen crosslinks per collagen molecules. The ascending *oim* aortas exhibited a significant 35% reduction in collagen content per tissue weight (0.168 ± 0.012) as compared to wildtype (0.257 ± 0.025) (Figure 3.3 A), with a significant increase in corresponding hydroxylysyl-pyridinoline crosslinks per collagen molecule in the *oim* ascending aortas (0.541 ± 0.036) relative to wildtype ascending aortas (0.366 ± 0.061). This represents a 48% increase in hydroxylysyl- pyridinoline crosslinks per collagen molecule on *oim* aortas (Figure 3.3 B). Heterozygote ascending aortas exhibited intermediate levels of increased pyridinoline crosslinks and decreased collagen content between *oim* and wildtype aortas, although differences were not statistically significant. Descending *oim* aortas demonstrated a similar increase in pyridinoline crosslinks per collagen molecule as the ascending aorta; however, this increase was not significantly different from
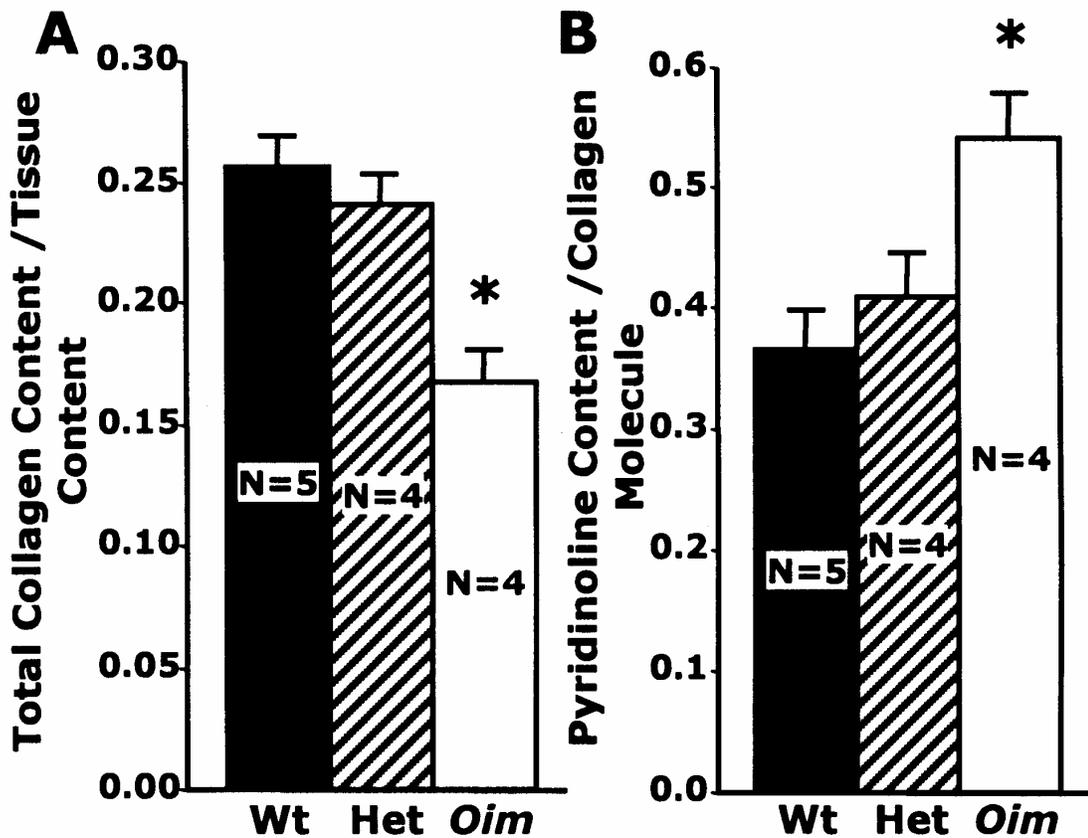
Figure 3.3 Collagen Content per Tissue Weight and Pyridinoline Crosslinks per Collagen Molecule of Ascending Thoracic Aortas. Collagen content per tissue weight and pyridinoline crosslinks per collagen molecule of ascending aortas from *oim*, heterozygote, and wildtype mice. A, mean collagen content per aortic weight for wildtype (Wt – *solid bars*), heterozygote (Het – *striped bars*), and *oim* (*Oim* – *open bars*). B, mean pyridinoline crosslinks per collagen molecule. Data are expressed as mean ± S.D. (*) indicates a p < 0.05 relative to wildtype. Figure is from Pfeiffer, *et al.* Matrix Biol 2005; 24, 7: 451-8

wildtype. The descending *oim* aortas did exhibit a significant 34% reduction in collagen content per tissue weight (0.204 ± 0.016) as compared to wildtype (0.311 ± 0.037) (Figure 3.4 A). Descending heterozygote aortas also demonstrated a similar increase in hydroxylysyl-pyridinoline crosslinks as descending *oim* aortas, although not significantly different from wildtype. Descending heterozygote aortas did demonstrate a significant 22% reduction in collagen content per tissue weight (0.244 ± 0.016) as compared to wildtype (0.311 ± 0.016) (Figure 3.4 A). No lysyl-pyridinoline crosslinks were detected in any of the aortic samples, and the hydroxylysine content per collagen molecule was equivalent between all genotypes and between ascending and descending aortas: wildtype ascending and descending (25.5 ± 0.5) and (24.9 ± 0.7), heterozygote ascending and descending (24.0 ± 1.6) and (24.6 ± 1.1), *oim* ascending and descending (25.0 ± 1.6) and (24.2 ± 1.0), respectively.

Discussion

The absence of the proα2(I) collagen chains in the *oim* mouse has been extensively studied in bone tissue and tightly correlated with bone fragility (Landis 1995; Fratzl, Paris et al. 1996; Saban, Zussman et al. 1996; McBride, Choe et al. 1997; Misof, Landis et al. 1997; Camacho, Hou et al. 1999; Phillips, Bradley et al. 2000). Whereas much less has been done to evaluate the extra-
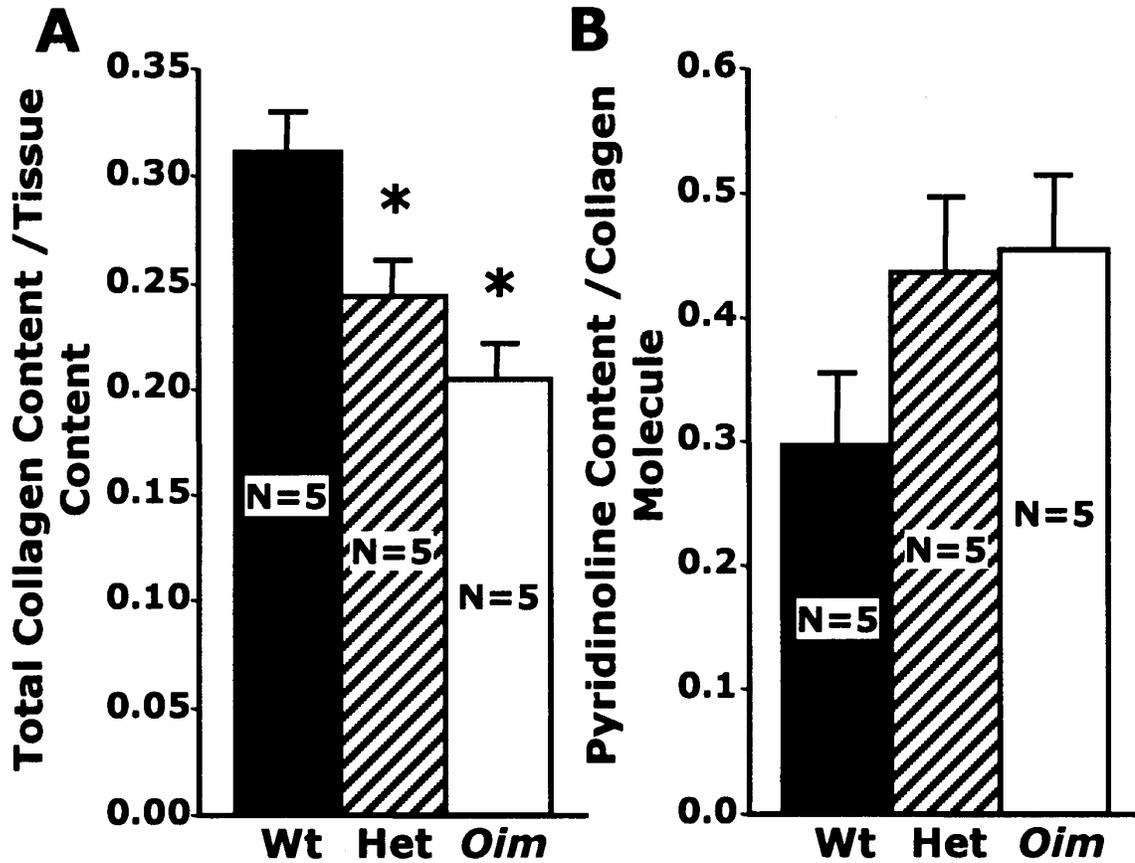
Figure 3.4 Collagen Content per Tissue Weight and Pyridinoline Crosslinks per Collagen Molecule of Descending Thoracic Aortas. Collagen content per tissue weight and pyridinoline crosslinks per collagen molecule of descending aortas from *oim*, heterozygote, and wildtype mice. A, mean collagen content per aortic weight for wildtype (Wt – *solid bars*), heterozygote (Het - *striped bars*), and *oim* (*Oim – open bars*) groups. B, mean pyridinoline crosslinks per collagen molecule. Data are expressed as mean ± S.D. (*) indicates a p < 0.05 relative to wildtype. Figure is from Pfeiffer, *et al.* Matrix Biol 2005; 24, 7: 451-8

skeletal consequences of the absence of the proα2(I) collagen chains and/ or presence of homotrimeric type I collagen in non-mineralized tissues (McBride, Choe et al. 1997; Camacho, Hou et al. 1999; Weis, Emery et al. 2000). To examine the extra-skeletal role of the α2(I) collagen chain, we evaluated *oim*, heterozygote and wildtype thoracic aortic tissue for histological / morphological parameters, circumferential biomechanical properties, and aortic collagen and lysyl-oxidase initiated collagen crosslinking levels.

Histological evaluation was driven in part by a previous report of Vetter et al that patients with OI type III were predisposed to aortic dilatation (ecstatic aorta) (Vetter, Maierhofer et al. 1989), and more recently reports that patients null for proα2(I)collagen expression have cardiovascular and valvular involvement (Schwarze, Hata et al. 2004). Histological evaluation of wall thickness, lumen diameter, and ECM components demonstrated no differences between the genotypes in aortic wall thickness; however, the outer aortic wall diameter was decreased in *oim* and heterozygote aortas. Theoretically, a decrease in vessel diameter can influence systolic pressure (Poiseuille's law $\Delta P = 8 \eta l / \pi r^4$; which is inversely equal to vessel compliance) (Dobrin 1997). Inhibition of lysyl oxidase initiated crosslinking is known to result in increased aortic diameters, so perhaps inversely an increase in pyridinoline crosslinks per collagen molecule reduces aortic diameter (Bruel, Ortoft et al. 1998). It is however difficult to assess whether this is a true in vivo difference or a reflection of the genotypic differences in material properties of the aortas in response to the

same perfusion pressure.   There was no evidence of aortic dilatation for any

genotype at 3 months of age. The ECM histology did reveal a reduction in

collagen picrosirius red staining localized to the adventia layer in *oim* and

heterozygote aortas, suggesting decreased fibrillar collagen deposition in the

adventia.

     We verified the significant decrease in collagen content in both *oim* and

heterozygote aortas by hydroxyproline analyses, which suggests that the

reduced thoracic aortic breaking strength and stiffness may reflect in part a

decrease in total collagen content. Heterozygote aortas demonstrated

biomechanical alterations intermediate of *oim* and wildtype implying that the

absence of α2(I)collagen and/or presence of homotrimeric collagen has a dosage

affect, in which reduced heterotrimeric type I collagen amounts decrease aortic

strength and stiffness. Studies by McBride et al., using enzyme degradation and

x-ray diffraction analyses, suggest the presence of homotrimeric and

heterotrimeric type I collagen in heterozygote tendons (McBride, Choe et al.

1997). Due to the limited tissue amounts it is difficult to assess the amount of

homotrimeric type I collagen present in heterozygote aortas. In this study we

found that total collagen content in *oim* aortas was not statistically different from

that of heterozygous aortas, yet *oim* aortas had significantly greater reductions in

F_{max} and IEM relative to heterozygote. This implies that a reduction in type I

collagen is not the only factor responsible for altered aortic integrity of *oim* aortas,

and that the presence of solely homotrimeric type I collagen or the complete

absence of the proα2(I) collagen chain imparts other effects upon thoracic aorta integrity.

Our findings are consistent with other collagen and force bearing tissues studied in the *oim* mouse (Camacho, Hou et al. 1999; Weis, Emery et al. 2000; Vouyouka, Pfeiffer et al. 2001). *Oim* femurs are reported to have 20% less collagen than wildtype mouse femurs with reduced biomechanical integrity (Camacho, Hou et al. 1999). Weis et al. evaluated the collagen content and mechanical properties of the *oim* left ventricular myocardium and found a 45% reduction in collagen content (hydroxyproline analyses) and altered ventricular mechanics as compared to wildtype (Weis, Emery et al. 2000). We previously reported no difference in aortic collagen content in Vouyouka et al. However, the determination of collagen content was based on a colorimetric assay for hydroxyproline instead of quantitative amino acid analyses and the ability to detect a 35% decrease in collagen content in such small amounts of aortic tissue was beyond the sensitivity of the colorimetric assay.

We also investigated other post-translational components of type I collagen including the lysyl oxidase (LO) initiated collagen crosslinks (hydroxylysyl-pyridinoline/lysyl-pyridinoline) and hydroxylysine/lysine. LO enzymatically modifies lysine residues of type I collagen molecules, in which divalent crosslinks and eventually trivalent crosslinks (hydroxylysyl-pyridinoline/lysyl-pyridinoline) are formed between adjacent collagen molecules (Reiser, McCormick et al. 1992). This process is essential for proper cardiovascular function as evidenced by in vivo inhibitor studies with β-

aminopropionitrile (BAPN, LO inhibitor) in rats (Bruel, Ortoft et al. 1998) and the Menkes and LOX knock out mice (Kodama and Murata 1999; Hornstra, Birge et al. 2003). Brüel *et al.* demonstrated treatment of rats with BAPN significantly decreased thoracic aortic pyridinoline crosslinks, increased aortic diameters, and significantly reduced the maximum load and stiffness of the thoracic aortas (Bruel, Ortoft et al. 1998). Menkes mice have a copper transport defect, an essential cofactor for LO activity (Rucker, Kosonen et al. 1998), and the Menkes defect significantly reduces LO activity predisposing the mouse to arterial rupture due to improper elastin and collagen crosslinking (Kodama and Murata 1999; Hornstra, Birge et al. 2003). The LOX knock out mouse, (lysyl oxidase 1 gene knock-out), demonstrates abnormal aortic and diaphragmatic development with normal skeletal development, and reduced di-functional collagen crosslinks, as compared to wildtype LOX mice (Hornstra, Birge et al. 2003). This reiterates the importance of hydroxylated lysines for proper cardiovascular function; however, both Menkes and the LOX knock out mouse demonstrate reduced elastin crosslinking, which may contribute significantly to their abnormal cardiovascular development. Though the *oim* mouse also exhibits reduced mechanical integrity we found LO-initiated collagen crosslinks were increased in *oim* aortas suggesting that homotrimeric type I collagen molecules may actually have a greater potential to form crosslinks with adjacent collagen molecules and/or that there might be a compensatory mechanism for reduced biomechanical strength to sustain viability. These results are further supported by Weis *et al.* in which

oim left ventricular myocardium demonstrated a 22% increase in pyridinoline crosslinks/collagen as compared to wildtype (Weis, Emery et al. 2000).

In humans, mutations in COLIA2 gene resulting in the absence of functional proα2(I) collagen chains have demonstrated various mineralized and non-mineralized connective tissue phenotypes, ranging from Ehlers Danlos syndrome (EDS) to OI (Pihlajaniemi, Dickson et al. 1984; Sasaki, Arai et al. 1987; Nicholls, Valler et al. 2001; Schwarze, Hata et al. 2004). The first patient described was a child who exhibited clinically OI type III without indications of cardiovascular involvement. This child's OI was a result of homozygosity for a 4bp deletion in the coding region that corresponded to the carboxy-propeptide domain (Nicholls, Osse et al. 1984; Pihlajaniemi, Dickson et al. 1984). Subsequently another patient was described whom exhibited a mixed EDS/OI phenotype, whose COL1A2 mutation was a splicing defect that resulted in significantly reduced levels of functional proα2(I) collagen mRNA, and at age 9 years had no evidence of cardiovascular involvement (Nicholls, Valler et al. 2001). Recently a series of EDS patients with cardiovascular valvular dysfunction were described by Schwarze et al. whom had COL1A2 splicing mutations activating a nonsense-mediated RNA decay pathways resulting in complete absence of proα2(I) collagen expression (Schwarze, Hata et al. 2004). The OI patient produces normal amounts of stable mutant proα2(I) collagen mRNA, and the OI/EDS patient has minor amounts of mutant proα2(I) collagen mRNA, but it is unknown if these patients have any cardiovascular dysfunction because of loss to follow up or adolescent age (Pihlajaniemi, Dickson et al. 1984;

Nicholls, Valler et al. 2001). Molecularly, biochemically and phenotypically the

oim mouse is most similar to the original OI patient. The EDS and the EDS/OI

patients all exhibit some if not complete nonsense mediated decay of the mutant

COL1A2 transcript, whereas the OI patient and *oim* mouse express and maintain

the mutant COL1A2 transcript with evidence for the accumulation of abnormal

proα2(I) collagen intracellularly in the human OI fibroblasts (Nicholls, Valler et al.

2001). Whether *oim* mice also produce mutant proα2(I) collagen chains

intracellularly is not clear. The OI and EDS patients and the *oim* mouse suggest

that expression of stable nonfunctional proα2(I)collagen mRNA and/or protein

exhibits pathogenically dominant negative mechanisms that are tissue specific,

with a greater impact on mineralized tissue, in contrast to mutations that result in

the complete absence of functional proα2(I) collagen transcripts and exhibit

greater cardiovascular involvement. Further studies are needed to clarify the role

of proα2(I)collagen in connective tissue disease and mutation specific

pathogenesis.

CHAPTER IV

ROLE OF PROα2(I) COLLAGEN CHAINS AND COLLAGEN CROSSLINKING IN THORACIC AORTIC BIOMECHANICAL INTEGRITY DURING AGING USING THE *OIM* MOUSE MODEL

Brent J. Pfeiffer[1], David A. Wirth[1], Craig L. Franklin[2], Fu-hung Hsieh[3], Rudolf A. Bank[4], Charlotte L. Phillips[1] Departments of Biochemistry[1], Veterinary Pathobiology[2], Biological and Agriculture Engineering[3], University of Missouri-Columbia, Columbia, MO 65212, and TNO Prevention and Health, Zernikedreef 9 Box 2215, 2301 CE Leiden, Netherlands[4]

Introduction

Vascular tissue extracellular matrix (ECM) confers unique biomechanical properties crucial to maintaining vascular wall integrity in the presence of hemodynamic anisotropic forces (Fung 1993). Elastin and collagens are the major passive determinants of arterial wall integrity. Vascular tissue maturation and age-related changes in collagen have been associated with increased stiffness and are tightly linked to vascular tissue structural and functional alterations (Vogel 1983; Bailey, Paul et al. 1998). Proposed mechanisms for age-related tissue stiffening include non-reducible enzyme-initiated collagen crosslinking and advanced glycation end-products (AGEs) (Oxlund, Rasmussen et al. 1989; Bailey, Paul et al. 1998; Bruel, Ortoft et al. 1998).

Abnormalities in the vascular components elastin, fibrillin, and collagen are known to cause cardiovascular pathology (Yeowell and Pinnell 1993; Chowdhury and Reardon 1999; Arteaga-Solis, Gayraud et al. 2000). Whereas the molecular and pathogenic basis for elastin and fibrillin defects have been elucidated, the role of type I collagen is still largely undefined. The heritable connective tissue disorder, osteogenesis imperfecta (OI) is characterized by type I collagen mutations primarily affecting mineralized tissue (Byers 2001). Case reports describing OI patients with cardiovascular dysfunction and two investigations into extra-skeletal complications associated with OI have been reported since the 1980's (Hortop, Tsipouras et al. 1986; Kalath, Tsipouras et al. 1987; Wheeler, Cooley et al. 1988; Vetter, Maierhofer et al. 1989; Wong, Follis et

76

al. 1995). These early studies determined the prevalence of cardiovascular dysfunction, in particular aortic root dilatation, to be 12% in the OI population studied, with a correlation between cardiovascular dysfunction and OI severity (Hortop, Tsipouras et al. 1986; Kalath, Tsipouras et al. 1987; Vetter, Maierhofer et al. 1989). However, these studies examined heterogeneous OI populations, and due to the genetic and phenotypic heterogeneity of OI, it is unclear whether there is a phenotype-to-genotype correlation.

The predominant type I collagen molecule is the heterotrimeric isotype composed of two α1(I) collagen chains and one genetically distinct α2(I) collagen chain; however, a minor isotype also exists comprised of three α1(I) chains (Kietly 1993; Byers 2001). In vertebrates, the evolutionary conservation of the heterotrimeric isotype is believed to contribute to greater mechanical stability and to be utilized for tissue specialization, suggesting a potential physiological and developmental role for the type I collagen isotypes (Jimenez, Bashey et al. 1977; Rojkind, Giambrone et al. 1979; Uitto 1979; Bernard, Myers et al. 1983; Exposito and Garrone 1990).   However, the precise role of heterotrimeric type I collagen, and more specifically, the α2(I) chain is still unclear and remains a subject of great interest. We use the *oim* mouse model to study vascular tissue alterations associated with the absence of α2(I) collagen chains from type I collagen and/or presence of homotrimeric type I collagen molecules. *Oim* mice produce only the homotrimeric type I collagen isotype, as result of COL1A2 homozygosity for non-functional proα2(I) collagen chains (Chipman, Sweet et al. 1993). Skeletal consequences associated with the *oim* mutation have been well documented;

however, the extra-skeletal effects of homotrimeric type I collagen are not as well studied (Chipman, Sweet et al. 1993; McBride, Shapiro et al. 1998; Camacho, Hou et al. 1999; Sims, Miles et al. 2003).

Recently, we demonstrated that *oim* thoracic aortas have reduced breaking strength and stiffness, reduced collagen content, and increased pyridinoline crosslinking relative to age-matched 3-month-old wildtype mice (Pfeiffer, Franklin et al. 2005). We present here a continuation of our investigation into the role of α2(I) collagen chains, pyridinoline crosslinks, and AGE crosslinks in aortic integrity and aging.

Materials and Methods

Mice

Heterozygous B6C3Fe-*a/a-Col1a2^{oim}/+* mice were purchased from Jackson Laboratory (Bar Harbor, ME) and bred to produce homozygous *oim*, heterozygous, and wildtype mice. All animals were housed, fed, and handled as previously described (Vouyouka, Pfeiffer et al. 2001; Pfeiffer, Franklin et al. 2005). Genotypes were confirmed by PCR restriction fragment length polymorphism analysis, and mice were euthanized via CO_2 asphyxiation for analyses at 3, 8, and 18 months of age ± one week, as previously described

78

(Phillips, Bradley et al. 2000; Pfeiffer, Franklin et al. 2005). A total of 185 mice were used to complete this study.

Biomechanical Analysis

Thoracic aortas were dissected, separated into 5-millimeter (mm) ascending and descending portions, with stainless steel hooks placed in the lumen for circumferential studies (Vouyouka, Pfeiffer et al. 2001; Pfeiffer, Franklin et al. 2005). For longitudinal studies, descending thoracic aortas were harvested similarly and placed into small vice grips at each end to be attached to the texture analyzer clamps. Load-extension curves were obtained using a TA-XT2 texture analyzer (Stable MicroSystems, NY), as described previously (Vouyouka, Pfeiffer et al. 2001). Load-extension curves were analyzed for thoracic aortic maximal breaking strength (F_{max}) and incremental elastic modulus (IEM), as described previously (Vouyouka, Pfeiffer et al. 2001). Following mechanical testing, aortas were delipified and weighed prior to biochemical analyses (Pfeiffer, Franklin et al. 2005).

Histological/Morphological Analysis

Aortas from each genotype were perfusion fixed and harvested for histological and morphological studies, as previously described (Pfeiffer, Franklin et al. 2005).

Immunohistochemistry (*IHC*)

Aortas harvested for histology/morphometry studies were also used in *IHC* studies. Aortas were sectioned transversely at five micron thicknesses. *IHC* was performed using a pepsin epitope retrieval solution (0.02%pepsin/0.01N HCl/PBS); endogenous peroxidases blocking solution (10%MeOH/3%H_2O_2/PBS); primary monoclonal anti-AGE (6D12) antibody (TransGenic Inc., Kumamoto, Japan) at a working concentration of 2mg/ml; endogenous mouse IgG blocking with the Histomouse-Max Kit (Zymed Lab. Inc., San Francisco, CA) per instructions; and secondary anti-mouse IgG-HRP conjugated antibody plus substrate-chromogen (DAB) per Histomouse-Max Kit instructions. After chromogen development, sections were stained with hematoxylin per Histomouse-Max Kit instructions. Histological images were captured digitally and analyzed as previously described (Pfeiffer, Franklin et al. 2005).

Biochemical Analysis

Following biomechanical testing, dried delipified aortic tissue was evaluated for total collagen content, hydroxylysine/lysine content, hydroxyproline/proline content, and enzyme-initiated collagen crosslink content (hydroxylysyl-pyridinoline/lysyl-pyridinoline) using reverse phase high performance liquid chromatography (HPLC), as previously described (Bank,

Beekman et al. 1997; Bank, Bayliss et al. 1998). Amino acid analysis of purified

α1(I) and α2(I) collagen chains was evaluated using isolated tail tendon collagen

from wildtype, heterozygote, and *oim* mice, as previously described (Woodson,

Fujita et al. 1991; Pfeiffer, Franklin et al. 2005).

In situ hybridization (*ISH*)

To evaluate the steady-state mRNA levels of elastin, proα1(I) collagen,

proα2(I) collagen, and proα1(III) collagen, we performed *ISH* on ascending and

descending thoracic aorta paraffin embedded sections. Aortas harvested from

the histology/morphology studies were used. Five-μm transverse sections were

obtained under RNase-free conditions and the following procedures occurred as

follows: dewaxing, pretreatment, prehybridization, hybridization, stringency

washes, and autoradiography/imaging, which has been previously described

(Reneker, Silversides et al. 1995). However, the following modifications were

followed: ^{35}S-rUTP source (MP Biomedicals, Irvine, CA), RNA probe construction

using MEGAscript T3 RNA polymerase kit (Ambion Inc., Austin, TX), 1mg of PCR

generated DNA template with the T3 RNA polymerase sequence placed at the 5'

end of the sense or anti-sense strands, and RNasin (Promega, Madison, WI).

Bright field and dark field images were captured at 100X magnification, using a

Leica (Leica Microsystems, Wetlzar, Germany) microscope mounted with an in-

line Optronics Digital Camera (Optronics, Goleta, CA). Steady-state mRNA

expression was captured using dark-field microscopy, and nuclear location via hematoxylin staining was captured using bright field microscopy.

RNA Harvest and Isolation

Aortic tissue was collected from mice within 10 minutes of euthanasia and place into 2ml of RNAlater (Ambion Inc., Austin, TX) solution per instructions. Samples were stored at 4°C for 6 hours and then transferred to -20°C for long term storage. After all samples have been collected, ascending and descending portions were separated and homogenized in a 2-inch mortar/pestle with liquid nitrogen. Total RNA was isolated using the RNAeasy RNA Isolation Kit (Qiagen, Valencia, CA) per instructions. Total RNA was stored at -80°C until prior to use in reverse transcription.

Reverse Transcription PCR

Reverse transcription (RT) was performed using Improm-II Reverse Transcriptase and reagents (Promega, Madison, WI), as per instructions, in a RoboCylcer Gradient40 (Stratagene, La Jolla, CA) with the following modifications: 4ul of RNA template and 3mmol/L $MgCl_2$ working concentration.

Real-Time (RT) PCR

PCR primers were designed for proα1(I) collagen, proα2(I) collagen, proα1(III) collagen, elastin, and lysyl oxidase transcripts using the PrimerQuest primer design program at the integrated DNA technologies website http://scitools.idtdna.com/Primerquest/ (Integrated DNA Technologies, Coralville, IA) see table 4.1 for primer sequences.

External standards were produced from PCR amplicons isolated via agarose gel extraction using Qiagen's Gel Extraction kit (Qiagen, Valencia, CA), and cloned separately into a Topo TA cloning vector per manufactures instructions (Invitrogen, Carlsbad, CA). Clones were grown in Luria B Broth culture media, harvested using Promega's Wizard mini-preps (Promega, Madison, WI) per instructions, and linearized with NotI or BamHI restriction endonucleases. The linearized clones were quantified using UV spectrophometric readings at 260nm, and copy numbers/μL were calculated for each clone. Real-time PCR was performed using the LightCycler System (Roche, Indianapolis, IN) and QuantiTect SYBR Green PCR Kit (Qiagen, Valencia, CA) per instructions at an activation temperature of 95°C for 15 minutes, denaturation temperature of 94°C for 15 seconds, annealing at 62°C for 20 seconds, elongation at 72°C for 30 seconds, and acquisition at 78°C for each cycle for a total of 40 cycles.

Table 4.1 Primer sequences for RT-PCR

Transcript (ascension number)	Ampilcon Size (bp)	Forward Primer	Reverse Primer
COL1A1 (U08020)	335	5'-AGC CTG AGT CAG CAG ATT GAG A	5'-CTT GCA GTG ATA GGT GAT GTT CT
COL1A2 (X58251)	235	5'-TGA AGT GGG TCT TCC AGG TCT TTC	5'-CAC CCT TGT TAC CGG ATT CTC CTT
COL3A1 (X52046)	419	5'-ATC AGA TGG TCA GCC AGG TC	5'-GAT GCC CAC TTG TTC CAT CT
ELASTIN (XM_109452)	78	5'-CAT CCA TCC ATC CGT CCA TCT TGA	5'-ACA GGT GAA CCA GGT TGA TAG T
LYSYL OXIDASE (NM_010728)	316	5'-ATC CCT ACA AGT ACT CCG ACG ACA	5'-AAG TCC GAT GTC CCT TGG TTC TTC
HPRT (O'Garra, Chang et al. 1992)	NA	Provided by Dr. Craig Franklin	Provided by Dr. Craig Franklin

Aortic Collagen Isolation, Western Blot, and ELISA for AGEs

Harvested aortas were collected and stored at -20°C until ready for use. Collagen from aortas was isolated in the following manner. Aortic cells were lysed with 7.5ml of Tris/TritonX^{100} buffer (10mmol/L Tris/2% TritonX^{100}/pH7.5) incubated on ice for 15 minutes followed by sonication using a Branson Sonifier250 (Branson Ultrasonics Corp, Danbury, CT) with a micro tip probe and settings of duty cycle at 100% and output at 6. Samples were sonicated at four 15-second intervals interrupted with 2 minute incubations on ice between each interval to prevent thermal denaturation. Samples were centrifuged at 10,000xg at 4°C for 30 minutes, and the supernatant discarded. The tissue pellet was rinsed with sterile ddH$_2$O three times (5ml/wash), discarding the wash solution. Samples were lyophilized for 4 hours. The pellet was resuspended in 5ml of 0.5N acetic acid (pre-chilled to 4°C). 250μl of pepsin (1mg/ml) (Sigma-Aldrich, St Louis, MO) was added to each resuspended aortic sample. Samples were incubated at 4°C for 72 hours with continuous agitation using a micro-stir bar. Pepsin was inactivated with 50μl of pepsatinA (1mg/ml) (Sigma-Aldrich, St Louis, MO). The quality of the isolated collagen was visualized via 8% SDS-PAGE/2mol/L Urea gels and quantified via Sircol assays (Biocolor, Newtownabbey, Northern Ireland).

Five μg of collagen from each aortic sample was evaluated by 5% SDS-PAGE/2M urea gel electrophoresis loaded with procollagen sample buffer (20%

Glycerol/0.1mol/L Tris pH 6.8/2% SDS/ddH2O/1mol/L Urea/Bromophol Blue),

and ran at 100 Volts using a Tris/Glycine/SDS/Urea running buffer (0.02mol//L

Tris/0.2mol/L Glycine/0.1%SDS /2mol/L Urea/pH8.3). Proteins were transferred

to a BioRad PVDF membrane (BioRad, Hercules, CA) per instructions using a

Tris/Glycine/SDS/ transfer buffer (12mmol/L Tris/96mmol/L Glycine/3%

SDS/pH8.3). Transfers were performed at 200mA for 3 hours at 4°C with the

assembly packed on ice. Membranes were rinsed in a TBS Tween[20] buffer

(100mmol/L Tris/400mmol/L NaCl/0.1% Tween[20]/pH7.4) three times for 5

minutes. Westerns preceded by inhibiting non-specific binding with 5%

condensed milk/TBS Tween[20] buffer incubated for 1 hour at RT. In between all

steps six, 5 minutes TBS Tween[20] buffer washes were performed. Primary

antibody binding was done incubating for 1 hour at RT using the monoclonal anti-

AGE (6D12) antibody (TransGenic Inc., Kumamoto, Japan) prepared at a

1:10,000 dilution in the TBS Tween[20] buffer. Membranes were then washed, and

secondary antibody binding was done incubating for 1 hour at RT with the anti-

mouse IgG-HRP conjugated antibody (Santa Cruz Biotech, Inc, Santa Cruz, CA)

prepared at a 1:25,000 dilution in the TBS Tween[20] buffer. Following this step,

membranes were washed and antibody binding was visualized via

chemiluminescence per Pierce Dura-chemilumenscence kit (Pierce, Rockford, IL)

using autoradiography.

Statistical Analysis

Data were analyzed using a 3 by 3 factorial generalized linear model (GLM), expressed as means ± standard deviation using SAS (SAS Institute Inc., NC) statistical software. Individual p-values between preset treatment groups were expressed and significance was set at 0.05. If the standard deviation was equal to or greater than the mean value, then the data was evaluated for outliers via the NMR outlier test and table. In addition, qRT-PCR data was log transformed to stabilize variance and evaluate for differences among genotype and age treatments; the presented data are the actual means and standard error.

Results

Load-Extension Curves Analyses

Circumferential load extension curve analyses demonstrated the expected significant decreases in F_{max} and IEM of *oim* ascending and descending thoracic aortas at each age class. The greatest impact was evident in descending aortic segments (Figure 4.1; Table 4.2). *Oim* descending aortas demonstrated F_{max} values at 39%, 46%, and 56% and IEM values at 33%, 40%, and 57% of wildtype for 3, 8, and 18 months of age, respectively. Heterozygote descending aortas
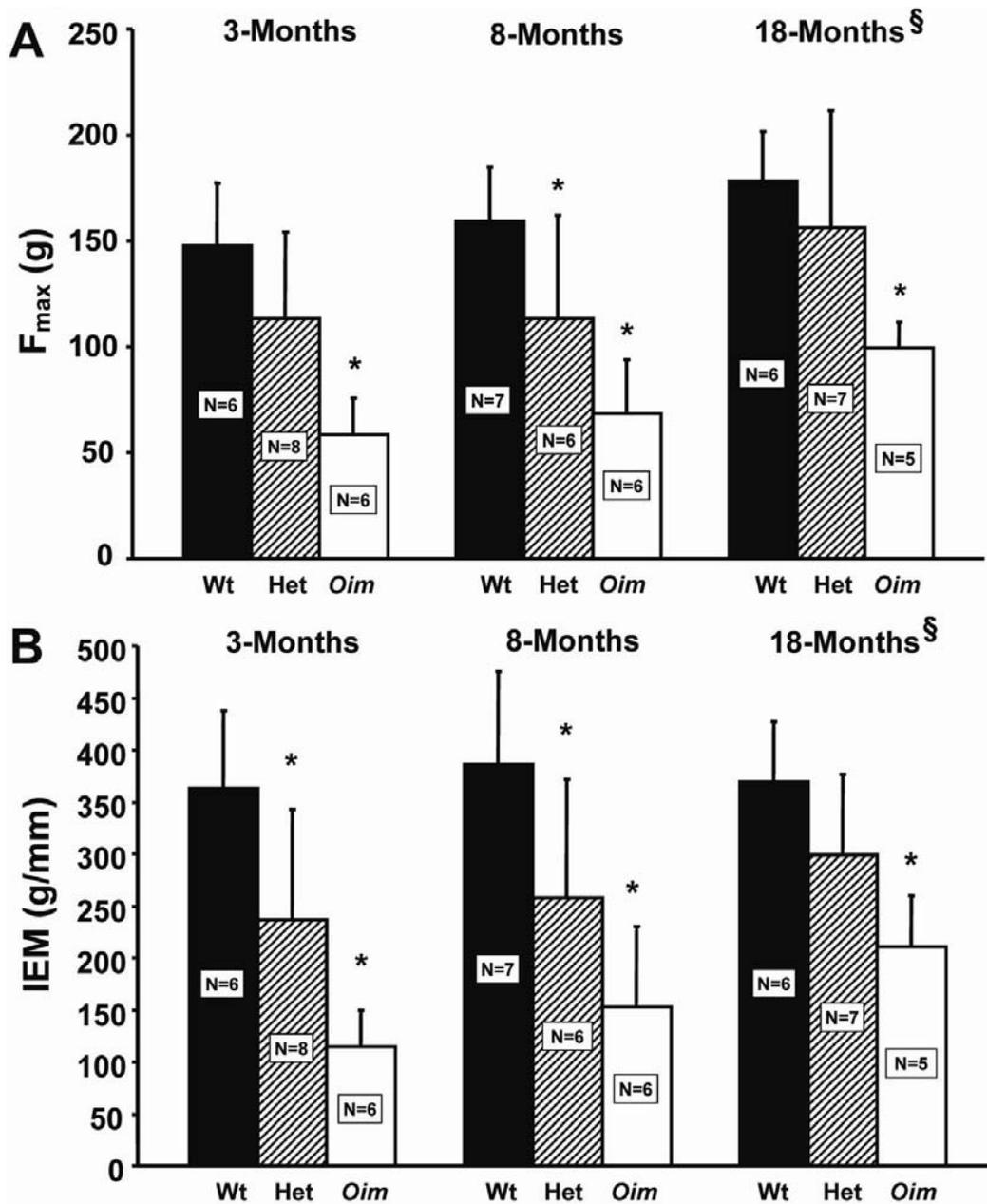
Figure 4.1 Circumferential Breaking Strength and Stiffness of Descending Thoracic Aortas at 3, 8, and 18 Months of Age. Circumferential breaking strength (F_{max}) (A) and circumferential stiffness (IEM) (B) of descending *oim* aortas are significantly weaker than wildtype aortas at each age class. Age-associated increases in F_{max} and IEM in *oim* and heterozygote aortas at 18 months as compared to 3 months. Values are expressed as means ± standard deviation. (*) indicates a p-value <0.05 relative to wildtype. (§) indicates a p-value <0.05 relative to relative to the same genotype at 3 months of age.

Table 4.2 Summary of Circumferential and Longitudinal Biomechanical Properties of the Throacic Aorta

Circumferential

	Oim			Heterozygote			Wildtype		
	3-months	8-months	18-months	3-months	8-months	18-months	3-months	8-months	18-months
Afm	83±12*	73±18*	84±12*	125±24*	133±25	165±28§	148±23	141±21	148±24
Aiem	153±33*	129±39*	147±38*	226±0	217±66	280±65§	219±33	212±32	250±26
Ave	-0.0153±.002	-0.0208±.01	-0.0178±.008	-0.0153±.004	-0.0152±.001	-0.0153±.004	-0.0180±.003	-0.0158±.005	-0.0178±.005
Dfm	62±16*	72±22*	92±19*§	118±38*	136±38	147±49§	158±26	155±27	164±31
Diem	120±35*	164±71*	216±53*§	248±98*	315±106*	303±63*§	364±58	405±63	376±47
Dve	-0.0153±.002	-0.0191±.002	-0.0138±.002	-0.0201±.006	-0.0186±.008	-0.0174±.004	-0.0191±.003	-0.0173±.005	-0.0184±.007

Longitudinal

	Oim			Heterozygote			Wildtype		
	3-months	8-months	18-months	3-months	8-months	18-months	3-months	8-months	18-months
Dfm	30±5	29±8*	29±9*	40±5	42±8	60±20	38±5	47±12	53±13
Diem	0.84±.14	0.77±.28	0.79±.32*	1.85±.40	1.49±.25	2.24±.90	1.27±.63	1.52±.67	1.92±.73

Afm is ascending Fmax (g). Aiem is ascending IEM (g/mm). Ave is ascending viscoelastic property (ln). Dfm is descending Fmax (g). Diem is descending IEM (g/mm). Dve is descending viscoelastic property (ln). Values expressed as mean ± standard deviation. (*) represents a p-value <0.05 relative to wildtype. (§) represents a p-value <0.05 relative to 3 months of age.

demonstrated F_{max} and IEM intermediate of *oim* and wildtype values; though

these changes were not always statistically significant. Examination of

longitudinal load extension curve data revealed a trend towards reduced F_{max} at

8 and 18 months and IEM at 8 months in *oim* descending aortas as compared to

age-matched wildtype (Table 4.2).   Circumferential aortic viscoelastic

properties, a measure of tissue hydration, did not demonstrate significant

genotype or age-associated differences (Table 4.2). Age-associated increases in

F_{max} and IEM were demonstrated in *oim* and heterozygote descending aortas at

18 months compared to 3 months. No significant genotype-associated difference

in aortic mass was demonstrated; however, a significant increase in aortic weight

was seen for each genotype by 18 months as compared to 3 months. The

percent increase in aortic weight at 18 months relative to 3 months for ascending

and descending aortas were: *oim*, 26% and 15%; heterozygote, 83% and 63%;

and wild type, 38% and 36%, respectively.

Histological and Morphometric Studies

        For both *oim* and heterozygote aortas there were no gross histological

differences in cell numbers, elastin, or proteoglycan staining as compared to

wildtype (Figures 4.2, 4.3, and 4.4). As was seen previously 3 month old *oim*

aortas exhibited reduced picrosirius red (PSR) fibrillar collagen staining relative

to wildtype aortas. Further, this reduction in PSR staining of *oim* aortas relative

to wildtype aortas was maintained at 8 and 18 months of age (Figure 4.5 and
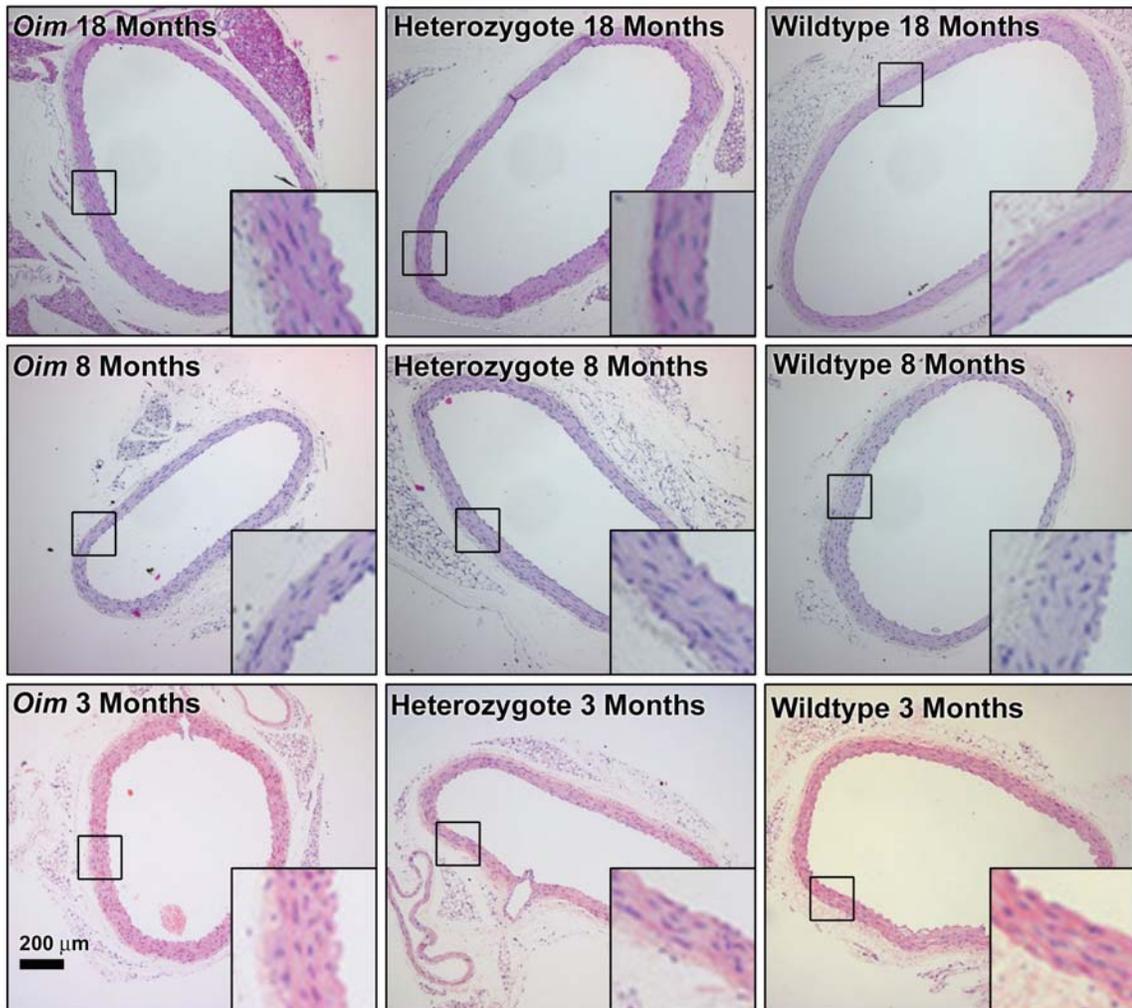
Figure 4.2 Hematoxylin & Eosin Stain of Thoracic Aorta Sections. Hematoxylin & eosin (H&E) stain demonstrating cell numbers in O*im*, Heterozygote, and Wildtype descending thoracic aortas at 3, 8, and 18 months of age. There were no genotype-associated or age-associated changes in cell numbers or cell size. The inset displayed in the lower right corner is a magnified view of the thoracic aortic wall to demonstrate histological details from the outlined black box.
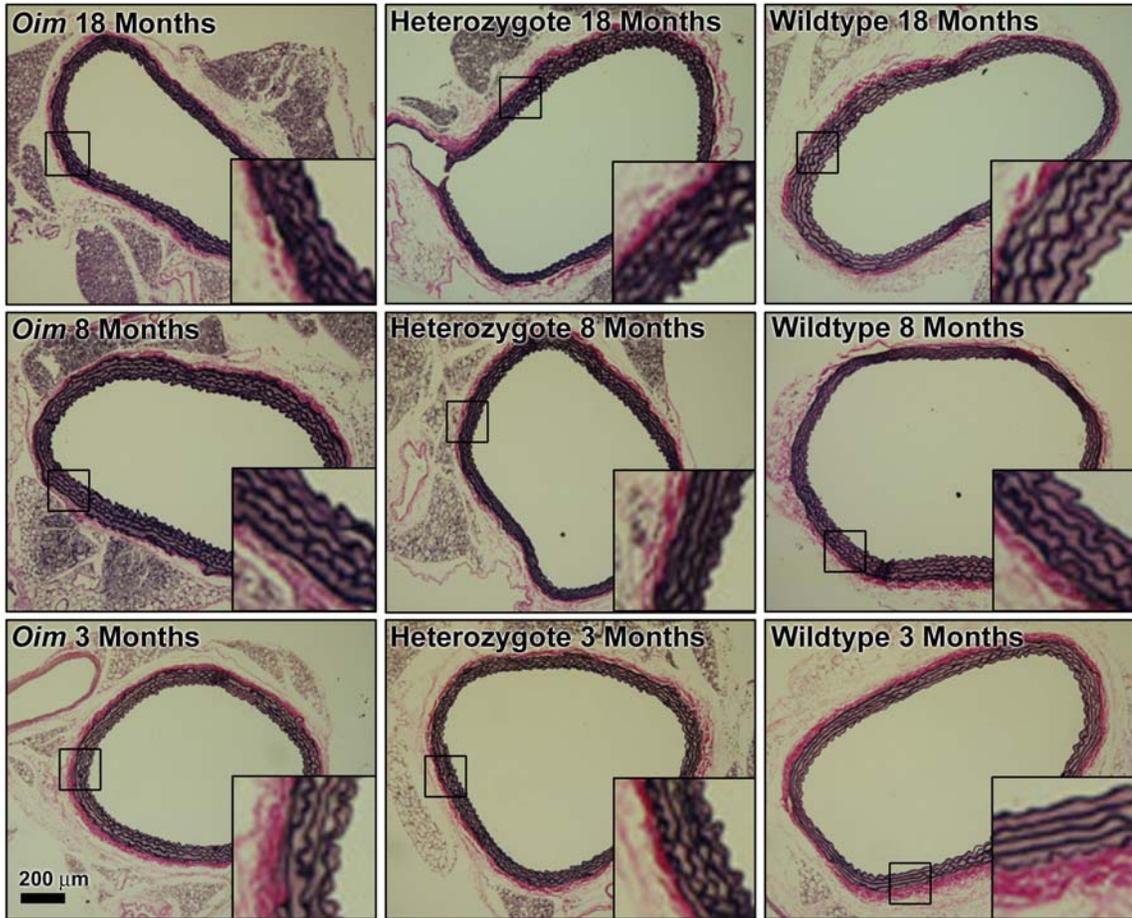
Figure 4.3 Verhoff's van Gieson Stain of Thoracic Aorta Sections. Verhoff's van Gieson stain demonstrating elastin lamella in *Oim*, Heterozygote, and Wildtype descending thoracic aortas at 3, 8, and 18 months of age. There were no genotype-associated or age-associated changes in elastin staining as compared to batch controls. The inset displayed in the lower right corner is a magnified view of the thoracic aortic wall to demonstrate histological details from the outlined black box.
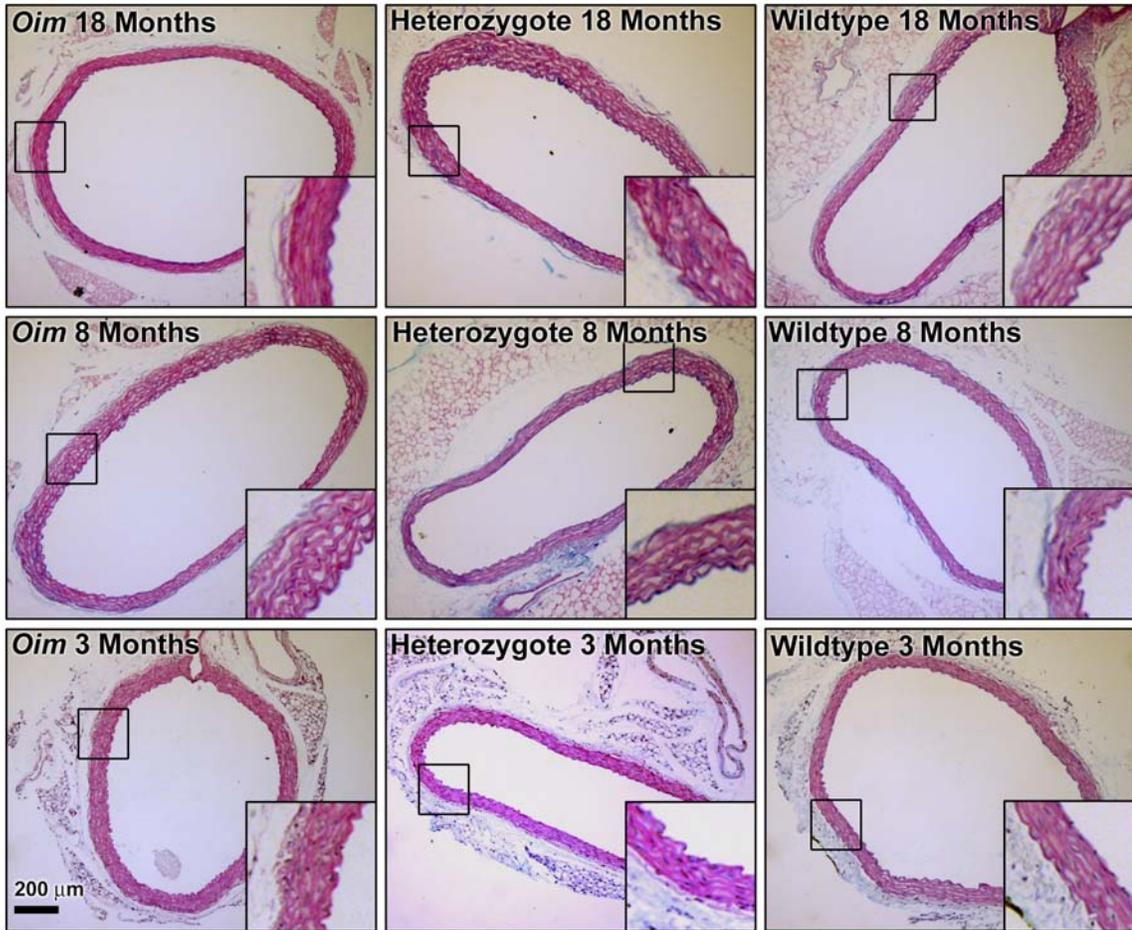
Figure 4.4 Alcian Blue Stain of Thoracic Aorta Sections. Alcian blue pH 1.0 and Periodic Acid Schiff (PAS) counter stain demonstrating proteoglycan content in O*im*, Heterozygote, and Wildtype descending thoracic aortas at 3, 8, and 18 months of age. There were no genotype-associated or age-associated changes in proteoglycan content. The inset displayed in the lower right corner is a magnified view of the thoracic aortic wall to demonstrate histological details from the outlined black box.
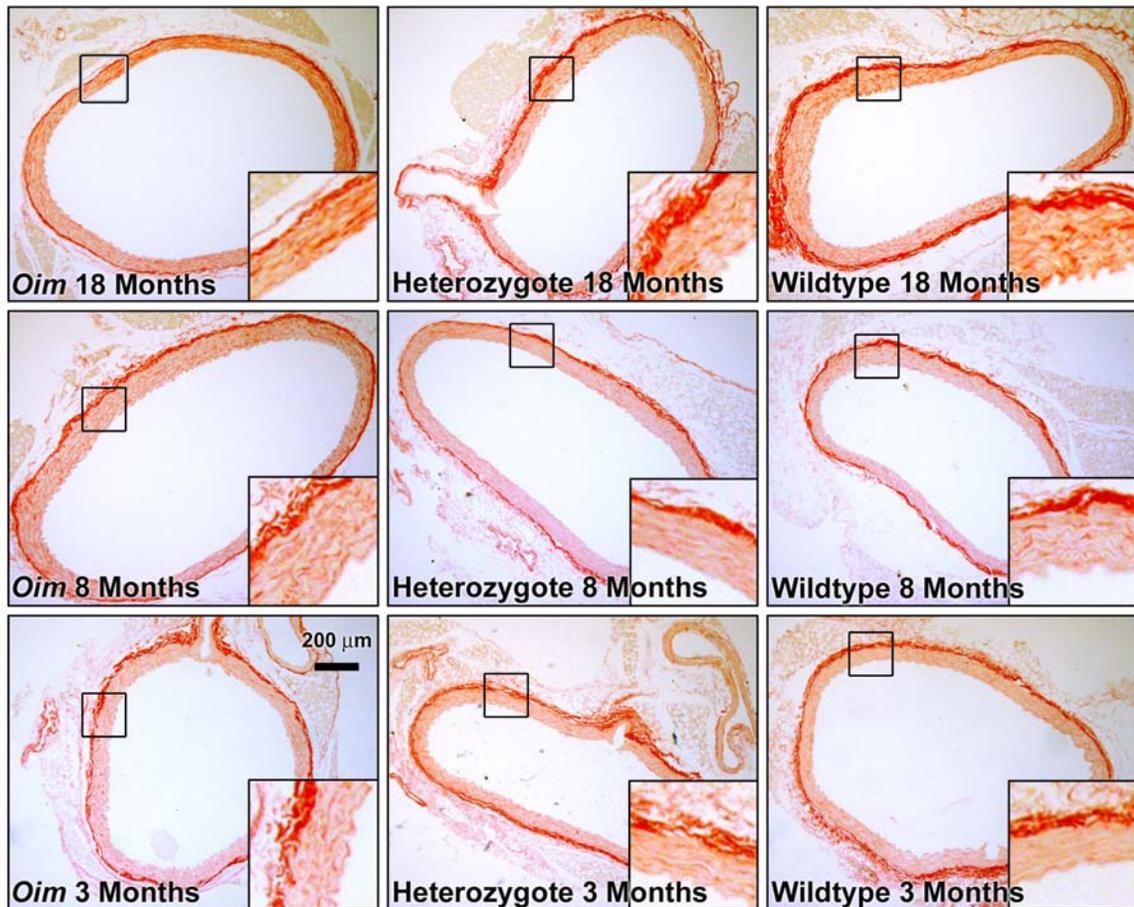
Figure 4.5 Picrosirius Red Stain of Thoracic Aorta Secitons. Picrosirius red (PSR) stain visualized by brightfield demonstrating fibrillar collagens in O*im*, Heterozygote, and Wildtype descending thoracic aortas at 3, 8, and 18 months of age. There were genotype-associated and age-associated changes in fibrillar collagen staining. *Oim* descending thoracic aortas demonstrated less fibrillar collagen staining localized to the adventitia layer. All genotypes demonstrate an increase in fibrillar collagen staining at 18 months of age as compared to 3 months. The inset displayed in the lower right corner is a magnified view of the thoracic aortic wall to demonstrate histological details from the outlined black box.
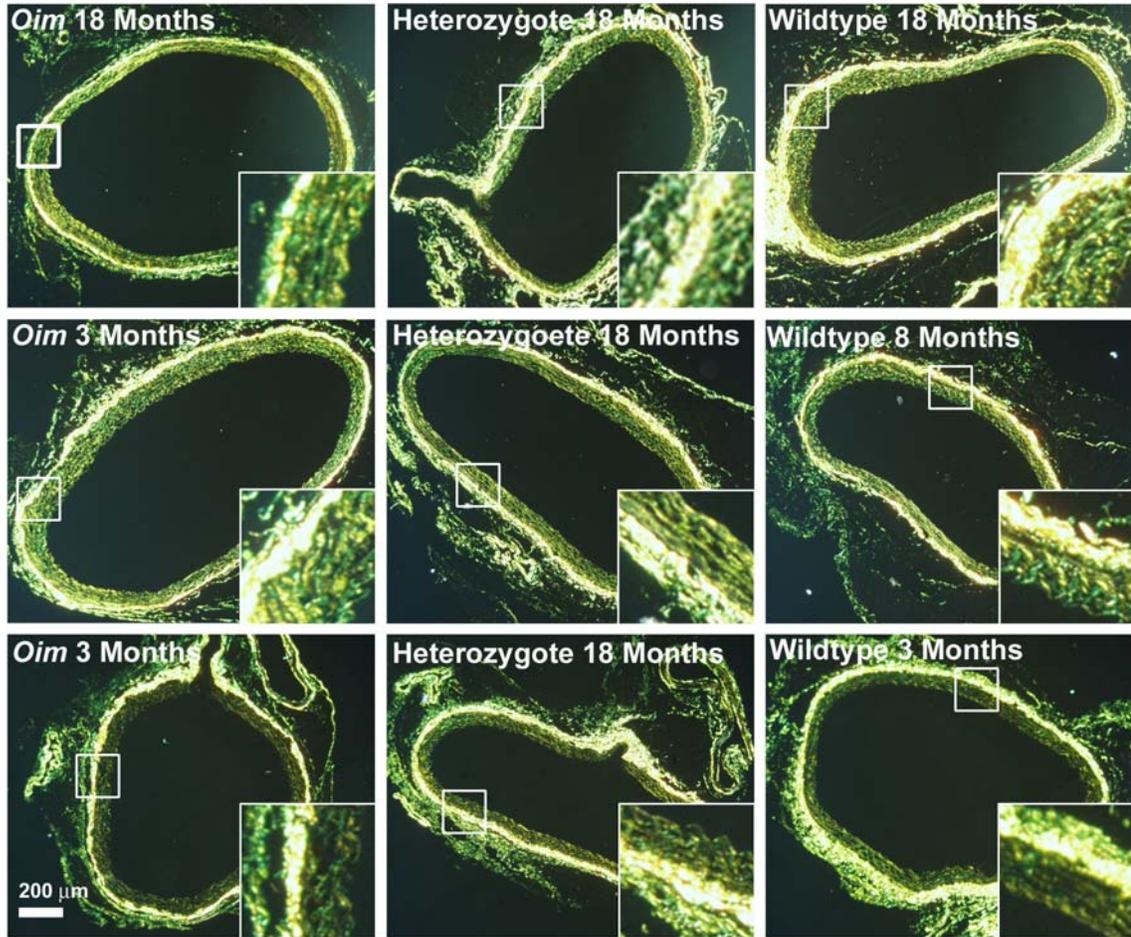
Figure 4.6 Picrosirius Red Stain of Thoracic Aorta Sections Viewed with Polarized Light.

Picrosirius red stain under polarized light (PSRP) demonstrating fibrillar collagens in O*im*, Heterozygote, and Wildtype descending thoracic aortas at 3, 8, and 18 months of age. Areas of fibrillar collagen staining are easily viewed under polarized light and allows for improved visualization of the vessel adventitia layer. There were genotype-associated and age-associated changes in fibrillar collagen staining. *Oim* descending thoracic aortas demonstrated less fibrillar collagen staining localized to the adventitia layer. All genotypes demonstrate an increase in fibrillar collagen staining at 18 months of age as compared to 3 months. The inset displayed in the lower right corner is a magnified view of the thoracic aortic wall to demonstrate histological details from the outlined black box.

4.6).

Morphometry studies of aortic diameter and wall thickness demonstrated significant age-associated increases in aortic diameter and aortic wall thickness independent of genotype (Figure 4.7). The only genotype-associated difference was aortic diameter of *oim* (569±32μm) and heterozygote (566±37μm) descending aortas at 3 months of age, which were significantly smaller than wildtype aortas (656±77μm). However, this genotype-associated difference was not maintained at 8 and 18 months. Eighteen months, intra-genotypic comparisons with 3 months old aortas, demonstrated a significant increase in aortic diameter for all genotypes. The percent increases in aortic diameters by 18 months were: *oim* 18%, heterozygote 25%, and wildtype 9% as compared to 3 months. Aortic wall thickness did not exhibit genotype-associated differences, but there were age-associated increases exhibited at 18 months (*oim* 74±4μm, heterozygote 74±9μm, and wildtype 76±5μm) when compared to the 3 month wall thickness (*oim* 68±8μm, heterozygote 66±6μm, and wildtype 70±5μm). However, the wildtype intra-genotypic age-associated comparison was not significant.

Total Collagen Content and Pyridinoline crosslink/Collagen Molecule

We previously confirmed that the hydroxyproline content is a valid measure of collagen content and found no genotype-associated differences in
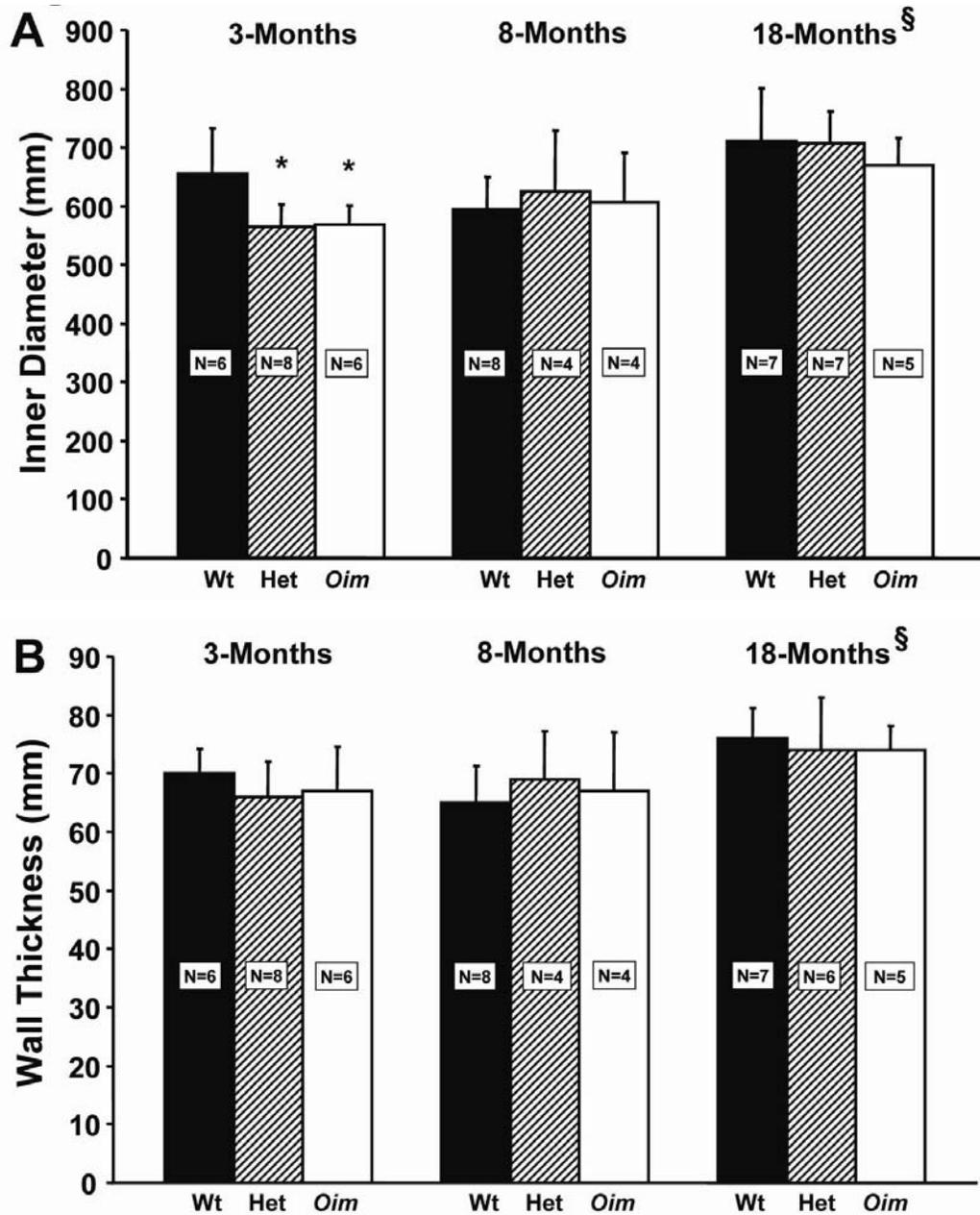
Figure 4.7 Thoracic Aorta Morphometry, Inner Diameter and Wall Thickness at 3, 8, and 18 Months of Age. Inner diameter (A) and aortic wall thickness (B) of descending *oim*, heterozygote, and wildtype aortas at 3, 8, and 18 months of age. Values are expressed as means ± standard deviation in millimeter. (*) indicates a p-value <0.05 relative to wildtype. (§) indicates a p-value <0.05 relative to the same genotype in the 3 month age class.

hydroxyproline content between wildtype, heterozygote, and *oim* mice (Pfeiffer,

Franklin et al. 2005). Total collagen content/tissue weight and hydroxylysyl-

pyridinoline (pyridinoline) content/collagen molecule demonstrated significant

genotype and age-associated differences (Figure 4.8 and 4.9). *Oim* and

heterozygote ascending and descending thoracic aortas maintained decreased

collagen content/tissue weight relative to age matched wildtype mice at 3, 8, and

18 months of age, respectively (Figure 4.8). *Oim* ascending and descending

aortas exhibited significant reductions in collagen content/tissue weight;

ascending reductions were 35%, 34%, and 24% and descending reductions were

34%, 26%, and 30% relative to age-matched wildtype controls (Figure 4.8).

Heterozygote ascending and descending aortas exhibited decreased collagen

content with intermediate values ranging in reduction of 0-21% as compared to

wildtype (Figure 4.8). In addition to the genotype-associated reduction in

collagen, there was an age-dependent increase in total collagen content/tissue

weight for all genotypes by 8 months of age in both ascending and descending

aortas. The percent increase from 3 months to 18 months of age in collagen

content/tissue weight for ascending and descending aortas were: *oim*, 209% and

211%; heterozygote, 189% and 202%; and wild type, 166% and 194%;

respectively.

Lysyl oxidase initiated collagen crosslinks, hydroxylysyl-pyridinoline

(pyridinoline), maintained an increased number of crosslinks/collagen triple helix

in oim and heterozygote ascending and descending thoracic aortas relative to

age-matched wildtype aortas for each age class (Figure 4.9). *Oim* ascending
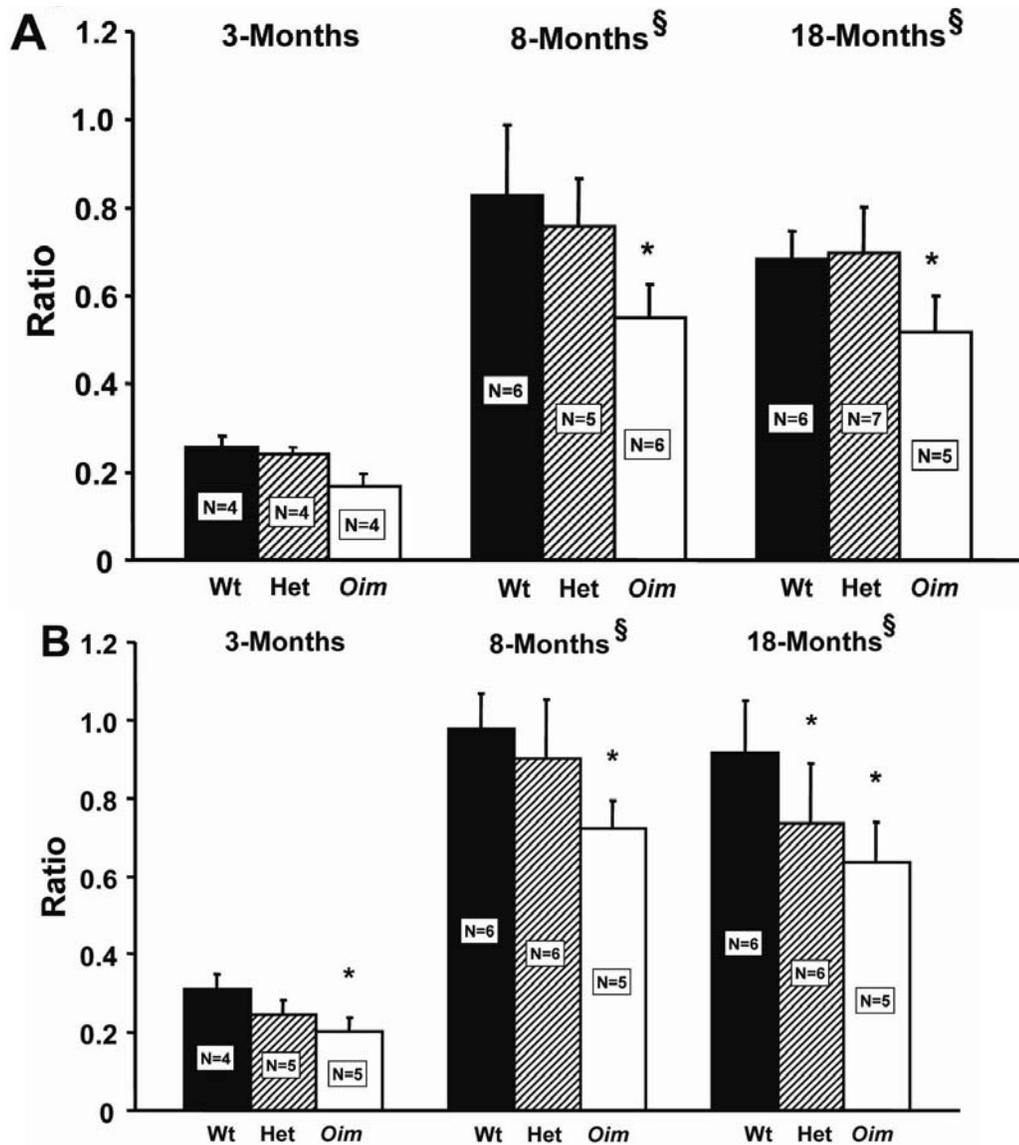
Figure 4.8 Collagen Content In Thoracic Aortas at 3, 8, and 18 Months of Age. Collagen content is significantly reduced in *oim* ascending (A) and descending (B) aortas as compared to wildtype for most age classes, except *oim* ascending 3 month old aortas; however, there was a trend of reduced collagen. In addition, ascending and descending aortas increased in collagen content at 8 and 18 months of age relative to 3 months for all genotypes. Values are expressed as mean ± standard deviation of collagen (mg) per dried tissue content (mg). (*) indicates a p-value <0.05 relative to wildtype. (§) indicates a p-value <0.05 relative to the same genotype in the 3 month age class.
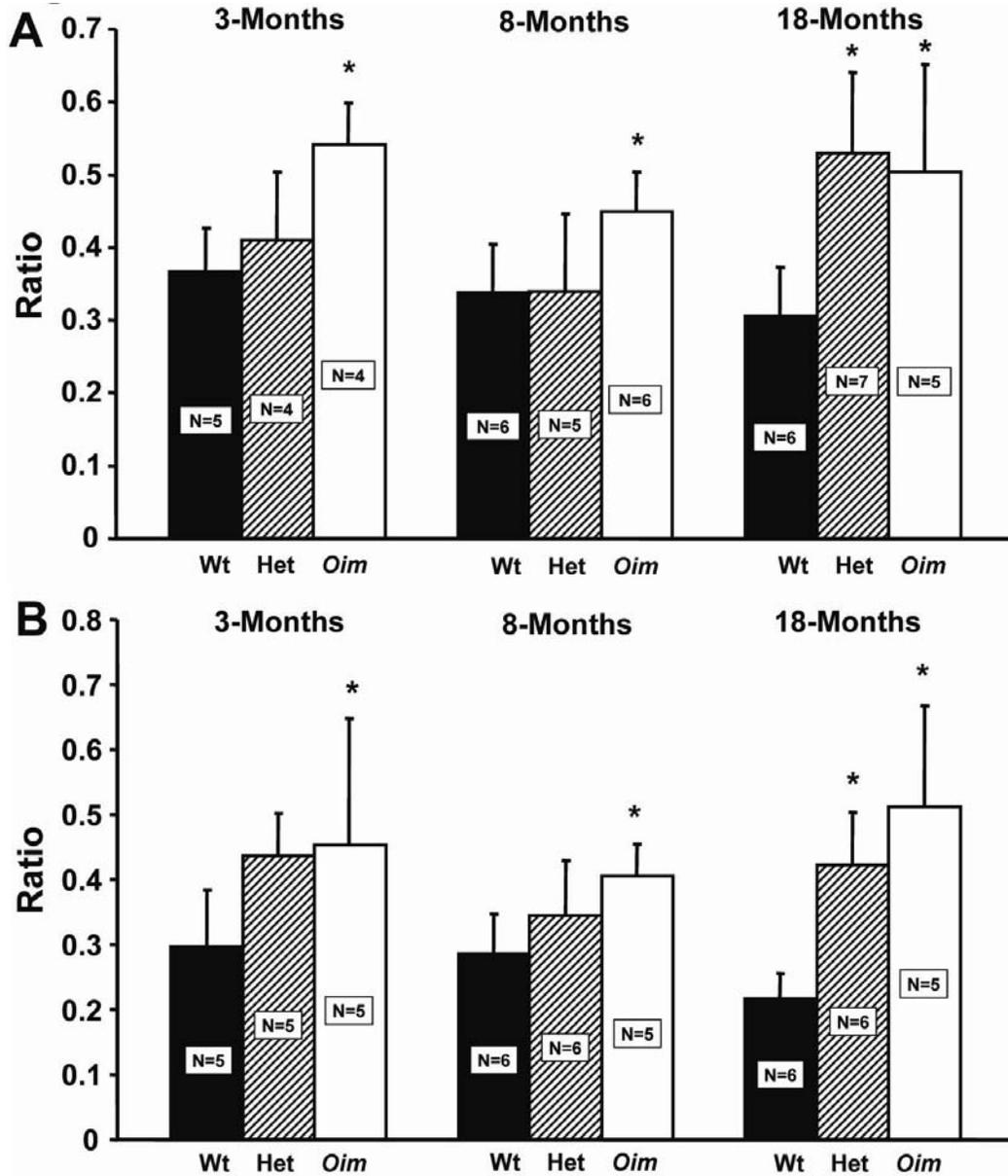
Figure 4.9 Hydroxylysyl-Pyridinoline Crosslinks/Collagen Molecule in Thoracic Aortas at 3, 8, and 18 Months of Age. Ratios of hydroxylysyl-pyridinoline crosslinks/collagen molecule are significantly increased in *oim* ascending (A) and descending (B) aortas as compared to wildtype. Heterozygote descending aortas demonstrate a trend of increased crosslinks intermediate of *oim* and wildtype. No lysyl-pyridinoline crosslinks were detected in our samples. Values are expressed as mean ± standard deviation of pryridinoline/collagen molecule. (*) indicates a p-value <0.05 relative to wildytpe.

and descending aortas demonstrated increases of 48%, 33%, and 64% and

53%, 47%, and 136% in pyridinoline crosslinking/collagen molecule relative to

wildtype aortas at 3, 8, and 18 months, respectively (Figure 4.9). Heterozygote

ascending and descending aortas did not demonstrate a significant increase in

pyridinoline crosslinking/collagen molecule until 18 months of age as compared

to wildtype (increases of 77% and 94%, respectively).

In situ Hybridization (ISH) and Quantitative RT-PCR (qRT-PCR)

In situ hybridization was performed on formalin fixed aortic tissue to

localize proα1(I) collagen, proα2(I) collagen, proα1(III) collagen, and elastin

mRNA steady-state expression. No significant differences in steady-state mRNA

expression or localization were demonstrated (Figures 4.10, 4.11, 4.12, and

4.13).

Quantitative RT-PCR further confirmed that there were no significant

genotype-associated differences in proα1(I) collagen, proα1(III) collagen, elastin,

and lysyl oxidase steady-state mRNA levels in ascending and descending

thoracic aortas of *oim*, heterozygous, and wildtype mice (Table 4.3). However,

proα2(I) collagen steady-state mRNA levels in *oim* ascending and descending

aortas at 3 months of age were significantly reduced as compared to age

matched wildtype, with a similar trend at 18 months of age (Table 4.3). Age-

associated reductions in mRNA steady-state expression were significant for

proα1(I) collagen in *oim*, heterozygote, and wildtype ascending and
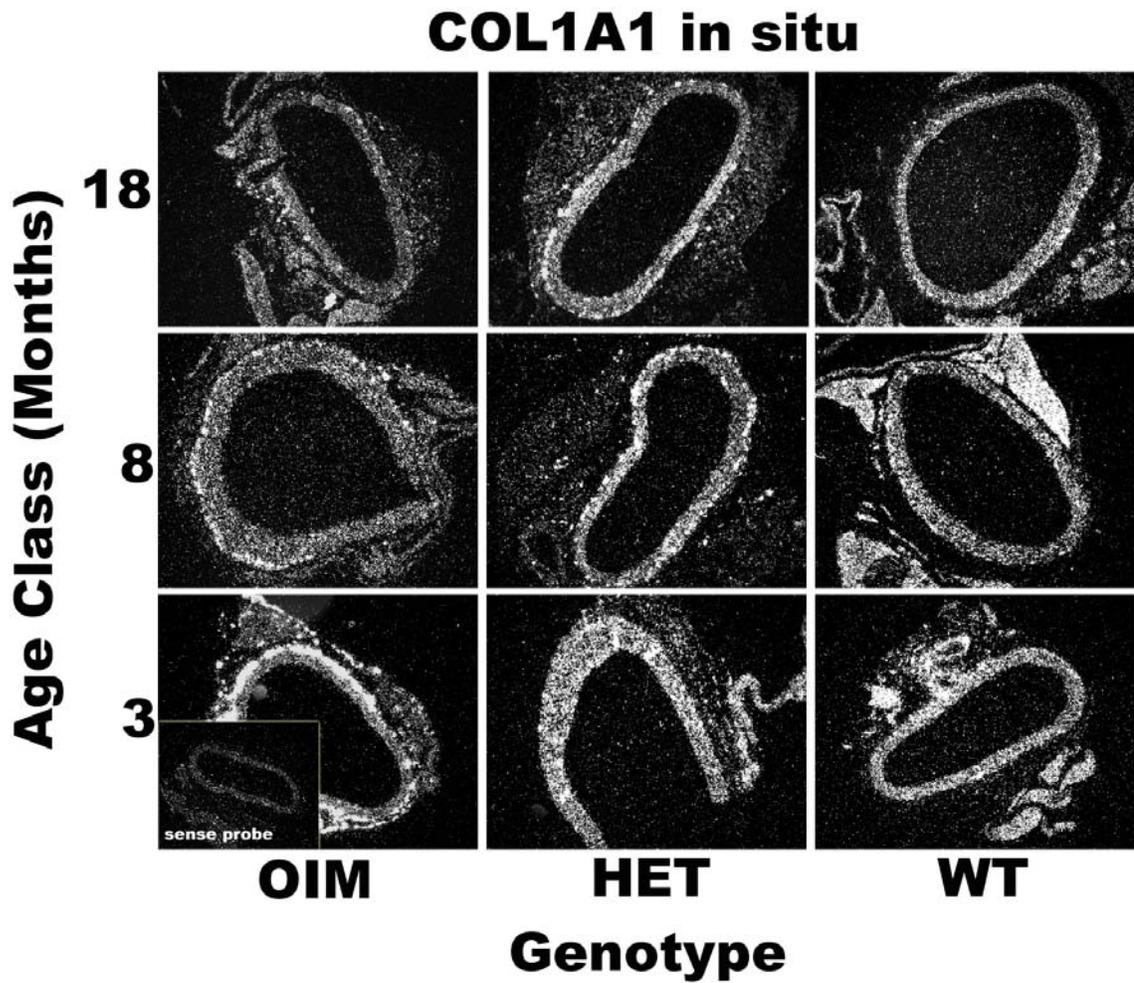
COL1A1 *in situ*

Figure 4.10 COL1A1 *in situ* **Hybridization. COL1A1** *in situ* **hybridization (*ISH*)**

demonstrating steady-state proα1(I) collagen mRNA expression localized in *Oim*,

Heterozygote, and Wildtype descending thoracic aortas at 3, 8, and 18 months of age.

There were no genotype-associated or age-associated changes in steady-state mRNA

expression. The inset in the lower left hand corner is the control sense probe

hybridized to an *oim* thoracic aorta segment.
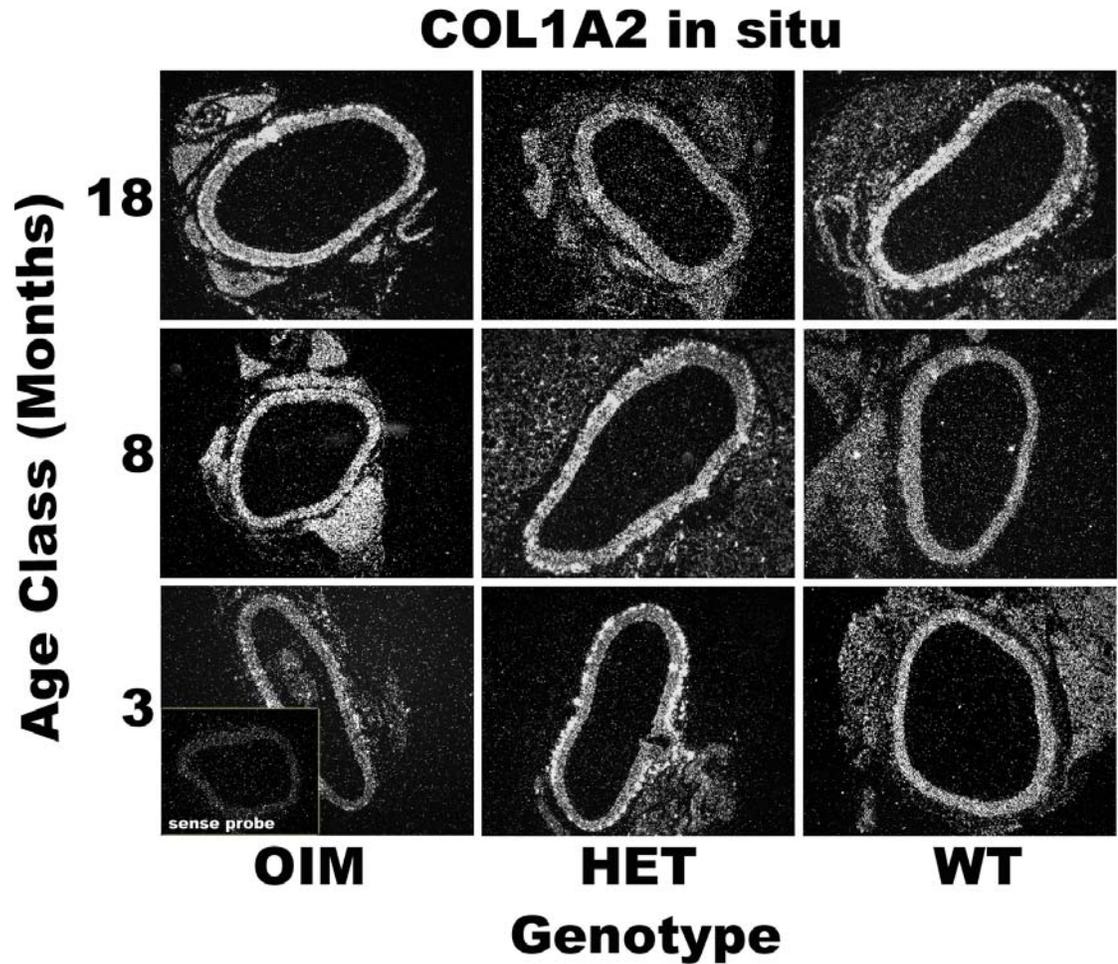
Figure 4.11 COL1A2 *in situ* Hybridization. COL1A2 *in situ* hybridization (*ISH*) demonstrating steady-state proα2(I) collagen mRNA expression localized in *Oim*, Heterozygote, and Wildtype descending thoracic aortas at 3, 8, and 18 months of age. There were no genotype-associated or age-associated changes in steady-state mRNA expression. The inset in the lower left hand corner is the control sense probe hybridized to a wildtype thoracic aorta.
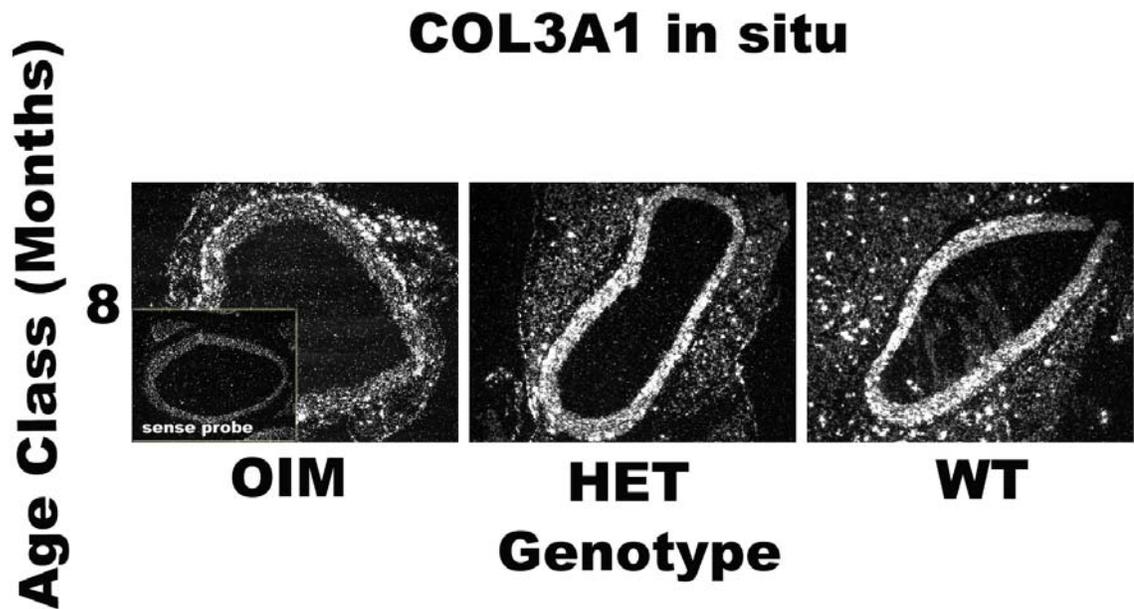
Figure 4.12 COL3A1 *in situ* Hybridization. COL3A1 *in situ* hybridization (*ISH*) demonstrating steady-state proα1(III) mRNA expression localized in O*im*, Heterozygote, and Wildtype descending thoracic aortas at 8 months of age. There were no genotype-associated changes in steady-state mRNA expression. The inset in the lower left hand corner is the control sense probe hybridized to an *oim* thoracic aorta. Thoracic aortas from 3 and 8 months of age were performed for each genotype; however, the data from the experiments was disregarded due to technical errors and was not repeated because of later real-time PCR data.
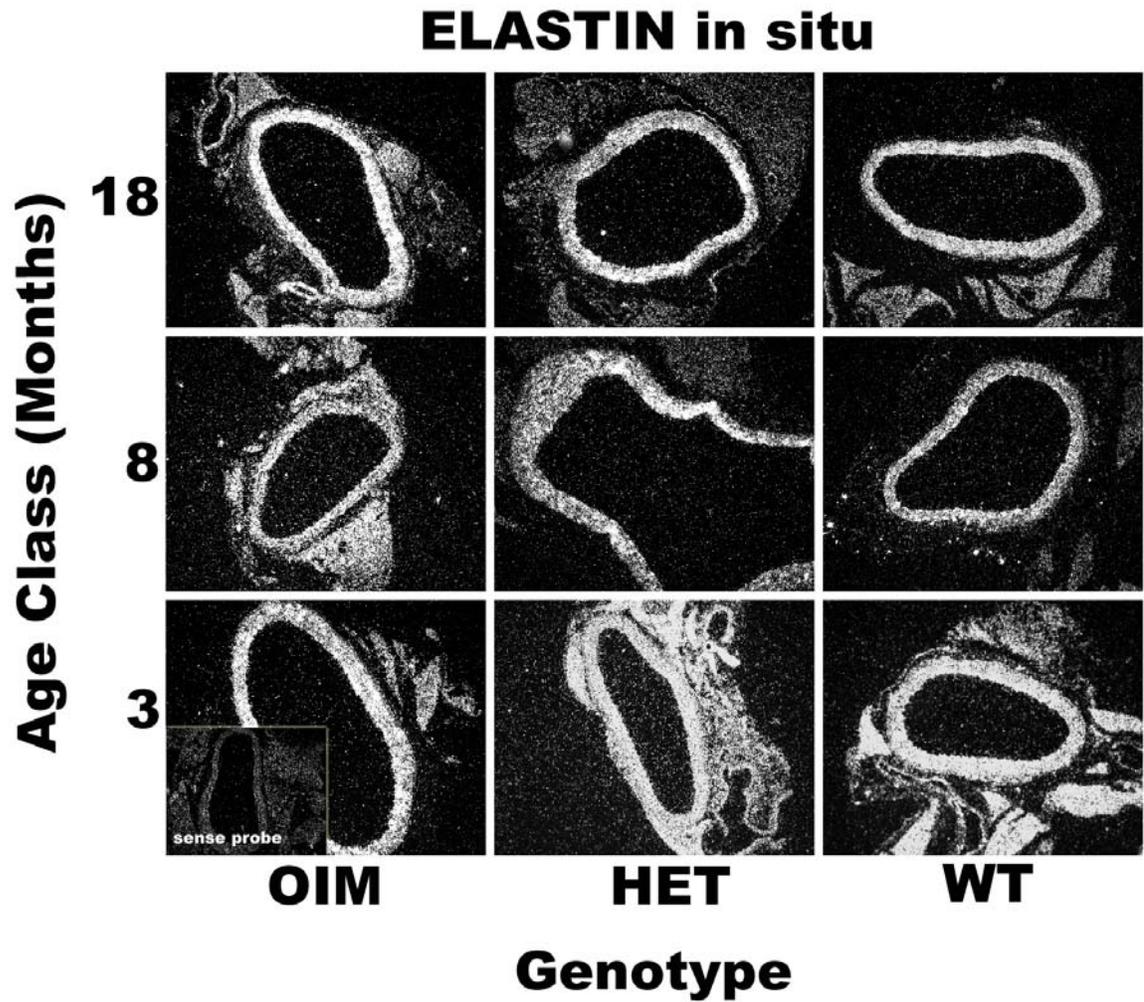
ELASTIN in situ

**Figure 4.13 ELASTIN *in situ* Hybridization. ELASTIN *in situ* hybridization (*ISH*) demonstrating steady-state elastin mRNA expression localized in O*im*, Heterozygote, and Wildtype descending thoracic aortas at 3, 8, and 18 months of age. There were no genotype-associated or age-associated changes in steady-state mRNA expression. The inset in the lower left hand corner is the control sense probe hybridized to a heterozygote thoracic aorta.**

Table 4.3 Quantitive Real-Time PCR Evaluating pProα1(I) collagen, Proα2(I) collagen, Proα1(III) collagen, Elastin and ILsyl Oxidase Steady-State mRNA

mRNA Transcripts	Oim		Heterozygote		Wildtype	
	3 Months	18 Months	3 Months	18 Months	3 Months	18 Months
Ascending COL1A1	16.8 ± 4.0	8.4 ± 1.2 ¥	14.8 ± 3.6	8.2 ± 1.0 ¥	15.1 ± 3.9	6.2 ± 1.5 ¥
Descending COL1A1	19.5 ± 3.5	8.0 ± 1.5 ¥	13.8 ± 2.4	6.6 ± 0.9 ¥	16.1 ± 4.0	11.6 ± 2.8 ¥
Ascending COL1A2	0.23 ± 0.04 *	0.18 ± 0.01	0.25 ± 0.04	0.15 ± 0.02	0.93 ± 0.35	0.76 ± 0.38
Descending COL1A2	0.28 ± 0.06 *	0.20 ± 0.04	0.37 ± 0.05	0.24 ± 0.06	0.69 ± 0.25	0.49 ± 0.14
Ascending COL3A1	2.43 ± 0.62	1.18 ± 0.53	2.24 ± 1.19	0.56 ± 0.17	4.04 ± 2.48	0.88 ± 0.30
Descending COL3A1	3.54 ± 1.56	1.28 ± 0.58	3.15 ± 1.57	1.02 ± 0.43	3.80 ± 1.95	1.64 ± 0.97
Ascending Elastin	258 ± 36	126 ± 18 ¥	328 ± 97	123 ± 31 ¥	209 ± 33	114 ± 20 ¥
Descending Elastin	237 ± 25	106 ± 8	444 ± 156	111 ± 36 ¥	218 ± 60	191 ± 58
Ascending Lysyl Oxidase	0.10 ± 0.02	0.10 ± 0.02	0.07 ± 0.02	0.06 ± 0.03	0.07 ± 0.03	0.05 ± 0.01
Descending Lysyl Oxidase	0.12 ± 0.02	0.08 ± 0.01	0.13 ± 0.03	0.07 ± 0.02	0.13 ± 0.03	0.06 ± 0.02

Specific transcript values were calculated using external standards and a standard curve. Transcript values were standardized to the aortic sample's HRPT expression. Values are expressed as mean / HPRT ± standard error. (¥) represents a p-value <0.05 for difference in age compared to the same genotype in the 3-month age.

descending aortas at 18 months as compared to 3 months. However, mRNA

steady-state expression for proα2(I) collagen, proα1(III) collagen, and elastin

demonstrated trends of age-associated reductions in expression, but were not

significantly different. Lysyl oxidase did not demonstrate genotype- or age-

associated differences or trends in steady-state mRNA levels.

Advanced Glycation End Products

Analyses using immunohistochemistry (IHC) demonstrated AGE epitopes

localized to the aortic adventia in 3, 8, and 18 month old mice in all genotypes

(Figure 4.14). In addition, surrounding adipose tissue demonstrated AGE

staining, a known cross reaction process with lipid peroxides. In 18 month aortas

AGE epitopes localized to the collagenous material within the aortic media, which

was not well visualized in 3 and 8 month aortas. In addition, AGE modification

was confirmed to be present in isolated aortic collagen from 3, 8, and 18 month

old *oim*, heterozygote, and wildtype aortas via direct chemiluminescent ELISA

and western blot (data not shown). However, neither of these analyses were

quantitative.
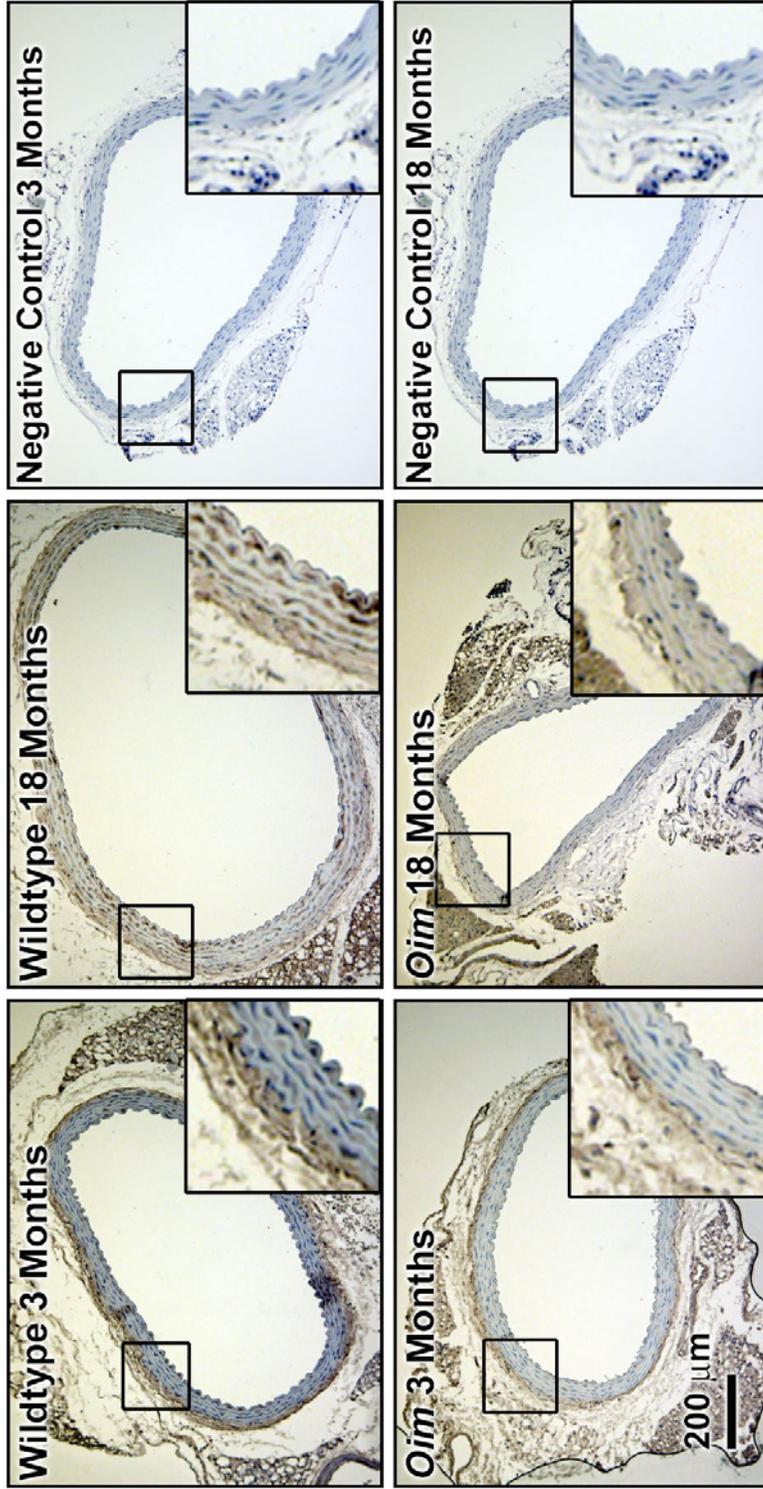
Figure 4.14 Immunohistochemistry (*IHC*) of Advanded Glycation End-Products. Immunohistochemical evaluation of Advanced Glycation End-products (AGE) using a monoclonal anti-AGE (6D12) antibody demonstrates AGE epitopes localized to the aortic adventia in 3 and 18 month old mice in all genotypes (only *oim* and wildtype aortas are shown for image clarity). The right lower corner inset demonstrates positive AGE marker, indicated via brown staining, localized to the media and adventitia layers. The anti-AGE mAb also localized to the surrounding adipose tissue and has previously been shown to bind to lipid peroxide epitopes. Magnification is at 100X.

Discussion

Collagen is primarily responsible for contributing to aortic wall integrity by increasing vessel strength and stiffness (Fung 1993). The reduction of F_{max} and IEM in *oim* aortas demonstrates the important role of collagen in determining proper circumferential aortic integrity and is consistent with the greatest impact occurring in the descending thoracic aorta, due to the increase in collagen/elastin ratios as the distance from the heart increases (Fung 1993). Another relevant observation was the significant increase in aortic weight in the 18 month age class regardless of genotype. We originally standardized our biomechanical data to both aortic weight (mg, milligrams) and aortic length (5-mm, millimeters). When evaluating biomechanical parameters in relation to aortic weight we observed decreasing strength and stiffness with increasing age. This was contrary to well documented studies demonstrating increased aortic stiffness with increasing age (Bruel and Oxlund 1996; Bailey, Paul et al. 1998; Corman, Duriez et al. 1998). When we normalized F_{max} and IEM values to aortic length, a more physiological relevant parameter, *oim* and heterozygote aortas exhibited age-associated increases in aortic strength and stiffness consistent with aging studies in humans and rats (Bruel and Oxlund 1996; Bailey, Paul et al. 1998). Wildtype aortas did not demonstrate significant increases in F_{max} and IEM with aging, which may be related to the outbred noncongenic B6C3 genetic background of the *oim* mice; outbred mice generally live longer then congenic strains (Silver 1995). The genotype-associated improvement in aortic integrity with aging in *oim*

109

and heterozygote aortas is not unlike the structural/functional improvement of bones in certain forms of OI as noted by fracture rate reduction during the post-pubertal period (Byers 2001).

Morphometric analyses provided further insight into the increased aortic weight observed at 18 months. No genotype- or age-associated changes in cellular, elastin or proteoglycan content were observed (data not shown). Our observed increase in aortic weight is associated with increased collagen content seen in morphometric analysis of fibrillar collagen PSR staining and later confirmed by hydroxyproline quantification using HPLC.

HPLC analyses demonstrated significant reductions in total collagen content/tissue weight in both *oim* and heterozygote aortas as compared to wildtype, independent of age. This finding is consistent with other *oim* studies of bone, tail tendons, and myocardium (Chipman, Sweet et al. 1993; McBride, Choe et al. 1997; Weis, Emery et al. 2000). This suggests that our observation of reduced total collagen content/tissue weight in *oim* and heterozygote aortas may play a role in their reduced thoracic aortic integrity. However, it should be noted that age-associated increases in total collagen content/tissue weight for each genotype were significantly increased at 8 months of age by 160% or greater as compared to 3 months without corresponding increases biomechanical strength or stiffness, implying that total collagen content is not the main factor responsible for reduced thoracic aorta integrity seen in *oim* and heterozygote aortas. With such a large increase in the amount of total collagen content/tissue weight, we would expect to have observed a change in biomechanical parameters unless

collagen maturation was a factor. However, the ratios of pyridinoline crosslink/collagen molecule were not statistically different at 3, 8, and 18 months of age. This indicates that the collagen present in the aortas is fully matured. In addition heterozygote aortas demonstrated aortic biomechanical parameters intermediate of *oim* and wildtype suggesting that heterotrimeric and homotrimeric collagen molecules are both present in heterozygote aortic tissue. McBride *et al.* found evidence of this observation in heterozygote tail tendons by thermodynamic studies (McBride, Choe et al. 1997). This also implies it is the presence of the homotrimeric type I collagen molecule that is responsible for the observed alteration of aortic integrity.

Steady-state levels of extracellular matrix component mRNAs were analyzed via in situ hybridization and quantitative real-time PCR to determine if a pretranslational mechanism may explain the observed reduced collagen content in heterozygote and *oim* aortas or other differences in vascular ECM components. In situ data exhibited no genotype associated or age-associated differences in steady-state mRNA localization within the aortic architecture for proα1(I), proα2(I), and proα1(III) collagen or elastin. Collagen expression was localized mainly to the aortic media and adventia, while elastin expression was localized mainly to the aortic media. qRT-PCR proved to more informative, demonstrating reduced proα2(I) collagen mRNA expression in *oim* ascending and descending 3 month aortas as compared to age-matched wildtype. Since *oim* mice do not produce functional proα2(I) collagen chains, the decreased collagen content observed in *oim* aortas as compared to wildtype is likely related

to the stoichiometric use of proα1(I) chains, which must replace the missing

proα2(I) chains with proα1(I) chains for homotrimeric type I collagen to be

produced. However, other mechanisms may also exist that influence type I

collagen gene expression, such as cytokine sequestering (Bornstein 2002).

Collectively, our steady-state mRNA data suggests that there is no

pretranslational mechanism influencing the genotypic difference in total collagen

content in *oim* and heterozygote aortas. It also demonstrates that cells in aortic

ECM undergo an age-associated decrease in steady-state mRNA expression of

ECM components. Lysyl oxidase steady state mRNA expression was the

exception demonstrating no genotype or age-associated differences and thus

cannot explain the increased pyridinoline crosslinks/collagen molecule seen in

oim and heterozygote aortic tissue.

Collagen crosslinking, a co-translational and post-translational

modification, provides critical links important to tissue structure/function. Lysyl

oxidase (LO) initiated crosslinks have been shown to be essential for proper

tissue function, i.e.: lathyritic models, Menkes syndrome, and LOX (lysyl oxidase)

knock out mice (Bruel, Ortoft et al. 1998; Kodama and Murata 1999; Hornstra,

Birge et al. 2003). LO initiated collagen crosslinks, pyridinoline, demonstrated

significant genotype-associated increases in both *oim* and heterozygote aortas.

Oim mice exhibited increased pyridinoline crosslinks/collagen molecule relative

to age matched wildtype. This suggests that homotrimeric type I collagen

molecules have a greater potential to form intra-/intermolecular pyridinoline

crosslinks and may represent a compensatory mechanism to sustain tissue

viability for reduced biomechanical strength and stiffness. With the addition of another $\alpha 1$(I) chain replacing the $\alpha 2$(I) chain, there are 7 additional lysine/hydroxylysine residues for potential crosslinking, including one lysine/hydroxylysine residue in each telopeptide domain available for LO modification. However, it is unknown if the additional lysines participate in crosslink formation, since proximity and fibril alignment are important determinants of intermolecular crosslinks formation (McBride, Choe et al. 1997; Miles, Sims et al. 2002). Increased pyridinoline crosslinking has also been reported in *oim* left ventricle myocardium (Weis, Emery et al. 2000; Pfeiffer, Franklin et al. 2005). Kalath et al. reported increased circumferential stiffness in OI patients and postulated that the increased aortic root stiffness seen in a few OI patients may be explained by an increase in collagen crosslinking (Kalath, Tsipouras et al. 1987). It is postulated that in skin, tendon, and bone homotrimeric type I collagen alters fibril packing in addition to intermolecular crosslinking (Miles, Sims et al. 2002).

There were no age-associated differences in pyridinoline crosslinks/collagen molecules for any genotype, further evidence that pyridinoline crosslinks do not correspond with the age-associated increases in biomechanical parameters observed in *oim* and heterozygote aortas. Previous aging studies and our data support the hypothesis that pyridinoline crosslinks between adjacent collagen molecules are responsible for maturation of tissue ECM, but do not account for age-associated increases in tissue biomechanical strength and stiffness (Bailey, Paul et al. 1998; Corman, Duriez et al. 1998; Reiser 1998).

Current hypotheses for the age-associated increases in biomechanical stiffness implicate the detrimental accumulation of carbohydrate adducts and their derived crosslinks on collagen. These crosslinks, known as advanced glycation end-products (AGE), represent stable intra- and inter-molecular crosslinks, and are non-enzymatic adducts of a reducing sugars to the ε-amino group of lysines or hydroxylysines within long lived proteins. The Schiff base rearranges to an Amadori product in which further rearrangements occur forming fluorophoric structures. Several AGE crosslinks have been discovered and are hypothesized to be the reason for the deleterious function of tissues associated with aging (Bailey, Paul et al. 1998). However, no particular AGE crosslink has been identified to be exclusively formed in the vascular system. It is known that aortic collagen-associated fluorescence positively correlates with increasing aortic stiffness and age (Bruel and Oxlund 1996). Using HPLC, we attempted to detect collagen-associated fluorescence outside the pyridinoline and pentosidosine fluorescence spectra. No significant pentosidosine signal was detected. The reasons for this paucity of information likely reflect that no one particular AGE product is predominant in aortic tissue. Because of limited tissue amounts, we were unable to identify specific aortic AGE compounds. Instead, we used a monoclonal antibody, a marker of AGE formation, to provide evidence that AGE crosslinks are potentially modifying aortic collagen, and thus may impact aortic integrity with increasing age. *IHC*, western blot, and ELISA assays confirmed that the AGE marker was present in aortic collagen and localized to media and adventitia layers of the thoracic aorta via *IHC*. But, due to sample and

114

assay limitations, we were unable correlate increased AGE marker with increased AGE modification.

Studies have extensively investigated the skeletal manifestations in the *oim* mouse; however, the extra-skeletal impact of homotrimeric type I collagen and OI has been less explored. In the present study we demonstrate that the absence of $\alpha2$(I) collagen chains and/or presence of homotrimeric type I collagen molecules in the thoracic aorta are responsible for the reduced aortic integrity, which improves in *oim* and heterozygote aortas with aging, and cannot be accounted for by increases in total collagen content and aortic wall thickness alone. The increased pyridinoline crosslinks/collagen molecule may represent a tissue specific mechanism compensating for the altered vascular biomechanical properties. Therefore, we postulate that homotrimeric fibrils in *oim* and homotrimeric/heterotrimeric fibrils in heterozygote aortas are inherently weaker than heterotrimeric fibrils despite the observed increase in pyridinoline crosslinking/collagen molecule associated with homotrimeric type I collagen. Interestingly, pyridinoline crosslinks/collagen molecule did not increase with increasing age and cannot account for observed increased biomechanical stiffness. We postulate that the increased aortic wall strength and stiffness in heterozygote and *oim* ascending and descending aortas at 18 months is likely due to other mechanisms, such as non-specific collagen crosslinking from advanced glycation endproducts (AGE).

CHAPTER V

SUMMARY AND FUTURE DIRECTIONS

Arterial components that determine vascular integrity are collagen and elastin. Age-associated increases in vascular stiffness are accompanied by altered collagen content and structure, but the relationship between these changes remains unclear. Type I collagen, a major component of vascular tissue, is a heterotrimeric molecule composed of two proα1(I) chains and a proα2(I) chain, undergoing co- and posttranslational modifications, fibrillar assembly, and cross-link formation. The osteogenesis imperfecta model mouse (*oim*) provided an excellent system for the examination of type I collagen's proα2(I) chains impact upon thoracic aortic integrity. We hypothesized that the absence of the proα2(I) chain alters cardiovascular integrity by interfering with fibrillar assembly, collagen content, and/or cross-linking formation. By addressing the following specific aims we were able to illustrate the importance of the proα2(I) collagen chain in determining aortic wall integrity.

Will *oim* mice with their reduced breaking strength and stiffness exhibit age-associated increases in vascular stiffness as age-matched heterozygote and wildtype mice? Hypothesis: *Oim*, heterozygous, and wildtype mice will have age-associated increases in their thoracic aorta stiffness. The reduction of F_{max} and IEM in *oim* aortas demonstrates the important role of type I collagen in determining proper circumferential aortic integrity and is consistent with the greatest impact occurring in the descending thoracic aorta, since collagen/elastin ratios increase as the distance from the heart increases. However, even with increasing age *oim* aortas were significantly reduced in breaking strength and stiffness as compared to age-matched wildtype controls. *Oim* and heterozygote

117

ascending and descending thoracic aortas demonstrated age-associated increases in both breaking strength and stiffness. This genotype-associated improvement in aortic integrity with aging in *oim* and heterozygote aortas is not unlike the structural/functional improvement of bones in some forms of OI as noted by fracture rate reduction during the post-pubertal adulthood periods.

Wildtype thoracic aortas did not demonstrate age-associated increases in breaking strength or stiffness; however, there is evidence of AGE modification in the wildtype thoracic aortas. This potentially reflects that wildtype thoracic aortas may require a longer aging period in order to demonstrate age-associated increases in strength and stiffness. This is most likely because mouse outbred/hybrid strains, in which the *oim* mutation is maintained, generally live longer than cogenic inbred strains.

Will age-associated changes in biomechanical properties of *oim*, heterozygote, and wildtype aortas reflect changes in collagen content and/or cross-linking, and will these alterations be age dependent or reflect genotypic differences? Hypothesis: Increases in *oim*, heterozygote, and wildtype thoracic aortic stiffness will reflect age-associated increases in collagen content and cross-links, yet the *oim* aortic strength and stiffness relative to age-matched wildtype aortas will maintain genotypic differences in collagen content and cross-links. *Oim* ascending and descending thoracic aortas maintained genotype-associated reduction in collagen content as compared to age-matched wildtype aortas. However, all genotypes experienced age-associated increases in collagen content per tissue weight at 8 and 18 months of age. In addition,

118

collagen specific crosslinking in *oim* ascending and descending thoracic aortas demonstrated significantly increased content per collagen molecule as compared to age-matched wildtype. This may represent a compensatory mechanism in response to reduced aortic integrity or a mechanism in which there is a greater potential to form collagen specific crosslinks. All genotypes maintained the same level of collagen specific crosslink content per collagen molecule at 3, 8, and 18 months of age. This indicates that the collagen present in the thoracic aortas was fully matured, and that the increased strength and stiffness observed in *oim* and heterozygote aortas at 18 months is most likely due to other mechanisms, such as non-enzymatic collagen crosslinking AGE modification. Unfortunately, via HPLC analyses we were unable to detect specific AGE increases. However, by immunological techniques we were able to demonstrate the presence of AGE modification, which localized to the aortic collagen molecules or α chains.

Will age-associated and genotype-associated differences in collagen expression reflect differences at the pre-translational level? Hypothesis: *oim*, heterozygote, and wildtype aortas will reflect age-associated decreases in pre-translational collagen expression, yet *oim* aortas will reflect genotypic differences in pre-translational collagen expression as compared to age-matched wildtype controls. *Oim* thoracic aortas did not demonstrate significant genotype-associated differences in procollagen α1(I), procollagen α1(III), or elastin steady-state mRNA expression. There was a significant reduction in procollagen α2(I) steady state mRNA expression in *oim* thoracic aortas; however, this does not result in functional proα2(I) collagen chain expression in *oim* tissues. All

genotypes demonstrate either a significant or trend of reduced ECM steady state mRNA expression at 18 months of age. This suggest that the reduced collagen content in *oim* and heterozygote thoracic aortas is likely due to the stoichiometric use of an additional $pro\alpha1(I)$ collagen chain to form homotrimeric type I collagen molecules. However, a possible signaling pathway or ligand sequestration mechanism may cause a reduction in collagen and was not specifically examined in this study.

Future directions for this project include the following. 1) Create an iRNA for $pro\alpha2(I)$ mRNA in the *oim* mouse attempting to mimic the EDS phenotype and molecular defect demonstrated by Shwarze et al. 2004. This may identify a unique molecular mechanism that differentiates between a bone (OI) or skin (EDS) phenotype based upon mRNA expression and translation of the $pro\alpha2(I)$ collagen chain. 2) Create a knock in mouse with specific regions of the $pro\alpha2(I)$ collagen chain, such as the C- and/or N-telopeptide domains. The chimeric $pro\alpha2(I)$-$pro\alpha1(I)$ chains produced in the newly created knock-in mouse may establish important tissue specific sites in the $pro\alpha2(I)$ collagen chain. 3) Confirm the presence of homotrimeric type I collagen in heterozygote and possibly in wildtype tissues. This may be done via an immunological assay that differentiates heterotrimeric and homotrimeric type I collagen. 4) Use the *oim* as a clinical model for OI in a diseased state. For example, induce hypertension in *oim* mice and examine the response of the thoracic aorta. 5) Attempt to identify specific vascular AGE crosslinks via MALDI by pooling aortas from different genotypes.

APPENDIX

CHAPTER VI

MURINE MODEL OF THE EHLERS-DANLOS SYNDROME (EDS): COL5A1 HAPLOINSUFFICIENCY DISRUPTS COLLAGEN FIBRIL

Introduction

This portion of my work was a collaboration with Dr. Richard Wenstrup at the Division of Human Genetics, Children's Hospital Research Foundation, Cincinnati, OH. Dr. Wenstrup generated a col5a1 knock out mouse into the Kg-1/C57BL/6 genetic background (Wenstrup, Florer et al. 2006). Ehlers-Danlos syndrome (EDS) classical type is associated with a high prevalence of aortic root dilation and infrequently aortic rupture or dissection (Wenstrup, Florer et al. 2004; Wenstrup, Florer et al. 2006). Easy bruising is a hallmark of the condition and is evidenced by capillary fragility. Classic type EDS has been associated with type V collagen defects (Wenstrup, Florer et al. 2000; Wenstrup, Florer et al. 2004; Wenstrup, Florer et al. 2006). Type V collagen has been demonstrate to be involved in the regulation of type I collagen fibril diameters and fibril numbers (Wenstrup, Florer et al. 2000; Wenstrup, Florer et al. 2004; Wenstrup, Florer et al. 2006). Homozygous Col5a1 -/- mice died in utero demonstrating cardiovascular involvement. Col5a1 -/- mice embryos and yolk sacs demonstrated blood pooling and reduced circulation at E10 before cessation of the heart's rhythmic contractions, indicating that cardiovascular insufficiency was a factor in embryonic demise (Wenstrup, Florer et al. 2004). However, heterozygous col5a1 +/- survive and were available for thoracic aortic analyses (Wenstrup, Florer et al. 2004; Wenstrup, Florer et al. 2006). To determine whether aortic integrity was measurably altered in col5a1 haploinsufficient animals, biomechanical analyses were performed on ascending and descending

aortas from 12 week old animals (Wenstrup, Florer et al. 2004; Wenstrup, Florer et al. 2006).

Materials and Methods

Dr. Wenstrup provided col5a1 +/- and +/+ mice at 12 weeks of age. The thoracic cavities of the mice were shipped by overnight delivery on ice in 50ml conical tubes filled with Dulbecco's Modified Eagle Medium (DMEM). Aortas were harvested immediately upon arrival, as previously described (Vouyouka, Pfeiffer et al. 2001). To ensure that aortic integrity was not altered by the 24 hour DMEM 4°C incubation, we treated six heterozygote (oim/+) thoracic cavities as described above and compared breaking strength and stiffness data with that from the heterozygote (oim/+) 3 month old aortas described in Chapter III of this dissertation. Our findings demonstrated no significant difference between breaking strength and stiffness when aortas were harvested immediately after sacrifice and aortas harvested 24 hours after DMEM incubation at 4°C (data not shown). Circumferential biomechanical analysis was performed as previously described (Vouyouka, Pfeiffer et al. 2001). Biomechanical data analyzed using Microsoft Excel (Microsoft Corporation, Seattle, WA) to determine F_{max} and IEM. Data tabulated and analyzed for statistical differences using SAS (SAS Institute Inc., Charlotte, NC) testing the treatment of genotype via ANOVA. Results were reported as means ± standard deviation.

Results

Col5a1 haploinsufficiency aortas demonstrated decreased aortic stiffness and breaking strength (Figure 1). There was a 36% [97.4 ± 5.7 (g) vs. 62.4 ± 4.9 (g); $p<0.05$] decrease in breaking strength and a 37% [120.3 ± 7.1 (g/mm) vs. 76.0 ± 6.5 (g/mm); $p<0.05$] decrease in incremental elastic modulus for the ascending thoracic aortas (Wenstrup, Florer et al. 2006). There was a 60% [104.2 ± 14.1 (g) vs. 42.1 ± 4.2 (g); $p<0.05$] decrease in breaking strength and a 68% [194.1 ± 18.0 (g/mm) vs. 61.1 ± 10.2; $p<0.05$] decrease in incremental elastic modulus for the descending thoracic aorta (Wenstrup, Florer et al. 2006). The greatest difference between col5a1 +/- and +/+ aortic integrity was seen in the descending thoracic aorta.

Discussion

Col5a1 haploinsufficient mice demonstrate the classical form of EDS characterized by tissue fragility, hyperextensible skin, and aortic integrity compromise. This mouse demonstrates the importance of type V collagen in determining type I fibrillogenesis, which affects fibril organization, disrupts lateral type I fibrillar growth, and reduces type I collagen content by ~50%. My portion

of this work demonstrates that type V collagen content affects aortic integrity either by altering proper type I collagen fibril morphology and/or total type I collagen content. In addition, it provides an explanation for the observed high prevalence of aortic root dilatation found in EDS type I/II patients suggesting that abnormal type I collagen fibrillogenesis is likely impairing aortic integrity. To further this study, collagen content and collagen crosslinking data may provide an explanation for the observed reduction in aortic breaking strength and stiffness.
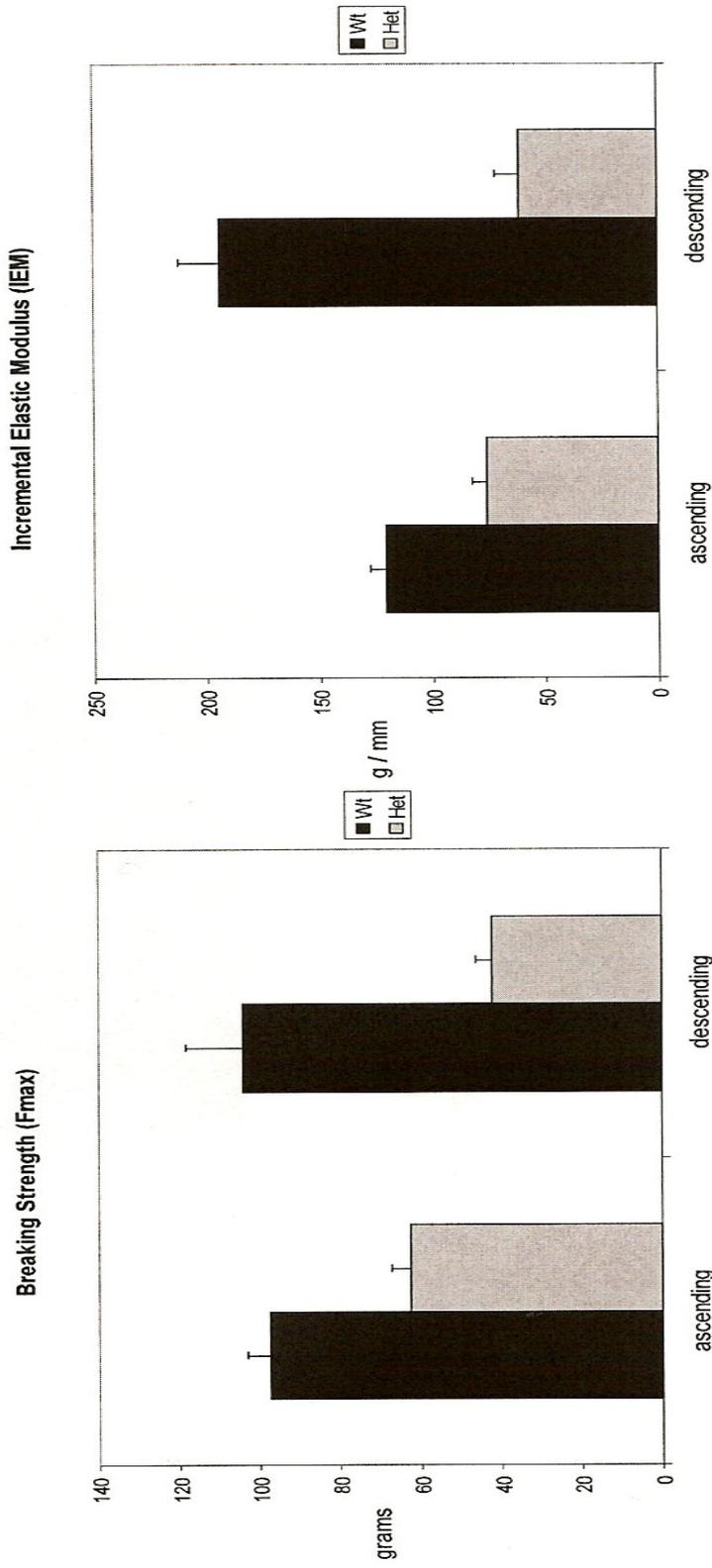
Figure 1 Summary of aortic load-extentsion curves from col5a1 +/- mice (grey columns, N=8) demonstrating reduced breaking strength and stiffness as compared to col5a1 +/+ mice (black columns, N=5). (A) is the breaking strength (Fmax) and (B) is the incremental elastic modulus (IEM) of ascending and descending thoracic aortas.

CHAPTER VII

BRTL MOUSE THORACIC AORTA STUDY

Introduction

This portion of my work was in collaboration with Dr. Joan C. Marini at the Heritable Disorders Branch and Laboratory of Mammalian Genes and Development, NIH Bethesda, MD. Dr. Marini generated a col1a1 Gly[349] → Cys substitution allele knock in mouse using the Cre/lox recombination system in a Sv129/CD-1/C57BL/6S genetic background (Forlino, Porter et al. 1999). The resultant mouse was a non-lethal murine model for osteogenesis imperfecta (OI) named Brittle IV (BrtlIV). BrtlIV IV mice demonstrate phenotype variability ranging from perinatal lethal to long term survival (Forlino, Porter et al. 1999).

Material and Methods

Dr. Marini provided BrtlIV +/- and +/+ mice at 2 and 6 months of age. The thoracic cavities of the mice were shipped by overnight delivery on ice in 50ml conical tubes filled with Dulbecco's Modified Eagle Medium (DMEM). To ensure that aortic integrity was not altered by the 24 hour DMEM 4°C incubation, we treated six heterozygote (oim/+) thoracic cavities as described above and compared breaking strength and stiffness data with that from the heterozygote (oim/+) 3 month old aortas described in Chapter III of this dissertation. Our findings demonstrated no significant difference between breaking strength and

stiffness when aortas were harvested immediately after sacrifice and aortas harvested 24 hours after DMEM incubation at 4°C (data not shown). Aortas were harvested immediately upon arrival, as previously described (Vouyouka, Pfeiffer et al. 2001). Circumferential biomechanical analysis was performed as previously described (Vouyouka, Pfeiffer et al. 2001). Biomechanical data analyzed using Microsoft Excel (Microsoft Corporation, Seattle, WA) to determine F_{max} and IEM. Data tabulated and analyzed for statistical differences using SAS (SAS Institute Inc., Charlotte, NC) testing treatments of genotype and age via a general linear model (GLM). Results were reported as means ± standard deviation.

Results

BrtIIV mice at 2 months of age demonstrated significantly reduced thoracic aortic integrity in the descending aorta (104 ± 12 g, F_{max} and 258 ± 23 g/mm, IEM), relative to wildtype-BrtIIV aortas (161 ± 11g, F_{max} and 369 ± 39 g/mm). BrtIIV ascending thoracic aortas at 2 months of age demonstrated a trend of reduced thoracic aortic integrity; however, it was not significantly different relative to wildtype aortas. By 6 months of age, the observed reduced thoracic integrity of 2 month old BrtIIV aortas had improved and did not demonstrate any genotype-associated difference as compared to wildtype aortas.

Discussion

BrtlIV mice were generated as a model for osteogenesis imperfecta (OI). The mutation generated in this mouse model represents a common genotypic cause for the OI phenotype, which is a glycine substitution. The BrtlIV mouse represents an excellent model for autosomal dominant OI resulting from a glycine substitution in which the abnormal type I collagen molecule is incorporated in the ECM. BrtlIV mice demonstrate increased bone fragility and reduced body size. As observed in OI individuals, as BrtlIV mice age there is improved mechanical integrity of bone breaking parameters. We demonstrated similar findings in the thoracic aorta of BrtlIV mice. Younger BrtlIV mice demonstrated significantly reduced breaking strength and stiffness. This difference was not maintained at 6 months of age. Unfortunately, it has not been reported whether the BrtlIV mice have reduced collagen content and/or collagen crosslinking as compared to wildtype BrtlIV mice, because this has yet to be done.
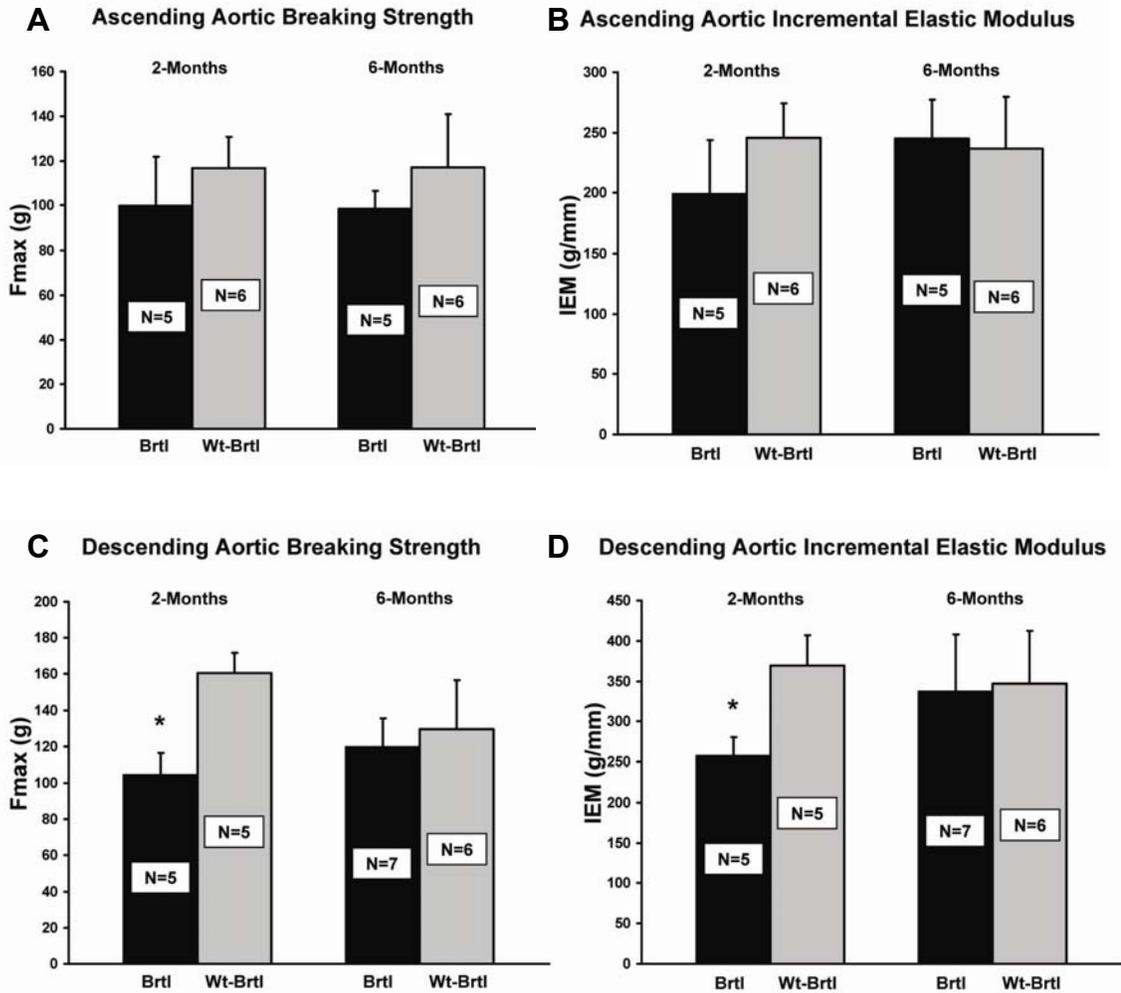
Figure 2.1 Summary of aortic load-extentsion curves from BrtIIV +/- mice (black columns) demonstrating reduced breaking strength and stiffness as compared to BrtIIV-wildtype +/+ mice (grey columns). (A and C) are the breaking strength (Fmax) at 2 and 6 months of age for ascending and descending thoracic aortas. (B and D) are the incremental elastic modulus (IEM) at 2 and 6 months of age for ascending and descending thoracic aortas.

BIBLIOGRAPHY

Alvares, K., F. Siddiqui, et al. (1999). "Assembly of the type 1 procollagen molecule: selectivity of the interactions between the alpha 1(I)- and alpha 2(I)-carboxyl propeptides." Biochemistry **38**(17): 5401-11.

Arteaga-Solis, E., B. Gayraud, et al. (2000). "Elastic and collagenous networks in vascular diseases." Cell Struct Funct **25**(2): 69-72.

Ashraf, S. S., N. Shaukat, et al. (1993). "Type I aortic dissection in a patient with osteogenesis imperfecta." Eur J Cardiothorac Surg **7**(12): 665-6.

Autio, P., J. Risteli, et al. (1994). "Collagen synthesis in human skin in vivo: modulation by aging, ultraviolet B irradiation and localization." Photodermatol Photoimmunol Photomed **10**(5): 212-6.

Bader, H. (1967). "Dependence of wall stress in the human thoracic aorta on age and pressure." Circ Res **20**(3): 354-61.

Bailey, A. J., R. G. Paul, et al. (1998). "Mechanisms of maturation and ageing of collagen." Mech Ageing Dev **106**(1-2): 1-56.

Bank, A. J., H. Wang, et al. (1996). "Contribution of collagen, elastin, and smooth muscle to in vivo human brachial artery wall stress and elastic modulus." Circulation **94**(12): 3263-70.

Bank, R. A., M. T. Bayliss, et al. (1998). "Ageing and zonal variation in post-translational modification of collagen in normal human articular cartilage. The age-related increase in non-enzymatic glycation affects biomechanical properties of cartilage." Biochem J **330 (Pt 1)**: 345-51.

Bank, R. A., B. Beekman, et al. (1997). "Sensitive fluorimetric quantitation of pyridinium and pentosidine crosslinks in biological samples in a single high-performance liquid chromatographic run." J Chromatogr B Biomed Sci Appl **703**(1-2): 37-44.

Baxter, B. T., G. S. McGee, et al. (1992). "Elastin content, cross-links, and mRNA in normal and aneurysmal human aorta." <u>J Vasc Surg</u> **16**(2): 192-200.

Beighton, P., A. De Paepe, et al. (1998). "Ehlers-Danlos syndromes: revised nosology, Villefranche, 1997. Ehlers-Danlos National Foundation (USA) and Ehlers-Danlos Support Group (UK)." <u>Am J Med Genet</u> **77**(1): 31-7.

Berg, R. A. and D. J. Prockop (1973). "The thermal transition of a non-hydroxylated form of collagen. Evidence for a role for hydroxyproline in stabilizing the triple-helix of collagen." <u>Biochem Biophys Res Commun</u> **52**(1): 115-20.

Bernard, M. P., J. C. Myers, et al. (1983). "Structure of a cDNA for the pro alpha 2 chain of human type I procollagen. Comparison with chick cDNA for pro alpha 2(I) identifies structurally conserved features of the protein and the gene." <u>Biochemistry</u> **22**(5): 1139-45.

Bornstein, P. (2002). "The NH(2)-terminal propeptides of fibrillar collagens: highly conserved domains with poorly understood functions." <u>Matrix Biol</u> **21**(3): 217-26.

Bornstein, P., V. Walsh, et al. (2002). "The globular domain of the proalpha 1(I) N-propeptide is not required for secretion, processing by procollagen N-proteinase, or fibrillogenesis of type I collagen in mice." <u>J Biol Chem</u> **277**(4): 2605-13.

Brodsky, B. and J. A. Ramshaw (1997). "The collagen triple-helix structure." <u>Matrix Biol</u> **15**(8-9): 545-54.

Bruel, A., G. Ortoft, et al. (1998). "Inhibition of cross-links in collagen is associated with reduced stiffness of the aorta in young rats." <u>Atherosclerosis</u> **140**(1): 135-45.

Bruel, A. and H. Oxlund (1996). "Changes in biomechanical properties, composition of collagen and elastin, and advanced glycation endproducts of the rat aorta in relation to age." <u>Atherosclerosis</u> **127**(2): 155-65.

Byers, P. (1996). Ehlers-Danlos Syndrome. <u>Emery and Rimoin's principles and practice of medical genetics</u>. C. J. Rimoin DL, and Pyeritz RE. New York, Churchhill Livingston**:** 1067-1081.

Byers, P. H. (2001). Disorders of Collagen Biosynthesis and Structure. <u>Metabolic and Molecular Bases of Inherited Disease 8th Ed</u>, McGraw-Hill**: 5241-5285.

Byers, P. H. (2001). "Folding defects in fibrillar collagens." <u>Philos Trans R Soc Lond B Biol Sci</u> **356**(1406): 151-7; discussion 157-8.

Byers, P. H., E. M. Click, et al. (1975). "Interchain disulfide bonds in procollagen are located in a large nontriple-helical COOH-terminal domain." <u>Proc Natl Acad Sci U S A</u> **72**(8): 3009-13.

Byers, P. H., J. C. Marini, et al. (1995). "Frontiers in rehabilitation medicine: osteogenesis imperfecta, overview of a conference." <u>Connect Tissue Res</u> **31**(4): 253-5.

Cabral, W. A., E. Makareeva, et al. (2005). "Mutations near amino end of alpha 1(I) collagen cause combined OI/EDS by interference with N-propeptide processing." <u>J Biol Chem</u>.

Camacho, N. P., L. Hou, et al. (1999). "The material basis for reduced mechanical properties in oim mice bones." <u>J Bone Miner Res</u> **14**(2): 264-72.

Camacho, N. P., W. J. Landis, et al. (1996). "Mineral changes in a mouse model of osteogenesis imperfecta detected by Fourier transform infrared microscopy." <u>Connect Tissue Res</u> **35**(1-4): 259-65.

Canty, E. G. and K. E. Kadler (2005). "Procollagen trafficking, processing and fibrillogenesis." <u>J Cell Sci</u> **118**(Pt 7): 1341-53.

Chipman, S. D., H. O. Sweet, et al. (1993). "Defective pro alpha 2(I) collagen synthesis in a recessive mutation in mice: a model of human osteogenesis imperfecta." <u>Proc Natl Acad Sci U S A</u> **90**(5): 1701-5.

Chowdhury, T. and W. Reardon (1999). "Elastin mutation and cardiac disease." <u>Pediatr Cardiol</u> **20**(2): 103-7.

Chu, M. L., W. de Wet, et al. (1984). "Human pro alpha 1(I) collagen gene structure reveals evolutionary conservation of a pattern of introns and exons." <u>Nature</u> **310**(5975): 337-40.

Clark, J. M. and S. Glagov (1985). "Transmural organization of the arterial media. The lamellar unit revisited." <u>Arteriosclerosis</u> **5**(1): 19-34.

Corman, B., M. Duriez, et al. (1998). "Aminoguanidine prevents age-related arterial stiffening and cardiac hypertrophy." <u>Proc Natl Acad Sci U S A</u> **95**(3): 1301-6.

Cusimano, R. J. (1996). "Repeat cardiac operation in a patient with osteogenesis imperfecta." <u>Ann Thorac Surg</u> **61**(4): 1294.

de Souza, R. R. (2002). "Aging of myocardial collagen." <u>Biogerontology</u> **3**(6): 325-35.

Deak, S. B., M. van der Rest, et al. (1985). "Altered helical structure of a homotrimer of alpha 1(I)chains synthesized by fibroblasts from a variant of osteogenesis imperfecta." <u>Coll Relat Res</u> **5**(4): 305-13.

DeBacker, C. M., A. M. Putterman, et al. (1998). "Age-related changes in type-I collagen synthesis in human eyelid skin." <u>Ophthal Plast Reconstr Surg</u> **14**(1): 13-6.

Dobrin, P. B. (1997). Physiology and Pathophysiology of Blood Vessels. <u>The Basic Science of Vascular Disease</u>. A. S. Sidway, BE; and DePalma, RG. Armonk, Futura Publishing Copmany Inc.**:** 69 - 105.

Dobrin, P. B., W. H. Baker, et al. (1984). "Elastolytic and collagenolytic studies of arteries. Implications for the mechanical properties of aneurysms." <u>Arch Surg</u> **119**(4): 405-9.

Dobrin, P. B. and T. R. Canfield (1984). "Elastase, collagenase, and the biaxial elastic properties of dog carotid artery." <u>Am J Physiol</u> **247**(1 Pt 2): H124-31.

Dumas, M., C. Chaudagne, et al. (1996). "Age-related response of human dermal fibroblasts to L-ascorbic acid: study of type I and III collagen synthesis." C R Acad Sci III **319**(12): 1127-32.

Exposito, J., C. Cluzel, et al. (2000). "Tracing the evolution of vertebrate fibrillar collagens from an ancestral alpha chain." Matrix Biol **19**(3): 275-9.

Exposito, J. Y., C. Cluzel, et al. (2002). "Evolution of collagens." Anat Rec **268**(3): 302-16.

Exposito, J. Y., M. D'Alessio, et al. (1992). "Sea urchin collagen evolutionarily homologous to vertebrate pro-alpha 2(I) collagen." J Biol Chem **267**(22): 15559-62.

Exposito, J. Y. and R. Garrone (1990). "Characterization of a fibrillar collagen gene in sponges reveals the early evolutionary appearance of two collagen gene families." Proc Natl Acad Sci U S A **87**(17): 6669-73.

Forlino, A., F. D. Porter, et al. (1999). "Use of the Cre/lox recombination system to develop a non-lethal knock-in murine model for osteogenesis imperfecta with an alpha1(I) G349C substitution. Variability in phenotype in BrtlIV mice." J Biol Chem **274**(53): 37923-31.

Franklin, S. S. (1999). "Cardiovascular risks related to increased diastolic, systolic and pulse pressure. An epidemiologist's point of view." Pathol Biol (Paris) **47**(6): 594-603.

Fratzl, P., O. Paris, et al. (1996). "Bone mineralization in an osteogenesis imperfecta mouse model studied by small-angle x-ray scattering." J Clin Invest **97**(2): 396-402.

Fratzl, P. M., K.; and Zizak, I (1997). "Fibrillar Structure and Mechanical Properties of Collagen." Journal of Structural Biology **122**: 119-122.

Fung, Y. (1993). Bioviscoelastic Solids. Biomechanics: Mechanical Properties of Living Tissues 2nd Ed. New York, Springer-Verlag**:** 220-320.

Fung, Y. (1993). Mechanical Properties and Active Remodeling of Blood Vessels. Biomechanics: Mechanical Properties of Living Tissues 2$\underline{^{nd}}$ Ed. New York, Springer-Verlag**:** 320-360.

Ghersi, G., A. M. La Fiura, et al. (1989). "Direct adhesion to type I and homotrimer collagens by breast carcinoma and embryonic epithelial cells in culture: a comparative study." Eur J Cell Biol **50**(2): 279-84.

Glasser, S. P., D. K. Arnett, et al. (1997). "Vascular compliance and cardiovascular disease: a risk factor or a marker?" Am J Hypertens **10**(10 Pt 1): 1175-89.

Greene, M. A., R. Friedlander, et al. (1966). "Distensibility of arteries in human hypertension." Proc Soc Exp Biol Med **121**(2): 580-5.

Gura, T., G. Hu, et al. (1996). "Posttranscriptional aspects of the biosynthesis of type 1 collagen pro-alpha chains: the effects of posttranslational modifications on synthesis pauses during elongation of the pro alpha 1 (I) chain." J Cell Biochem **61**(2): 194-215.

Guyton, A. C. and J. E. Hall (2000). Textbook of medical physiology. Philadelphia, Saunders.

Hall, D. A. and R. Reed (1957). "Hydroxyproline and thermal stability of collagen." Nature **180**(4579): 243.

Hata, R. (1995). "Transfection of normal human skin fibroblasts with human alpha 1(I) and alpha 2(I) collagen gene constructs and evidence for their coordinate expression." Cell Biol Int **19**(9): 735-41.

Hata, R., S. Kurata, et al. (1988). "Existence of malfunctioning pro alpha2(I) collagen genes in a patient with a pro alpha 2(I)-chain-defective variant of Ehlers-Danlos syndrome." Eur J Biochem **174**(2): 231-7.

Himmelmann, A., T. Hedner, et al. (1998). "Isolated systolic hypertension: an important cardiovascular risk factor." Blood Press **7**(4): 197-207.

Hornstra, I. K., S. Birge, et al. (2003). "Lysyl oxidase is required for vascular and diaphragmatic development in mice." J Biol Chem **278**(16): 14387-93.

Hortop, J., P. Tsipouras, et al. (1986). "Cardiovascular involvement in osteogenesis imperfecta." Circulation **73**(1): 54-61.

Hosokawa, N. and K. Nagata (2000). "Procollagen binds to both prolyl 4-hydroxylase/protein disulfide isomerase and HSP47 within the endoplasmic reticulum in the absence of ascorbate." FEBS Lett **466**(1): 19-25.

http://www.informatics.jax.org/mgihome/nomen/genefamilies/collagen.shtml (2006). Collagen Gene Family.

http://www.ncbi.nlm.nih.gov/entrez/query (2006). Human Collagen Genes.

Isotalo, P. A., M. M. Guindi, et al. (1999). "Aortic dissection: a rare complication of osteogenesis imperfecta." Can J Cardiol **15**(10): 1139-42.

Jimenez, S. A., R. I. Bashey, et al. (1977). "Identification of collagen alpha1(I) trimer in embryonic chick tendons and calvaria." Biochem Biophys Res Commun **78**(4): 1354-61.

Ju, H. and I. M. Dixon (1996). "Extracellular matrix and cardiovascular diseases." Can J Cardiol **12**(12): 1259-67.

Kadler, K. (1995). "Extracellular matrix 1: Fibril-forming collagens." Protein Profile **2**(5): 491-619.

Kadler, K. E., Y. Hojima, et al. (1987). "Assembly of collagen fibrils de novo by cleavage of the type I pC-collagen with procollagen C-proteinase. Assay of critical concentration demonstrates that collagen self-assembly is a classical example of an entropy-driven process." J Biol Chem **262**(32): 15696-701.

Kadler, K. E., Y. Hojima, et al. (1988). "Assembly of type I collagen fibrils de novo. Between 37 and 41 degrees C the process is limited by micro-unfolding of monomers." J Biol Chem **263**(21): 10517-23.

Kalath, S., P. Tsipouras, et al. (1987). "Increased aortic root stiffness associated with osteogenesis imperfecta." Ann Biomed Eng **15**(1): 91-9.

Kay, E. P. (1986). "Rabbit corneal endothelial cells modulated by polymorphonuclear leukocytes are fibroblasts. Comparison with keratocytes." Invest Ophthalmol Vis Sci **27**(6): 891-7.

Kietly, C. M. H., I.; and Grant, M.E. (1993). The Collagen Family: Structure, Assembly, and Organization in the Extracellular Matrix. Connective Tissue and Its Heritable Disorders, Wiley-Liss Inc**:** 103-147.

Kirk, T. Z., J. S. Evans, et al. (1987). "Biosynthesis of type I procollagen. Characterization of the distribution of chain sizes and extent of hydroxylation of polysome-associated pro-alpha-chains." J Biol Chem **262**(12): 5540-5.

Knott, L. and A. J. Bailey (1998). "Collagen cross-links in mineralizing tissues: a review of their chemistry, function, and clinical relevance." Bone **22**(3): 181-7.

Kodama, H. and Y. Murata (1999). "Molecular genetics and pathophysiology of Menkes disease." Pediatr Int **41**(4): 430-5.

Kojima, T., H. Shinkai, et al. (1988). "Case report and study of collagen metabolism in Ehlers-Danlos syndrome type II." J Dermatol **15**(2): 155-60.

Krafka, J. (1940). "Changes in the elasticity of the aorta with age." AMA Arch Patholo **29**: 303-309.

Landis, W. J. (1995). "The strength of a calcified tissue depends in part on the molecular structure and organization of its constituent mineral crystals in their organic matrix." Bone **16**(5): 533-44.

Li, D. Y., B. Brooke, et al. (1998). "Elastin is an essential determinant of arterial morphogenesis." Nature **393**(6682): 276-80.

MacLean, N. F., N. L. Dudek, et al. (1999). "The role of radial elastic properties in the development of aortic dissections." J Vasc Surg **29**(4): 703-10.

Marchant, J. K., R. A. Hahn, et al. (1996). "Reduction of type V collagen using a dominant-negative strategy alters the regulation of fibrillogenesis and

results in the loss of corneal-specific fibril morphology." <u>J Cell Biol</u> **135**(5): 1415-26.

Matsumura, S., S. Kawazoye, et al. (1995). "Organizations of extracellular matrices in aortic and mesenteric arteries of stroke-prone spontaneously hypertensive rat." <u>Ann N Y Acad Sci</u> **748**: 534-7.

McBride, D. J., Jr., V. Choe, et al. (1997). "Altered collagen structure in mouse tail tendon lacking the alpha 2(I) chain." <u>J Mol Biol</u> **270**(2): 275-84.

McBride, D. J., Jr., K. E. Kadler, et al. (1992). "Self-assembly into fibrils of a homotrimer of type I collagen." <u>Matrix</u> **12**(4): 256-63.

McBride, D. J., Jr. and J. R. Shapiro (1994). "Confirmation of a G nucleotide deletion in the Cola-2 gene of mice with the osteogenesis imperfecta mutation." <u>Genomics</u> **20**(1): 135-7.

McBride, D. J., Jr., J. R. Shapiro, et al. (1998). "Bone geometry and strength measurements in aging mice with the oim mutation." <u>Calcif Tissue Int</u> **62**(2): 172-6.

Meadows, R. S., D. F. Holmes, et al. (2000). "Electron cryomicroscopy of fibrillar collagens." <u>Methods Mol Biol</u> **139**: 95-109.

Menashi, S., J. S. Campa, et al. (1987). "Collagen in abdominal aortic aneurysm: typing, content, and degradation." <u>J Vasc Surg</u> **6**(6): 578-82.

Michalickova, K., M. Susic, et al. (1998). "Mutations of the alpha2(V) chain of type V collagen impair matrix assembly and produce ehlers-danlos syndrome type I." <u>Hum Mol Genet</u> **7**(2): 249-55.

Miles, C. A., T. V. Burjanadze, et al. (1995). "The kinetics of the thermal denaturation of collagen in unrestrained rat tail tendon determined by differential scanning calorimetry." <u>J Mol Biol</u> **245**(4): 437-46.

Miles, C. A., T. J. Sims, et al. (2002). "The role of the alpha2 chain in the stabilization of the collagen type I heterotrimer: a study of the type I homotrimer in oim mouse tissues." <u>J Mol Biol</u> **321**(5): 797-805.

Misof, K., W. J. Landis, et al. (1997). "Collagen from the osteogenesis imperfecta mouse model (oim) shows reduced resistance against tensile stress." J Clin Invest **100**(1): 40-5.

Moriyama, Y., T. Nishida, et al. (1995). "Acute aortic dissection in a patient with osteogenesis imperfecta." Ann Thorac Surg **60**(5): 1397-9.

Moro, L. and B. D. Smith (1977). "Identification of collagen alpha1(I) trimer and normal type I collagen in a polyoma virus-induced mouse tumor." Arch Biochem Biophys **182**(1): 33-41.

Morton, L. F. and M. J. Barnes (1982). "Collagen polymorphism in the normal and diseased blood vessel wall. Investigation of collagens types I, III and V." Atherosclerosis **42**(1): 41-51.

Murakami, H., H. Kodama, et al. (2002). "Abnormality of vascular elastic fibers in the macular mouse and a patient with Menkes' disease: ultrastructural and immunohistochemical study." Med Electron Microsc **35**(1): 24-30.

Nicholls, A. C., G. Osse, et al. (1984). "The clinical features of homozygous alpha 2(I) collagen deficient osteogenesis imperfecta." J Med Genet **21**(4): 257-62.

Nicholls, A. C., D. Valler, et al. (2001). "Homozygosity for a splice site mutation of the COL1A2 gene yields a non-functional pro(alpha)2(I) chain and an EDS/OI clinical phenotype." J Med Genet **38**(2): 132-6.

Nichols, W. O. R., MF (1990). Properties of the arterial wall. Philadelphia.

O'Garra, A., R. Chang, et al. (1992). "Ly-1 B (B-1) cells are the main source of B cell-derived interleukin 10." Eur J Immunol **22**(3): 711-7.

Oxlund, H., T. T. Andreassen, et al. (1984). "Effect of D-penicillamine on the mechanical properties of aorta, muscle tendon and skin in rats." Atherosclerosis **52**(2): 243-52.

Oxlund, H., L. M. Rasmussen, et al. (1989). "Increased aortic stiffness in patients with type 1 (insulin-dependent) diabetes mellitus." Diabetologia **32**(10): 748-52.

Pace, J. M., C. D. Kuslich, et al. (2001). "Disruption of one intra-chain disulphide bond in the carboxyl-terminal propeptide of the proalpha1(I) chain of type I procollagen permits slow assembly and secretion of overmodified, but stable procollagen trimers and results in mild osteogenesis imperfecta." J Med Genet **38**(7): 443-9.

Peleg, I., Z. Greenfeld, et al. (1993). "Type I and type III collagen mRNA levels in kidney regions of old and young rats." Matrix **13**(4): 281-7.

Pfeiffer, B. J., C. L. Franklin, et al. (2005). "Alpha 2(I) collagen deficient oim mice have altered biomechanical integrity, collagen content, and collagen crosslinking of their thoracic aorta." Matrix Biol **24**(7): 451-8.

Phillips, C. L., and Wenstrup, R.J. (1992). Biosynthetic and Genetic Disorders of Collagen. Wound Healing and Clinical Aspects. R. F. D. I.K. Cohen, and W.J. Linblad. Orlando, W.B. Saunders**:** 152-176.

Phillips CL, a. Y. H. (1997). Vitamin C, collagen synthesis and aging. Vitamin C in health and disease. P. L. a. F. J. New York, Marcel Dekker**:** 205-230.

Phillips, C. L., D. A. Bradley, et al. (2000). "Oim mice exhibit altered femur and incisor mineral composition and decreased bone mineral density." Bone **27**(2): 219-26.

Pihlajaniemi, T., L. A. Dickson, et al. (1984). "Osteogenesis imperfecta: cloning of a pro-alpha 2(I) collagen gene with a frameshift mutation." J Biol Chem **259**(21): 12941-4.

Pope, F. M. and N. P. Burrows (1997). "Ehlers-Danlos syndrome has varied molecular mechanisms." J Med Genet **34**(5): 400-10.

Powell, J. and R. M. Greenhalgh (1989). "Cellular, enzymatic, and genetic factors in the pathogenesis of abdominal aortic aneurysms." J Vasc Surg **9**(2): 297-304.

Prockop, D. J., K. E. Kadler, et al. (1988). "Expression of type I procollagen genes." Ciba Found Symp **136**: 142-60.

Reiser, K., R. J. McCormick, et al. (1992). "Enzymatic and nonenzymatic cross-linking of collagen and elastin." Faseb J **6**(7): 2439-49.

Reiser, K. M. (1991). "Nonenzymatic glycation of collagen in aging and diabetes." Proc Soc Exp Biol Med **196**(1): 17-29.

Reiser, K. M. (1994). "Influence of age and long-term dietary restriction on enzymatically mediated crosslinks and nonenzymatic glycation of collagen in mice." J Gerontol **49**(2): B71-9.

Reiser, K. M. (1998). "Nonenzymatic glycation of collagen in aging and diabetes." Proc Soc Exp Biol Med **218**(1): 23-37.

Reiser, K. M., M. A. Amigable, et al. (1992). "Nonenzymatic glycation of type I collagen. The effects of aging on preferential glycation sites." J Biol Chem **267**(34): 24207-16.

Reneker, L. W., D. W. Silversides, et al. (1995). "TGF alpha can act as a chemoattractant to perioptic mesenchymal cells in developing mouse eyes." Development **121**(6): 1669-80.

Rizzo, R. J., W. J. McCarthy, et al. (1989). "Collagen types and matrix protein content in human abdominal aortic aneurysms." J Vasc Surg **10**(4): 365-73.

Roach, M. a. B., AC. (1957). "The reason for the shape of the distensibility curves of arteries." Canadian Journal of Biochemistry and Physiology **35**: 681-690.

Rojkind, M. (1979). "Chemistry and biosynthesis of collagen." Bull Rheum Dis **30**(1): 1006-10.

Rojkind, M., M. A. Giambrone, et al. (1979). "Collagen types in normal and cirrhotic liver." Gastroenterology **76**(4): 710-9.

Rucker, R. B., T. Kosonen, et al. (1998). "Copper, lysyl oxidase, and extracellular matrix protein cross-linking." Am J Clin Nutr **67**(5 Suppl): 996S-1002S.

Rupard, J. H., S. J. Dimari, et al. (1988). "Synthesis of type I homotrimer collagen molecules by cultured human lung adenocarcinoma cells." <u>Am J Pathol</u> **133**(2): 316-26.

Saban, J., M. A. Zussman, et al. (1996). "Heterozygous oim mice exhibit a mild form of osteogenesis imperfecta." <u>Bone</u> **19**(6): 575-9.

Sasaki, T., K. Arai, et al. (1987). "Ehlers-Danlos syndrome. A variant characterized by the deficiency of pro alpha 2 chain of type I procollagen." <u>Arch Dermatol</u> **123**(1): 76-9.

Schwarze, U., M. Atkinson, et al. (2000). "Null alleles of the COL5A1 gene of type V collagen are a cause of the classical forms of Ehlers-Danlos syndrome (types I and II)." <u>Am J Hum Genet</u> **66**(6): 1757-65.

Schwarze, U., R. Hata, et al. (2004). "Rare autosomal recessive cardiac valvular form of Ehlers-Danlos syndrome results from mutations in the COL1A2 gene that activate the nonsense-mediated RNA decay pathway." <u>Am J Hum Genet</u> **74**(5): 917-30.

Silver, L. M. (1995). <u>Mouse genetics : concepts and applications</u>. New York, Oxford University Press.

Simon, A. and J. Levenson (1991). "Use of arterial compliance for evaluation of hypertension." <u>Am J Hypertens</u> **4**(1 Pt 1): 97-105.

Sims, T. J., C. A. Miles, et al. (2003). "Properties of collagen in OIM mouse tissues." <u>Connect Tissue Res</u> **44 Suppl 1**: 202-5.

Slack, J. L., D. J. Liska, et al. (1993). "Regulation of expression of the type I collagen genes." <u>Am J Med Genet</u> **45**(2): 140-51.

Spina, M., S. Garbisa, et al. (1983). "Age-related changes in composition and mechanical properties of the tunica media of the upper thoracic human aorta." <u>Arteriosclerosis</u> **3**(1): 64-76.

Stegemann, H. and K. Stalder (1967). "Determination of hydroxyproline." <u>Clin Chim Acta</u> **18**(2): 267-73.

Sumner, D. S., D. E. Hokanson, et al. (1970). "Stress-strain characteristics and collagen-elastin content of abdominal aortic aneurysms." Surg Gynecol Obstet **130**(3): 459-66.

Thornell, L. E., O. Norrgard, et al. (1986). "Abdominal aortic aneurysms: distribution of elastin, collagen I and III, and intermediate filament proteins desmin and vimentin--a comparison of familial and nonfamilial aneurysms." Heart Vessels **2**(3): 172-83.

Uitto, J. (1979). "Collagen polymorphism: isolation and partial characterization of alpha 1(I)-trimer molecules in normal human skin." Arch Biochem Biophys **192**(2): 371-9.

Vetter, U., B. Maierhofer, et al. (1989). "Osteogenesis imperfecta in childhood: cardiac and renal manifestations." Eur J Pediatr **149**(3): 184-7.

Vogel, H. G. (1978). "Influence of maturation and age on mechanical and biochemical parameters of connective tissue of various organs in the rat." Connect Tissue Res **6**(3): 161-6.

Vogel, H. G. (1983). "Age dependence of mechanical properties of rat tail tendons (hysteresis experiments)." Aktuelle Gerontol **13**(1): 22-7.

Vouyouka, A. G., B. J. Pfeiffer, et al. (2001). "The role of type I collagen in aortic wall strength with a homotrimeric." J Vasc Surg **33**(6): 1263-70.

Walker, L. C., M. A. Overstreet, et al. (2004). "Heterogeneous basis of the type VIB form of Ehlers-Danlos syndrome (EDS VIB) that is unrelated to decreased collagen lysyl hydroxylation." Am J Med Genet A **131A**(2): 155-62.

Weis, S. M., J. L. Emery, et al. (2000). "Myocardial mechanics and collagen structure in the osteogenesis imperfecta murine (oim)." Circ Res **87**(8): 663-9.

Wenstrup, R. J., J. B. Florer, et al. (2004). "Type V collagen controls the initiation of collagen fibril assembly." J Biol Chem **279**(51): 53331-7.

Wenstrup, R. J., J. B. Florer, et al. (2004). "Reduced type I collagen utilization: a pathogenic mechanism in COL5A1 haplo-insufficient Ehlers-Danlos syndrome." J Cell Biochem **92**(1): 113-24.

Wenstrup, R. J., J. B. Florer, et al. (2006). "Murine model of the ehlers-danlos syndrome: COL5A1 haploinsufficiency disrupts collagen fibril assembly at multiple stages." J Biol Chem.

Wenstrup, R. J., J. B. Florer, et al. (2000). "COL5A1 haploinsufficiency is a common molecular mechanism underlying the classical form of EDS." Am J Hum Genet **66**(6): 1766-76.

Wenstrup, R. J., S. Murad, et al. (1989). "Ehlers-Danlos syndrome type VI: clinical manifestations of collagen lysyl hydroxylase deficiency." J Pediatr **115**(3): 405-9.

Wheeler, V. R., N. R. Cooley, Jr., et al. (1988). "Cardiovascular pathology in osteogenesis imperfecta type IIA with a review of the literature." Pediatr Pathol **8**(1): 55-64.

Wilson, R., J. F. Lees, et al. (1998). "Protein disulfide isomerase acts as a molecular chaperone during the assembly of procollagen." J Biol Chem **273**(16): 9637-43.

Wong, R. S., F. M. Follis, et al. (1995). "Osteogenesis imperfecta and cardiovascular diseases." Ann Thorac Surg **60**(5): 1439-43.

Woodson, B. T., S. Fujita, et al. (1991). "Perilymphatic fistula: analysis of free amino acids in middle ear microaspirates." Otolaryngol Head Neck Surg **104**(6): 796-802.

Xu, Y., M. Bhate, et al. (2002). "Characterization of the nucleation step and folding of a collagen triple-helix peptide." Biochemistry **41**(25): 8143-51.

Yamada, Y., M. Mudryj, et al. (1983). "A uniquely conserved regulatory signal is found around the translation initiation site in three different collagen genes." J Biol Chem **258**(24): 14914-9.

Yeowell, H. N. and S. R. Pinnell (1993). "The Ehlers-Danlos syndromes." <u>Semin Dermatol</u> **12**(3): 229-40.

Zafarullah, K., A. L. Sieron, et al. (1997). "A recombinant homotrimer of type I procollagen that lacks the central two D-periods. The thermal stability of the triple helix is decreased by 2 to 4 degrees C." <u>Matrix Biol</u> **16**(5): 245-53.

VITA

Brent Pfeiffer was born in St. Louis, Missouri in 1975. He attended Francis Howell High School and graduated from the University of Evansville in 1998 with bachelor degrees in biology and chemistry. While in graduate school at the University of Missouri-Columbia, he applied to medical school and initiated a physician-scientist training program. Brent received his doctorate degree and medical degree from the University of Missouri-Columbia in May 2006. He will be beginning his residency training in pediatrics at the University of Miami, Holtz Children Hospital at the Jackson Memorial Medical Center in July 2006.